Preparation and characterization of biopolymer compounds containing poly-3-hydroxyalkanoates and polylactic acid

by

Manoj Nerkar

A thesis submitted to the Department of Chemical Engineering

In conformity with the requirements for the degree of

Doctor of Philosophy

Queen's University, Kingston, Ontario, Canada

(September, 2014)

Abstract

This thesis is focused on developing cost effective and environmentally friendly techniques to improve the properties and processability of biopolyesters through compounding and reactive modification. Specifically, elastomeric medium-chain-length poly(3-hydroxyalkanoates) (MCL PHA) have been evaluated as potential impact modifiers for poly(lactic acid) (PLA) and poly-3-hydroxybutyrate (PHB), using conventional melt compounding. The Mark-Houwink constants, absolute molecular weight distributions and the absolute molecular weight (MW) averages of MCL PHAs with predominantly 3-hydroxyoctanoate (PHO), 3-hydroxynonanoate (PHN) or 3-hydroxydodecanoate (PHDD) content were determined and ranged between 18,200 for PHN to 172,000 Da for PHO. Detailed thermal and rheological characterization revealed that PHO had the highest viscosity, and was thus the best candidate as impact modifier for PHB and PLA. Melt compounded PHB/PHO and PLA/PHO blends showed improved tensile strain at break and unnotched impact strength upon addition of up to 30 wt.% PHO in PHB and 15 wt.% PHO in PLA. This was counteracted by decreased Young's modulus due to lower blend crystallinity. The droplet-matrix morphology coarsened as PHO content increased beyond 5 wt.%, due to PHO coalescence attributed to viscosity mismatch between blend components. PHO was reacted using lauroyl peroxide to increase its viscosity through partial cross-linking, thus improving the morphology but the mechanical properties showed only moderate improvements, presumably due to high PHO gel content which compromised its elastomeric nature. Reactive compounding by radical mediated solvent-free grafting of triallyl trimesate (TAM) coagent was employed to improve blend properties. Reactively modified PLA had higher molar mass, melt viscosity and enhanced strain hardening. Additionally it showed a distinct crystallization peak upon cooling

with disappearance of the cold crystallization peak, indicative of a nucleation effect. PLA modified using a multi-functional epoxide oligomeric chain extender yielded similar improvements in rheological properties, but no considerable change in crystallization. This coagent modification approach also increased the viscosity of PHO, and improved both extrudate appearance and handling. Coagent modified PLA/PHO blends demonstrated significant improvement in crystallization and rheological properties, similar to those seen in the coagent modified PLA alone, while the mechanical properties remained unaffected.

Co-Authorship

This thesis contains seven chapters that present results that have been published in the form of original journal articles as well as material that is in preparation for submission. The complete citations for the published papers and chapter in which they appear are provided bellow:

- Chapter 3: Nerkar M, Ramsay J, Ramsay B, Kontopoulou M, Hutchinson R. Determination of Mark-Houwink parameters and absolute molecular weight of medium-chain-length poly(3-hydroxyalkanoates). Journal of Polymers and the Environment 2013 (21): 24-29
- Chapter 4: Nerkar M, Ramsay J, Ramsay B, Kontopoulou M. Melt compounded blends of short and medium-chain-length poly-3-hydroxyalkanoates. Journal of Polymers and the Environment 2014 (22): 236-243
- Chapter 5 : Nerkar M, Ramsay J, Ramsay B, Kontopoulou M. Dramatic Improvements in Strain Hardening and Crystallization kinetics of PLA by simple reactive modification in the melt state. Macromolecular Materials and Engineering (Accepted –May 2014)
- Chapter 6 : Nerkar M, Ramsay J, Ramsay B, Kontopoulou M. Improvements in the extensional rheology, thermal properties and morphology of poly(lactic acid)/ poly-3-hydroxyoctanoate blends through reactive modification (To be submitted)

All the papers and manuscripts were co-authored and reviewed prior to publication by Professors Marianna Kontopoulou, Juliana A. Ramsay and Bruce A. Ramsay. The first paper (chapter 3) was co-authored by Professor Robin Hutchinson who directed the experiments to determine true molecular weight of medium-chain-length polyhydroxyalkanoate. Dr. Alexandros Vasileiou helped in the synthesis and characterization of epoxidized

polyhydroxyoctanoate presented in Appendix A. Hang Li performed fermentations that made medium-chain-length polyhydroxyalkanoates. All the rest of the experimental work and manuscript preparation were performed by the author of this thesis.

Acknowledgements

It would not have been possible to complete my doctoral thesis without the support and help from my supervisors, staff members, lab mates, family and friends.

I consider myself lucky to have a supervisor like Professor Marianna Kontopoulou. I appreciate her for being a great support to me and to my family in a foreign land. Apart from her endless technical support and research guidance, she was always motivating and encouraging. She has been a wonderful person to work with. It's my great privilege to be co-supervised by Professor Juliana A Ramsay. I would like to thank her for her technical guidance and for taking time to critically reviewing all my work. I was privileged to have the opportunity to work closely with Dr. Bruce A Ramsay. He was instrumental in providing his expert opinion about biopolymers. I would like to thank him, along with his team members, Dr. Zhiyong Sun, Hang Li and Eric Potter for providing the polymers required for my research.

Professor Robin Hutchinson is greatly acknowledged for his support in molecular weight characterization of polymers. Timely support from Dr. Kalam Mir, Steven Hodgson and Kelly Sedore is highly appreciated. Charlie Cooney from the materials department provided judicious help in conducting SEM analysis of samples.

I would like to thank my lab mates Osayuki Osazuwa, Ying Zhang, Andrew Powell, Praphulla and Dr. Alexandros Vasileiou for their friendship, technical discussions and help.

Funding support from the Natural Science and Engineering Research Council (NSERC), Queen's University Graduate Award and Xerox Research Center of Canada is gratefully acknowledged.

I take this opportunity to thank my parents Mrs. Rajani Gokul Nerkar, Mr. Gokul Madhavrao Nerkar, and my in-laws, Mrs. Shailaja Arvind Sonar and the late Mr. Arvind

Lilachand Sonar and all family members including brothers, brother-in-laws and sister-in-laws and friends from around the world who provided all kinds of support throughout my life.

Poonam, my lovely wife, is the person who inspired me to get doctorate. I cannot thank her enough for all of her sacrifices and for being with me all the time. She took care of our kids and their illness single handedly when I was busy studying for exams, attending conferences or writing manuscripts.

My acknowledgement cannot be completed without mentioning my adorable son Aayush and my beautiful daughter Anishka. I thank them for their unconditional love.

Contents

List of Figures

List of Tables

List of Schemes

Nomenclature

a	Mark-Houwink exponent
G*	Complex modulus (Pa)
G'	Elastic or Storage modulus (Pa)
G''	Viscous or loss modulus (Pa)
K	Mark-Houwink constant (dL/g)
T	Temperature (°C)
t	Time (s)
T_C	Temperature of crystallization (°C)
T_M	Melting point (°C)
Xc	Degree of crystallinity (%)

Greek Symbols

ΔH_f	Heat of fusion (J/g)
[η]	Intrinsic viscosity (dL/g)
$3\eta^+$	Linear viscoelastic envelope in uniaxial extension (Pa.s)
η*	Complex Viscosity (Pa.s)
η_0	Zero shear viscosity (Pa.s)
ω	Angular frequency (rad/s)
λ	viscosity ratio
η_d	viscosity of the dispersed phase
η_m	viscosity of the matrix

Abbreviations

3HV	3-hydroxyvalerate
ASTM	American society for testing materials
CHS	cross head speed
DBP	Di n-butyl phthalate
DCP	Dicumyl peroxide
d*n*/d*c*	Refractive index
DRI	Differential refractive index
DSC	Differential scanning calorimetry
GMA	Glycidyl methacrylate
GMS	Glycerol monostearate
GPC	Gel permeation chromatography
GTA	Glycerol triacetate
GTB	Glycerol tributyrate
HDI	Hexamethylene diisocyanate
HDT	Heat distortion temperature
IV	Intrinsic viscosity
LALS	Low angle light scattering
LLDPE	Linear low density polyethylene
LS	Light scattering
LVE	Linear viscoelastic
MCL	Medium-chain-length
mCPBA	m-Chloroperbenzoic acid
MK	Mark-Houwink
MMT	Montmorillonite
M_n	Number-average
MSDS	Material safety data sheets
M_w	Weight-average
MW	Molecular weight
MWD	Molecular weight distribution
NCC	Nano-crystalline cellulose
NSERC	Natural sciences and engineering council
PBS	Polybutylene succinate
PCL	Polycaprolactone
PDI	Poly dispersity index
PEG	Polyethylene glycol
PEGCA	Poly (polyethylene glycol-co-citric acid)
PEGCA	Poly (polyethylene glycol-co-citric acid)
PET	polyethylene terephthalate
PETA	Pentaerythritol triacrylate
PHA	Poly-3-hydroxyalkanoate
PHB	poly(3-hydroxybutyrate

PHB-HV	poly(3-hydroxybutyrate-*co*-3-hydroxyvalerate
PHDD	Poly-3-hydroxydodecanoate
PHN	Poly-3-hydroxynonanoate
PHO	Poly-3-hydroxyoctanoate
PLA	Poly (lactic) acid
PLLA	Poly(L-Lactic Acid)
POM	Poly(methyleneoxide
PP	Polypropylene
PS	Polystyrene
PVA	Poly vinyl alcohol
RALS	Right angle light scattering
SEC	Size exclusion chromatography
SEM	Scanning electron microscopy
SNCC	Silylated cellulose nanocrystals
TAM	Triallyl trimesate
TAP	Triallyl phosphate
T_C	Crystallization temperature
TD	Triple detector
T_g	Glass transition temperature
TGA	Thermogravimetric analysis
THF	Tetrahydrofuran
T_M	Melt temperature
TMPTA	Trimethylol propanetrimethacrylate
TPEE	Thermoplastic polyester elastomer
UC	Universal calibration

Chapter 1 Introduction

The rapid progress in polymer science and technology in the latter half of the twentieth century has led to the use of synthetic polymers in almost every field, including household items, industrial applications, electrical appliances, electronic devices, automotive, construction, and the medical field. Polymer based compounds are found in every aspect of everyday life. The fast growth of the polymer industry is attributed to the unique properties of polymers including light-weight, corrosion resistance, design flexibility, and ease of manufacturing. Durability is one of the advantages of polymers, but it is also their shortcoming. Petroleum based polymers are generally not biodegradable. Their life span is longer than several hundred years. After the end of their use, the polymers end up either in landfills or littering the environment. Landfilling is becoming increasingly prohibitive, due to increasing costs, scarcity of land and other health and environmental considerations, such as ground water contamination.

Furthermore, conventional plastics are made from petroleum products or natural gases, which are non-renewable resources. Serious concerns about greenhouse gas emissions [1] and high oil prices, which accompany the use of conventional polymers, are key driving forces to reduce their usage. Therefore there is a need for new materials from renewable resources to replace conventional polymers [2,3]. The quest for alternative materials has put biopolymers at the forefront [4]. Biopolymers are promising candidates to replace conventional polymers, because of their biodegradable nature and they can be made from renewable resources as raw material. They can be categorized as a) bioresourced, b) biodegradable and c) bioresourced and biodegradable.

Polylactic acid (PLA) is one of the major bioplastics available on a large commercial scale. It is an aliphatic polyester made from α hydroxy acids. It is biodegradable and biocompatible and it is used in many biomedical applications, such as sutures, stents, dialysis media, and drug delivery devices. PLA is also used in commodity applications ranging from clothing, packaging, bottles, and office stationary to food containers [5].

Polyhydroxyalkanoate (PHA) is another polymer that has drawn considerable attention. It is produced by bacteria in a fermentation process, and is a water stable, biodegradable, biocompatible polymer. Past efforts to commercialize PHA have not been very successful, because they lack the engineering properties and processability needed to compete with conventional polymeric materials [6].

1.1 Thesis objectives

Upgrading the properties of biopolymers is an active area of research in academia and industry, with scientists and technologists striving to match performance of biopolymers with petroleum based polymers to find new applications. The objective of this thesis is to develop commercially viable biopolymer formulations containing PHA and PLA. To achieve this goal, medium-chain-length (MCL) PHA has been identified as a potential impact modifier. Following the detailed characterization and selection of suitable MCL PHA grades, challenges like the viscosity mismatch between the polymers and slow crystallization rates will be addressed with the ultimate goal of developing polymeric material with acceptable engineering properties and good processability in commercial polymer processing operations.

The approach followed in this thesis is outlined below.

1.1.1 Characterization of MCL PHA

Even though the synthesis of MCL PHAs has been reviewed extensively, their physical properties have not been yet fully characterized. Full characterization of the MCL PHAs used in this study is necessary to further understand their physical properties and processability and to choose suitable MCL PHA grades for formulations of biopolymers containing these materials. The first objective of this work is to fully characterize the molecular weight, melt and solid state properties of various MCL PHA grades, with different chain structures. This will aid with the choice of materials that will be used in subsequent steps.

1.1.2 Blends of MCL PHA with brittle biopolymers

Biopolymers such as PLA and poly-3-hydroxybutyrate (PHB) are brittle materials and thus cannot be used in certain applications like packaging, where flexibility of the material is essential. The second objective is to assess the ability of MCL PHA to impart flexibility into PHB and PLA. A suitable MCL PHA candidate will be chosen based on properties like melt viscosity, melting temperature, thermal stability and molecular weight, as described in the first objective. Various amounts of MCL PHA will be blended with PHB and PLA and the morphology and mechanical properties of the blends will be evaluated.

1.1.3 Enhancement of melt viscosity of MCL PHA for blending with PHB and PLA

It is expected that the inherently low melt viscosity of MLC PHAs will pose a problem when trying to blend them with other polymers. The significant difference in the melt viscosity of the blend components tends to give phase separation, and coarse morphology, resulting in poor mechanical properties. Therefore, the third objective will be to increase the melt viscosity of MCL PHAs, using chain extension and cross-linking techniques.

1.1.4 Improved melt strength and crystallization of PLA and its blends with MCL PHA by reactive modification

One of the main drawbacks that have hindered widespread implementation of biopolyesters, including PLA and PHAs, is their low crystallization rates, resulting in poor mechanical properties and processability. This makes them practically impossible to melt process in a cost-effective way using conventional techniques like injection molding, compression molding and extrusion. Poor melt strength restricts PLA's processability in operations involving high stretch rates, such as film blowing, thermoforming, and foaming. The last objective of this thesis is to improve crystallinity and melt strength of biopolymers through reactive processing without using any nucleating agents.

1.2 Thesis organization

This thesis contains seven chapters. **Chapter 1** gives an introduction of biopolymers specifically PHAs and PLA, their attributes and limitations. The chapter also defines the scope of the proposed research**. Chapter 2** summarizes the literature describing the various approaches that have been followed to address the limitations of PLA and PHAs. Relevant work is examined critically. **Chapter 3** discusses the characterization of a series of MCL PHAs including true molecular weight, melt viscosity, thermal stability, glass transition temperature (T_g), melting temperature and crystallinity**. Chapter 4** describes impact modification of brittle PHB, using a MCL PHA (i.e. polyhydroxyoctanoate (PHO)). **Chapter 5** describes the preparation of branched PLA with improved strain hardening and crystallinity by reactive modification in the melt state, using a peroxide and a multi-functional coagent. The performance of coagent-modified PLA is

compared with PLA modified with a multi-functional epoxide styrene-acrylic oligomeric chain extender, containing glycidyl methacrylate (GMA) functions. **Chapter 6** describes impact modification of PLA, and further utilizes the reactive modification approach described in chapter 5, to prepare reactively modified PHO and PLA/PHO blends to achieve a good balance of mechanical and melt-state properties. **Chapter 7** summarizes the overall outcomes and achievements of the thesis with recommendations for future work.

Chapter 2 Literature Review

2.1 Polyhydroxyalkanoates

Polyhydroxyalkanoates (PHAs) are linear polyesters that were first discovered in late 1920s, by Lemoigne who produced them using the *Bacillus megaterium* bacteria [7]. The chemical structure of PHA is shown in scheme 2.1 [8].

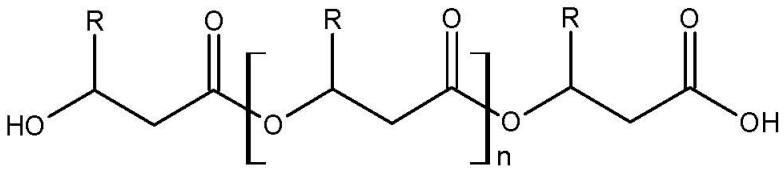

Scheme 2.1 Chemical structure of polyhydroxyalkanoate [8]

PHA can be divided into three categories based on number of carbons in side chain (the R group in Scheme 2.1): 1) Short-chain-length (SCL) PHA, 2) medium-chain-length (MCL) PHA and 3) hybrid (mix of SCL PHA and MCL PHA). SCL PHA contains 0-2 carbons whereas MCL PHA contains 3- 11 carbons in their backbone [9]. They can be found as homopolymers or co-polymers. PHAs can have thermoplastic or elastomeric properties, depending upon their composition. SCL PHAs behave like typical brittle thermoplastics, while MCL PHAs are elastomeric. Melting points of PHAs lie between 40^{o}C - 180^{o}C. PHAs can be processed by conventional polymer processing techniques.

Poly-3-hydroxybutyrate (PHB), a SCL PHA, is the most widely studied PHA. It is a brittle polymer and cannot be used without impact modification. The high crystallinity and low crystallization rate of PHB leads to embrittlement and an ageing effect of the polymer [10]. PHB is not

thermally stable [11], resulting in narrow processing windows [12]. The brittleness of PHB can be counteracted by adding impact modifiers or by using copolymers of the same polymer family, for example poly (3-hydroxybutyrate-co-3-hydroxyvalerate), P (3HB-co-3HV), which is more ductile and flexible than PHB. Increase in the 3-hydroxyvalerate (3HV) content improves flexibility with a decrease in melting temperature, tensile strength, modulus of elasticity and crystallinity. P (3HB-co-3HV) was commercialized in the 1980s by Imperial Chemical Industries Inc. (ICI) in the UK under the trade name Biopol®.

Medium-chain-length (MCL) PHA

SCL PHAs can be produced using a wide variety of bacteria under nutrient deprivation as an intracellular energy reserve [13]. On the other hand, very few microorganisms can be used to produce MCL PHA [14]. Accumulation of MCL PHA is restricted to *Pseudomonas rRNA* homology group I, like *Pseudomonas aeruginosa, P. chlororaphis, P. putida, P. syringae* and some *P. fluorescens* [14,15]. *P. putida* strains (formerly *P. oleovorans GPo1*) are used widely to produce MCL PHA. They have the ability to use alkanes, such as octane for synthesis of MCL PHA due to their octane (OCT) plasmid [13]. Alkanoates such as octanoate are a common carbon source to make MCL PHAs [16].

The properties of MCL PHAs depend on the polymer composition. The melting point of polyhydroxyoctanoate (PHO), a MCL PHA, is 61 °C with crystallinity of 30 % [17]. The glass transition temperature (T_g) is -35 °C. It is elastomeric in nature, having an extension at break value between 300-450 % and tensile strength between 6 and 10 MPa. The density of PHO is 1 $g.cm^{-3}$ [17]. Based on its properties listed above, MCL PHA is a potential bio-sourced, biodegradable impact modifier for brittle biopolymers.

Additives and chemical modification techniques that are commonly used to enhance the performance of PHAs and broaden its processing window are outlined below.

2.1.1 Impact modification of PHB

Blending brittle polymers with a ductile polymer, which forms a secondary phase, is the easiest way to impart flexibility in polymers. Polymer blends can either be miscible or immiscible. Immiscible blends that are compatible yield properties better than the parent polymers (synergistic effect) [18]. In the case of incompatible blends, compatibilizers can be used to enhance the blend properties. Some of the PHA-based blends that have been investigated are summarized below.

Parulekar et al. [19] used natural rubber to improve the ductility of PHB. They found that PHB-natural rubber blends were not compatible and there was a substantial viscosity mismatch between the two polymers. They used maleated polybutadiene with high graft content and low molecular weight to compatibilize the system. They concluded that epoxidized (25% epoxidation) natural rubber yielded better ductility compared to the non-functionalized natural rubber. A maleated polybutadiene- PHB – natural rubber (10:60:30) system showed 440% improvement in impact strength of PHB.

Block copolymers of polycaprolactone (PCL) and PHB have been used to compatibilize immiscible PCL/PHB blends. Optimization of the composition of the main blend components and compatibilizers is crucial to get substantial improvements in properties. 25 wt.% PCL and 5 wt.% of PCL-PHB block copolymers had only an elongation of 29 %, which increased dramatically to 855 % when there was 45 wt.% of PCL and 10 wt.% of PCL-PHB block copolymer [21]. Furthermore a 50:50 blend of PHB with a block copolymer of atactic poly ((R, S) -3-

hydroxybutyrate) and poly (ethylene glycol) resulted in increased elongation at break from 5 % to 90% with decrease in modulus and tensile strength [22]. An immiscible blend of PHB and acrylonitrile-g-(ethylene-co-propylene-co-diene)-g-styrene has also been studied and is composed of four phases of poly (ethylene-co-propylene-co-diene), poly (styrene-co-acrylonitrile), amorphous PHB and crystalline PHB. The blend exhibits 190% improvement in impact resistance of pristine PHB [23].

2.1.2 Plasticization

The ductility of PHB can be improved by adding low molecular weight plasticizers. Generally plasticizers decrease the intermolecular forces between polymer chains, thus increasing chain mobility. Plasticizers for PHB include 1) high boiling esters of polybasic acids such as phthalates, isophthalates, citrates, fumarates, glutamate, phosphates or phosphites 2) high boiling esters and part esters of polyhydric alcohols mainly glycols, polyglycols and glycerol 3) aromatic sulphonamides [24] and 4) a few high molecular weight polymers.

Ceccorulli et al. studied the effect of plasticization on the T_g of PHB [25]. They used a biodegradable plasticizer, di n-butyl phthalate (DBP) to improve the ductility of the PHB. 30 wt.% of DBP was sufficient to lower the T_g of PHB from 6 °C to -40 °C. The data is in agreement with Riande et al. [26] giving evidence of the existence of two concomitant phenomena, T_g depression of the polymer due to the plasticizing effect with up to 40 wt.% of plasticizer, and a small increase of the T_g of the plasticizer, due to hindrance in its mobility due to the dissolved polymer molecule, above 40 wt.% of the plasticizer. Plasticization did not affect the ability of PHB to crystallize. Increase in the plasticizer content decreases the crystallization temperature

as a result of reduced T_g that provides enough mobility to macromolecules for rearrangement and crystallization.

Other plasticizers include glycerol triacetate (GTA), glycerol tributyrate (GTB), and glycerol monostearate (GMS) [27]. Some high molecular weight polymers can also act as plasticizers. For example, addition of PEO, which has a T_g of -59 ^{o}C lowers the T_g and crystallization temperature of PHB [20].

2.1.3 Nucleation

One of the main drawbacks that have hindered widespread implementation of biopolyesters, including PHAs, is their low crystallization rates, which result in poor and inconsistent mechanical properties and processability. The time that these materials take to crystallize from the melt can be a few hours, which is too long compared to most conventional polymers. This makes them practically impossible to melt process in a cost-effective way using conventional processing techniques. Improvements in the crystallization behavior are necessary to obtain biopolymer-based formulations with good processability in polymer processing operations, such as extrusion, injection molding, and film processing.

Nucleating agents are commonly used to overcome slow crystallization rates and to increase the overall crystallinity, while maintaining small crystal sizes to achieve improved mechanical properties. Some of the common nucleating agents used in industry include talc, mica, calcium carbonate, chalk, and boron nitride. Environmentally friendly nucleating agents include saccharin, and phthalimide but they are not as effective as the conventional nucleating agents, such as boron nitride. They are both soluble in the melt and crystallize when solubility exceeds the relevant threshold [28].

High molecular weight polymers like poly vinyl alcohol (PVA) can also be used to nucleate PHB. PVA is a biodegradable, biocompatible and water soluble polymer with high crystallinity. A lot of research has been done on blends of PHB and PVA, which form a miscible blend with lower crystallinity. Alata et al. [29] showed that PVA particles can act as nucleating agents for PHB, and enhance the rate of crystallization of PHB. PVA has a melting point of ~ 225 °C, so blends processed at 190 °C ensure melting of PHB while PVA particles are still in the solid state. The nucleating performance of PVA is equivalent to that of talc and provides a complete bio and environment friendly material. Nano clays have also been used as nucleating agents for PHB. Addition of montmorillonite (MMT) clay increased the crystallization temperature by 29 °C [30]. In search of bio-sourced alternatives, which are considered more sustainable, cellulose, which is a naturally available crystalline material derived from wood (wood contains 40-50% cellulose [31]), has been suggested as a potential candidate. Cellulose has been proven to act as a nucleating agent for polymers like polypropylene. It reduces the size of the spherulites, while increasing the overall crystallinity and inducing trans-crystallinity [32,33]. Most of the work reported in this area has been done on microcrystalline cellulose. With recent advances in nanotechnology, it has been shown that high-aspect ratio nano-sized fillers are advantageous compared to their micron sized counterparts. Desired property improvements can be obtained at a fraction of the loading, while loss of ductility is minimized. Nano-crystalline cellulose (NCC) is a completely bioderived and biodegradable material, derived from cellulose through acid hydrolysis. NCC has been the subject of many recent research initiatives, including partnerships with the Canadian government [34]. In addition to being a promising candidate as a nucleating agent for PHAs, it can also offer substantial reinforcement given its high strength [35].

2.1.4 Chain extension

Chain extension is used widely to increase the molecular weight of polyesters. Diisocyanate forms urethane and amide linkages through a reaction with hydroxyl and carboxyl functional group, resulting in significant increase in molecular weight. Hexamethylene diisocyanate (HDI) has been used as a chain extender for PHO [4]. Scheme 2.2 illustrates the reaction of hydroxyl and carboxyl functional groups of polyester with isocyanate forming urethane, amide and allophanate linkages. This reaction increased the weight average molecular weight of PHO by 275 % and its number average molecular weight by 314 % [4].

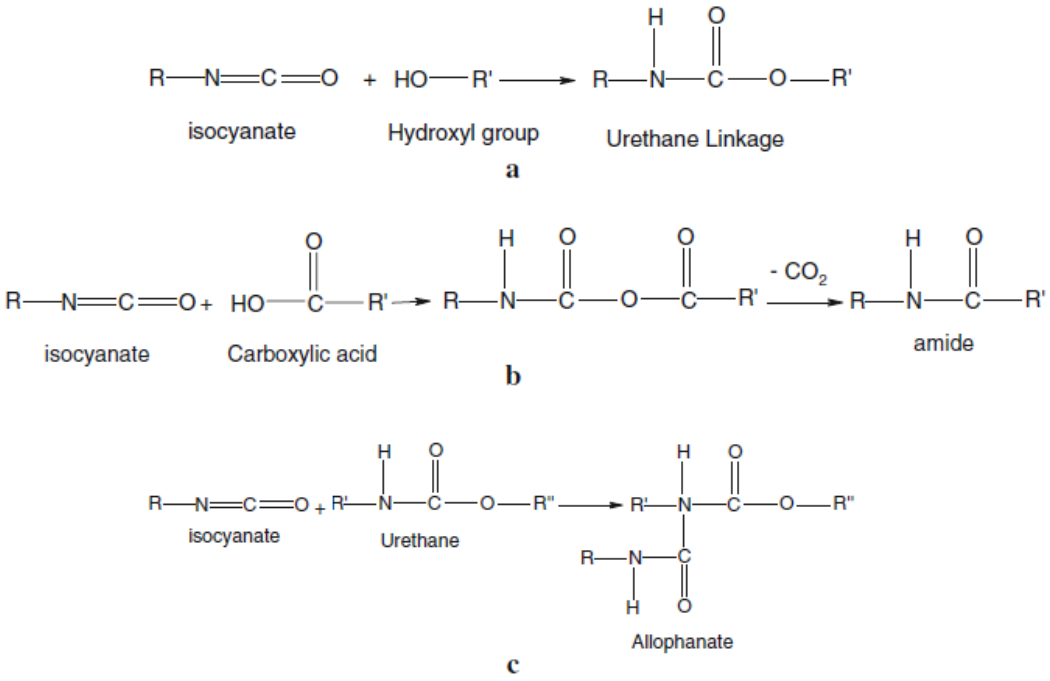

Scheme 2.2 Reaction of isocyanate with hydroxyl and carboxyl functional groups, adapted from Lee et al. 2009 [4]

2.2 Polylactic acid (PLA)

Poly (lactic acid) (PLA) (scheme 2.3) is an aliphatic polyester derived from renewable resources.

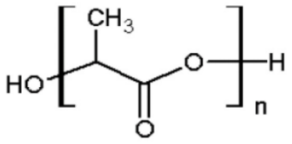

Scheme 2.3 Chemical structure of polylactic acid [36]

The properties of PLA depend significantly upon its molecular weight and the stereochemical makeup of the backbone, which is controlled by polymerization with D-lactide, L-lactide, or D,L-lactide, to form random or block stereocopolymers [37]. Some of the general properties of PLA are summarized in Table 2.1

Table 2.1 Properties of PLA [37]

	PLA
Density (Kg/m^3)	1.26
Tensile strength (MPa)	59
Elastic modulus (GPa)	3.8
Elongation at break (%)	4-7
Notched izod (J/m)	26
Heat deflection temperature (°C)	55

Some of the limitations of PLA are quite similar to PHB, for example brittleness and low crystallization rate. PLA has a very narrow processing window, because of the lack of melt strength and its slow crystallization rates. Its poor engineering properties, including impact strength and heat resistance have mainly confined its applications to food packaging [38], as

well as biomedical applications, such as drug delivery, where biocompatibility and biodegradability are desired. Extensive research has been done on PLA to address these problems. Various approaches to address the challenges of PLA are discussed below.

2.2.1 Impact modification

Blending with ductile polymers or elastomers is commonly used to counteract the brittleness of PLA. Thermoplastic polyester elastomer (TPEE) has been used as an impact modifier for PLA. Forming an immiscible blend with two phase morphology 4, 4-Methylenebis(phenylisocyanate) acts as a compatibilizer increasing the interfacial adhesion between PLA and TPEE to give 340 % increase in elongation at break while also maintaining modulus and tensile strength [39].

MCL PHA has been tested as an impact modifier for PLA. Immiscible blends of MCL PHA and PLA, produced by solution mixing, exhibited substantial improvement in impact strength and decreased tensile strength compared to the neat PLA [9]. Epoxy functionalized MCL PHA gave further improvement in mechanical properties. The epoxy groups react with the hydroxyl group of PLA, thus increasing the interfacial interaction and improving the blend morphology. Chain extension reduced the viscosity mismatch between PLA and PHO, so that eventually the melt viscosity of PHO and PLA blends was higher than that of blends without chain extension [4].

2.2.2 Plasticization

Polyethylene glycol (PEG) is often used to plasticize PLA. The system has improved elongation at break with limited impact strength. The PEG based polyester, poly (polyethylene glycol-co-citric acid) (PEGCA) forms a partially miscible blend with PLA. Addition of PEGCA diminishes the T_g of PLA. At 15 wt.% it gives 242 % elongation at break with impact strength as high as 103 J/m [40].

Adipates like (bis (2-ethylhexyl) adipate and glyceryl triacetate) and polymeric adipates exhibit excellent plasticization of PLA composites. They decrease T_g of PLA by 20 °C. 10 wt. % of plasticizer gives four times higher impact properties for PLA composite containing 40 wt. % of stable β -anhydrite. Adipates also help improve the dispersion of fillers and results in better tensile strength of composites [41].

2.2.3 Nucleation

Nucleating agents are used to address the slow crystallization rate of PLA. They increase nucleating density and thus increase crystallization rate. Talc exhibits effective nucleation in PLA, whereas other nucleating agents like calcium lactate and sodium stearate had little or no nucleating effect on PLA [42]. Talc contents of 1 wt.% significantly accelerate the crystallization process of the PLA matrix. The maximum crystallization rate was observed at an annealing temperature of 100 °C [43]. NCC has also been assessed in PLA. It has been shown that silylated cellulose nanocrystals (SNCC) exhibits enhanced nucleating efficiency. Addition of 1 wt.% SNCC resulted in substantial increase in crystallization rate. Increased crystallinity resulted in improvements of tensile strength and modulus [44].

2.2.4 Conditioning

Annealing is another approach to toughen PLA. The annealing temperature and annealing time have a significant effect on crystallization. As annealing time and temperature increase, the impact strength increases due to smaller spherulite size and a larger amount of the metastable phase. Quenching and subsequently annealing at an appropriate temperature (~90 °C) is crucial for PLA toughening [44].

2.2.5 Chain extension

As most polyesters, PLA has poor melt strength which restricts its use in processes involving extensional flow, such as film processing, thermoforming, and foaming. The processing window of PLA can be broadened by chain extension. Chain extenders such as isocyanate, glycidol, peroxides, and epoxy based styrene-acrylic oligomers have been used to increase the molecular weight of PLA, to improve its thermal stability and to increase its melt strength by introducing strain hardening [45], as explained in detail below.

2.2.6 Epoxy based chain extension

2.2.6.1 Glycidol

Deenadayalan et al. [46] achieved chain extension of PLA by reactive extrusion in the presence of glycidol. Chain extension was initiated by reaction of the carboxyl and the hydroxyl of PLA end groups with glycidol. The carboxylic end group of Poly(L-Lactic Acid) (PLLA) reacts with the primary hydroxyl end groups of glycidol and forms end-capped linear PLLA (scheme 2.4).

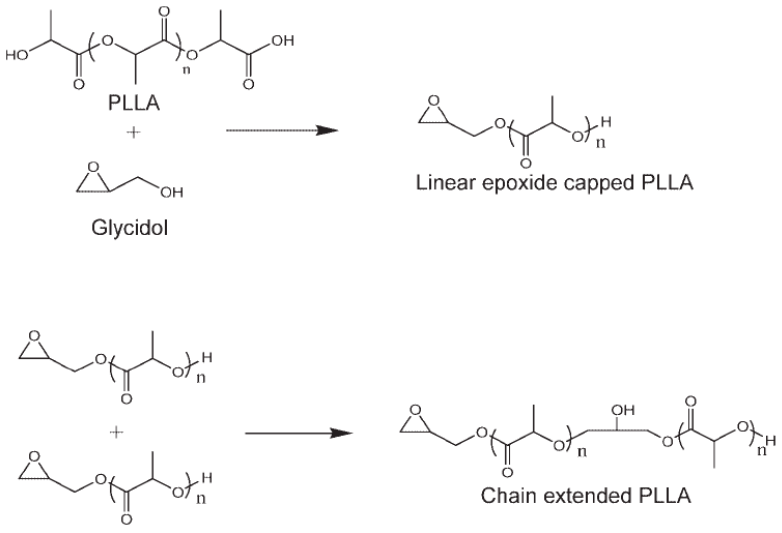

Scheme 2.4 Reaction between PLLA and glycidol adapted from Deenadayalan et al. 2009 [46]

A hydroxyl end group from another PLLA reacts with glycidol and initiates chain extension with formation of a pendant hydroxyl group that can react further with another end-capped PLLA to form a branch structure. Using this reaction, the resulting increase in molecular weight was more pronounced when low molecular weight as compared to high molecular weight PLA was used; this was attributed to the higher concentration of end groups in low molecular weight PLA, resulting in improved chain extension. The modified PLA showed higher T_g and melt temperature.

2.2.6.2 Multi-functional epoxy based chain extenders

Joncryl®, a multi-functional epoxide styrene-acrylic oligomeric chain extender, containing glycidyl methacrylate (GMA) functions (scheme 2.5) has been used successfully as a chain extender for polyesters, such as PLA [47]. It has following physical characteristics: T_g – 55 °C, epoxy equivalent weight – 285 g/mol.

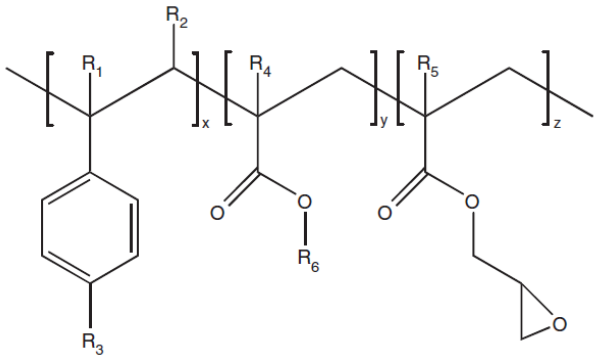

Scheme 2.5 General structure of Joncryl® styrene – acrylic multi-functional oligomeric chain extender, where R1 – R5 are H, CH_3, a higher alkyl group, or combinations of them, R6 is an alkyl group, and X, Y and Z are each between 1 and 20, adapted from Villalobos et al.2004 [48]

GMA contains epoxy groups, which participate in reactions with hydroxyl and carboxyl groups [49]. In polyesters, glycidyl esterification of carboxylic acid leads to hydroxyl end group etherification. Reaction of hydroxyl end group etherification competes with etherification of secondary hydroxyl group and main chain trans-esterification. The epoxy ring opening reaction results in covalent bonds via hydroxyl side group formation [50]. The reaction mechanism proposed by Al-Itry is depicted in scheme 2.6 [51].

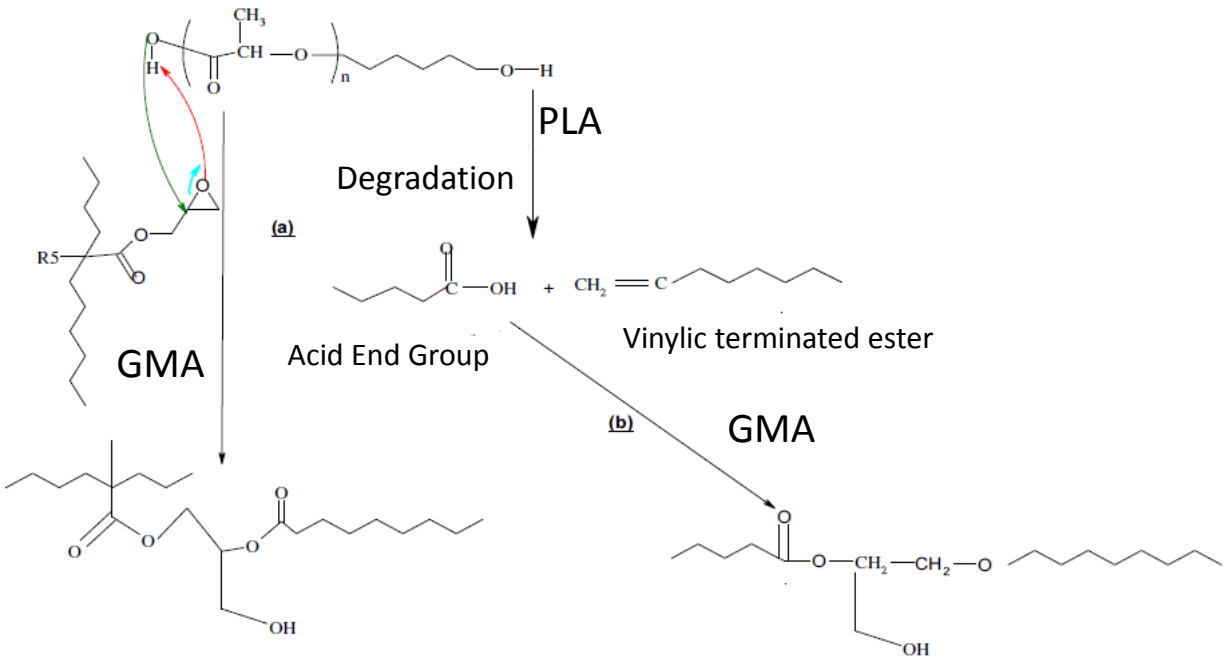

Scheme 2.6 Mechanism of PLA reaction with GMA, adapted from Al-Itry et al. 2012 [51]

2.2.7 Peroxide-mediated cross-linking

Peroxide curing is one of the oldest technologies to introduce branching and/or cross-linking in polymers. It is used widely in elastomers and polyolefin technology. A general scheme of peroxide cross-linking is shown in section 2.2.8. The peroxide undergoes hemolytic decomposition upon heating to generate free radicals. Free radicals abstract hydrogen from the polymer chain creating polymer radicals and decomposition products. The polymer radicals can

react with each other to form a C-C crosslinks. A competitive degradation reaction can also take place through β-chain session.

In PLA, peroxide-mediated chain extension has been achieved by reactive extrusion using lauroyl peroxide [52] dicumyl peroxide [53] and di-tertiary alkyl peroxide [54] with limited success. The choice of peroxide typically depends on the peroxide half-life time and the polymer processing temperature.

2.2.8 Multifunctional coagents

Multifunctional coagents are used widely to form branched polyolefins [55,56]. Parent et al. [57] studied triallyl trimesate (TAM), trimethylolpropane triacrylate (TMPTA) and triallyl phosphate (TAP) coagents (Scheme 2.7) in polypropylene. Depending on the type of coagent, different molecular weight and branching distributions may be obtained.

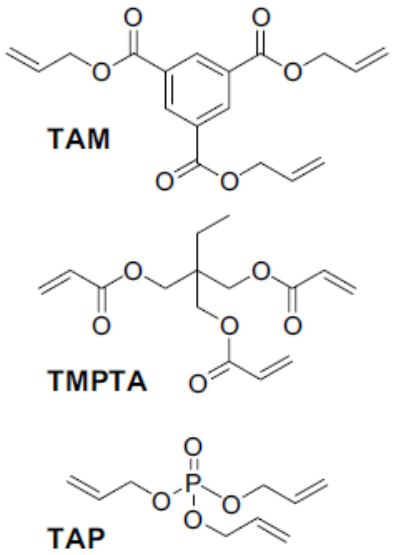

Scheme 2.7 Chemical structure of coagents, adapted from Parent et al. 2008 [56]

A typical peroxide assisted coagent modification scheme is illustrated below.

Initiation

$$ROOR \rightarrow 2\ RO\bullet$$

$$RO\bullet + P\text{-}H \rightarrow ROH - P\bullet$$

Propagation

$$P\bullet + M \xrightarrow{Kp} P\text{-}M\bullet$$

$$P\text{-}M\bullet + P\text{-}H \xrightarrow{Ktr} P\text{-}MH + P\bullet$$

Chain transfer

$$P\bullet + P\text{-}H \rightarrow P\text{-}H + P\bullet$$

Fragmentation -

$$P\bullet \rightarrow P^{=} + P\bullet$$

Termination

$$P\bullet + P\bullet \xrightarrow{Kt} P\text{-}P \text{ or } P\text{-}H + P^{=}$$

More specifically, the TAM activation reaction is discussed by Parent et al. [56].

Chapter 3 Determination of Mark-Houwink parameters and absolute molecular weight of medium-chain-length poly(3-hydroxyalkanoates)*

3.1 Introduction

Current global production of commodity plastics consumes up to 270 million tons of petroleum annually [58]. Despite recycling efforts, as much as 50% of the 100 million tons of plastic produced annually may end up in landfill sites. To address environmental and resource issues, "bio-based plastics" that are both biodegradable and made from renewable resources are being developed for a variety of applications. New applications and innovations are anticipated in the automotive, electrical/electronic, medical and packaging industries. Bioplastics include bio-polyethylene, polylactic acids (PLAs), polyhydroxyalkanoates (PHAs), and starch-based materials. Forecast analysts including Technavio and Helmut Kaiser Consultancy predict that the bioplastics market will experience significant growth (33.9-41% compound annual growth rate (CAGR)) from 2010 to 2015 [59].

As mentioned in section 2.1, the physical properties and solubilities of PHA are greatly affected by the length of the side group R (Scheme 2.1). Poly(3-hydroxybutyrate) (PHB), the most common short-chain-length (SCL) PHA, is stiff and brittle, whereas medium-chain-length (MCL) PHAs are more elastic and flexible. MCL PHAs are biodegradable materials with low crystallinity, low glass transition temperature ($T_{g)}$, high elongation, and low tensile strength [60], making them good candidates for applications where elastomeric properties are needed, such as for

*A version of this chapter has been published. Nerkar, M., Ramsay, J.A., Ramsay, B.A., Kontopoulou, M., Hutchinson, R.A. Journal of Polymers and the Environment 2013 (21): 24-29

impact modification of brittle biopolymers [47,61]. MCL PHAs are the only thermoplastics elastomers that have 100 % renewable content and are biodegradable.

Given the influence on many engineering properties such as strength, stiffness, toughness, elasticity, viscosity and thermal transitions, it is important to have access to reliable molecular weight data for PHAs, to assess the effect of synthesis conditions on their properties and evaluate the potential of these biopolymers in engineering applications.

Of the various PHA materials, PHB is by far the most investigated and characterized polymer. As PHB is not soluble in tetrahydrofuran (THF), molecular weight (MW) characterization is done in more aggressive solvents such as chloroform, 2,2,2-trifluoroethanol, and ethylene dichloride. Akita et al. [62] and Marchessault et al. [63] employed light scattering and osmometry to obtain absolute molecular weight (MW) data and to determine the Mark-Houwink (MH) calibration constants required to estimate PHB molecular weight distributions (MWD) from size exclusion chromatography (SEC) analysis coupled with a single detector calibrated using polystyrene (PS) standards. Ubbelohde type capillary viscometry and rotational viscometry have also been used to determine intrinsic viscosity data [62]. Miyaki et al. [64] and Cornibert et al.[65] covered a broader molecular weight range using osmometry. These efforts allow the estimation of absolute MW values from single-detector SEC analysis: a value of 1.0×10^5 Da as measured by PS calibration is transformed to 0.6×10^5 Da for PHB in chloroform using the MH constants published by Akita et al., a shift of 35%. PHB molecular weight is typically in the order of 1×10^6 Da in native granules but may decrease if exposed to depolymerases, base, oxidizing agents such as hypochlorite [66] or chlorinated solvents [67].

However, only limited MW data is available in the literature for MCL PHAs [60] and MCL SCL PHA materials [68], as measured by SEC analysis in THF eluent, and MW values are typically reported relative to PS calibrations. Absolute values of molecular weight for MCL PHAs are not reported in the literature to date, as the necessary SEC calibrations had not been performed. This information is required to better relate polymer structure to the processing properties and the degradation kinetics of these emerging biomaterials, such as those reported by Daly et al.[69] for poly (3-hydroxybutyrate-*co*- 3-hydroxyhexanoate).

In this chapter, absolute MW averages have been determined for four different MCL PHA copolymers from MWDs measured using multi-detector SEC, and MH parameters were estimated for the first time for these kinds of polymers in THF. Furthermore the melt viscosity is reported as a function of molecular weight.

3.2 Experimental

3.2.1 Materials

The four samples were copolymers with (3-hydroxyoctanoate) (PHO), (3-hydroxynonanoate) (PHN) and (3-hydroxydodecanoate) (PHDD) moieties produced from renewable starting materials including sugar and vegetable oil. PHO contained 98 mol % 3-hydroxyoctanoate and 2 mol % 3-hydroxyhexanoate. PHN 90 and PHN 70 contained 3-hydroxynonanoate and 3-hydroxyheptanoate at mole ratios of 90/10 and 70/30, respectively. PHDD contained 40 mol % 3-hydroxydodecanoate 39 mol % 3-hydroxydecanoate, 19 mol % 3-hydroxyoctanoate and 2 mol % 3-hydroxyhexanoate.

PHN 90 and PHO were produced in chemostat culture with addition of acrylic acid to inhibit β-oxidation [70]. PHN 70 and PHDD were produced in fed-batch culture [71]. The polymer samples were extracted from washed lyophilized biomass by Soxhlet extraction in acetone followed by precipitation in cold methanol [72], except for PHDD which was extracted in chloroform [67]. Cellular PHA content and composition were determined by gas chromatography as described by Sun et al. [71].

3.2.2 Methods

Samples were prepared for SEC analysis by dissolving 10 mg of polymer in 1 mL of distilled THF overnight to ensure complete dissolution, then passed through a 0.2 µm nylon filter. Polymer molecular weight distributions were measured using two different instruments to check consistency and reliability of the data. The first, a Viscotek 270max separation module with triple detection by differential refractive index (DRI), viscosity (IV) and light scattering (low angle LALS and right angle RALS), was maintained at 40 °C and contained two porous PolyAnalytik columns in series with an exclusion molecular weight limit of 20×10^6 Da. Distilled THF was used as the eluent at a flow rate of 1 mL/min. The MWDs were calculated using two methodologies. First, the results from the triple detector train and Viscotek Omnisec software were used to determine polymer MWDs and MW averages using the values of the refractive index (d*n*/d*c*) determined offline, using a Wyatt Optilab DSP refractometer as described below. The triple detection mode also yielded estimates for the polymer Mark-Houwink (MH) parameters, determined directly from the curve generated by the output from the IV and LS detectors. These MH parameters provided the means for a second analysis of the output data using the principle of universal calibration and the output from the DRI detector,

with a calibration curve constructed with narrow molecular weight polystyrene standards ranging from 6910 to 3.3×10^6 Da.

Samples were also characterized on a second SEC instrument consisting of a Waters 2960 separation module coupled with a Waters 410 differential refractometer (DRI) and a Wyatt Instruments Dawn EOS 690 nm laser photometer multiangle light scattering (LS) detector. THF was used as eluent at a flow rate of 1 mL/min through the four Styragel columns (HR 0.5, 1, 3, 4), maintained at 35 °C. The DRI detector was calibrated by 10 narrow polydispersity polystyrene standards in a broad MW range (870-3.55×10^5 Da), and the LS detector was calibrated by toluene, as recommended by the manufacturer. MWDs from this instrument were again calculated using two methods, using the output from the DRI detector and the MH parameters determined with the Viscotek setup, and by processing the data from the LS detector using the Wyatt Astra software and the refractive index (d*n*/d*c*) of the polymer in THF, according to standard procedures. The refractive index values were measured by a Wyatt Optilab DSP refractometer at 35 °C and 690 nm calibrated with sodium chloride. Five samples of 3–18 mg·mL^{-1} were prepared in THF for each polymer and injected sequentially to construct a curve with slope d*n*/d*c [73]*. The values for PHN 90 and PHO were 0.0601±0.0002 mL/g and 0.0603±0.0003 mL/g, respectively.

DSC experiments were performed using a Q100 DSC from TA Instruments, under dry nitrogen. Since MCL PHAs crystallize slowly, the samples were preconditioned to eliminate their thermal history as follows: the polymer was heated at 100 °C for 10 min in a convection oven, and then kept at room temperature for two weeks before characterization. Samples weighing 10-12 mg were sealed in aluminum hermetic pans, equilibrated at -70 °C and kept isothermally for 5 min.

Afterwards they were heated to 100 °C at a rate of 5 °C/min and held isothermally for 3 min before cooling to -70 °C at a rate of 5 °C/min. As MCL PHAs did not crystallize during second heating cycle data from first heating cycle was used for differentiation. The samples were finally reheated to 100 °C at a rate of 5 °C/min. The % crystallinity of the polymers, X_c, was estimated using equation (3.1).

$$X_c = \frac{\Delta H_m}{\Delta H_{100}} \times 100 \qquad (3.1)$$

where, ΔH_m is the enthalpy of fusion and ΔH_{100} is the theoretical fusion enthalpy of a 100% crystalline polymer, which is 146 J/g [74].

Rheological characterization was carried out in the constant rate mode under nitrogen blanket using a ViscoTech rheometer by Reologica, equipped with a cone and plate fixture having 25 mm diameter at 120 °C. All MCL PHAs had Newtonian behavior.

3.3 Results and Discussion

3.3.1 Molecular weight determination

Two different instruments, a triple detector Viscotec 270 max and a dual detector Waters/Wyatt, were used to characterize the polymer samples, as detailed in the Experimental Section. MWDs and molecular weight averages were calculated from each instrument using both multidetector and single detector (DRI) with universal calibration) output.

Log-log plots of polymer intrinsic viscosity ([η] in dL/g) vs. MW were constructed using the triple detector output from the Viscotec SEC; experimental results for the three PHO replicates are shown in Figure 3.1a. These curves were calculated using the d*n*/d*c* value of 0.0602 mL·g^{-1}

determined to be independent of the MCL PHA composition in THF at 35 °C. Linear regression was used to estimate the MH calibration parameters and for all four samples, as summarized in Table 3.1. Averages and standard deviations of three measurements are reported. The four sets of calibration parameters represent a very similar [η] vs MW behavior for the copolymer samples (Figure 3.1b). Thus, the values were averaged to provide an estimate of a "universal" set of MH parameters that may be applied to all MCL PHAs, independent of composition. The last column in Table 3.1 reports MW values calculated for a PS equivalent MW of 10^5 Da using the four individual pairs of MH parameters as well as that calculated according to the "universal" MH parameters. The difference between the various estimates is less than 15%, which is the typical error reported for MW measurements by SEC. Moreover, the calculated values are within 10% of 10^5 Da, the PS equivalent MW.

All of the copolymers were characterized at least three times on three different days to check reproducibility of the data. The MWD data of PHO (three replicates run on two instruments analyzed using multidetector and universal calibration) are shown in Figure 3.2. The peak positions of the three replicates are tightly grouped at 10^5 Da, independent of the SEC setup or analysis method chosen. This agreement, also observed for the other samples, demonstrates the validity of the polymer refractive index (d*n*/d*c*) and MH calibration parameters determined in this work for MCL PHA materials.

Before drawing generalized conclusions, it is useful to examine the number-average (M_n) and weight-average (M_w) molecular weight values as well as the dispersity index (PDI= M_w/M_n) for the four MCL PHA samples. Only the output from the Viscotek instrument was used, as the column set used in the Waters/Wyatt instrument is designed for analysis of lower MW samples

and the calibration for the DRI detector only extends to 3.5×10^5 Da. Thus, the polymer MWDs are cut off at higher molecular weights, most clearly seen in Figure 3.2a with the DRI detector.

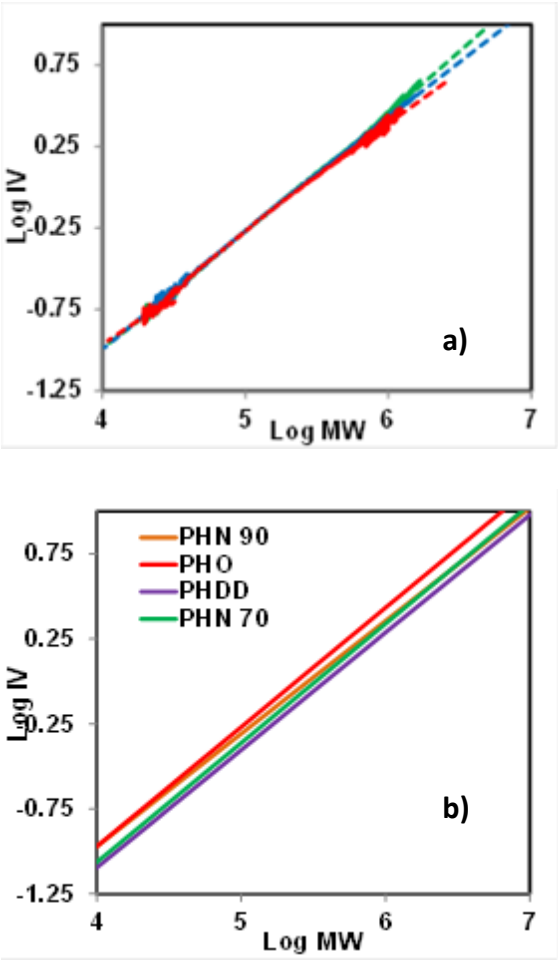

Figure 3.1 a) Experimental Mark-Houwink data for PHO (three replicates), b) best fit Mark-Houwink relationships for all copolymer samples.

(The Wyatt ASTRA software used for processing of the LS detector provides an estimate of the complete MWD; however, separation of the higher MW polymer will be incomplete due to the column set used.) MW averages and standard deviations are reported in Table 3.2 as estimated

by the full Viscotek triple detector (TD) analysis, as well as using only the output from the DRI detector coupled with universal calibration (DRI/UC). The universal calibration procedure is done using the sample-specific MH parameters reported in Table 3.1, as well as the averaged "universal" MH sample-specific MH parameters reported in Table 3.1, as well as the averaged "universal" MH parameters. Furthermore, the MW averages are also reported according to DRI analysis with PS calibration.

Table 3.1 Mark Houwink calibration constants from best fit to triple detector analysis of MCL PHA samples in THF ($[\eta]=K(MW)^a$).

	a	**Log(*K*/(dL·g^{-1}))**	**MW (kDa)[a]**
PS [75]	0.716	-3.943	100.0
PHO	0.701 (±0.013)	-3.77 (±0.07)	88.1
PHN 90	0.663 (±0.020)	-3.62 (±0.11)	92.7
PHN 70	0.701 (±0.031)	-3.86 (±0.16)	99.8
PHDD	0.691 (±0.013)	-3.86 (±0.07)	106.0
Universal PHA	0.689	-3.78	96.2

[a] Calculated for PS equivalent MW of 10^5 Da

As summarized in Table 3.2, the MWDs of the four samples have similar PDI values of 1.8-2.3. (The values obtained by TD-SEC are lower, as is often observed in MWDs measured by light-scattering techniques). However, as also seen in the MWDs plotted as Figure 3.3, the absolute

M_w averages vary from 3.0-3.4×10^4 Da for the PHN-70 sample to 1.4-1.7×10^5 Da for PHO. These values, controlled by the synthesis conditions for the different copolymers, are within the range

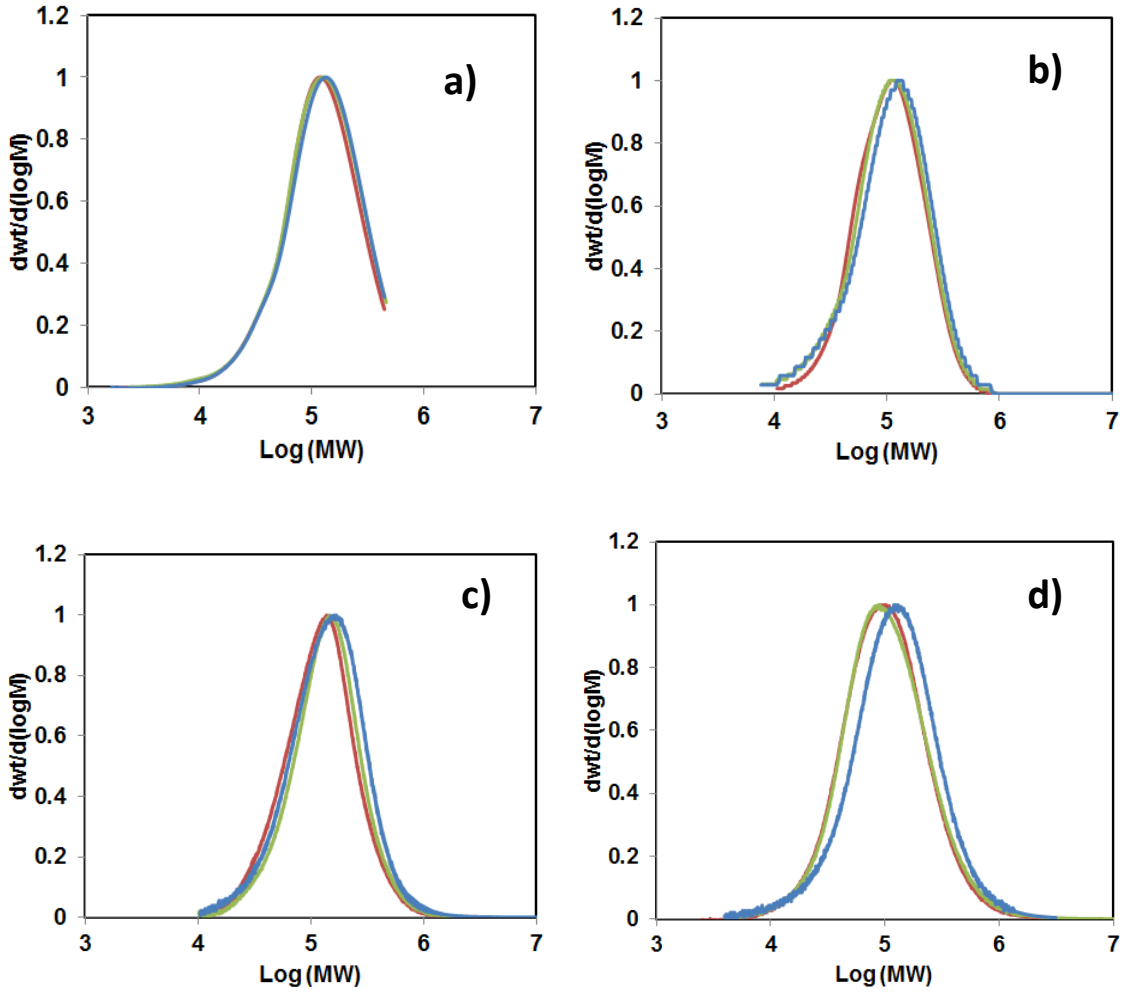

Figure 3.2 Molecular weight distributions for PHO (three replicates) as measured by a) Waters/Wyatt SEC, light-scattering detector; b) Waters/Wyatt SEC, universal calibration; c) Viscotek SEC, triple detection; and d) Viscotek –SEC, universal calibration.

Table 3.2 Number-average (M_n), weight-average (M_w), and dispersity (PDI) values determined from SEC analysis of MCL PHA samples.

	PS Calibration			UC, individual MH parameters			UC, averaged MH parameters			TD Analysis		
	M_n (kDa)	M_w (kDa)	PDI	M_n (kDa)	M_w (kDa)	PDI	M_n (kDa)	M_w (kDa)	PDI	M_n (kDa)	M_w (kDa)	PDI
PHO	73.7±4.5	150±16	2.02±0.11	61.6±5.7	140.7±15.3	2.28±0.22	67.2±6.3	155.2±17	2.31±0.22	98.2±6.7	172±17	1.75±0.10
PHN90	52.7±1.6	98.3±2.6	1.87±010	44.9±2.0	92.6±2.4	2.06±0.14	47.4±2.1	95.6±2.4	2.03±0.14	49.8±1.8	89.7±7.0	1.80±0.14
PHN70	15.4±0.7	33.6±0.5	2.18±0.11	13.6±0.8	31.1±0.4	2.29±0.14	12.9±0.7	29.9±0.4	2.32±0.14	18.2±3	31.9±2.3	1.77±0.17
PHDD	25.7±1.4	47.1±1.4	1.83±0.05	24.5±1.6	47.3±1.5	1.93±0.07	22.3±1.4	43.2±1.3	1.93±0.07	29.7±1.3	46.8±0.8	1.58±0.04

Values are reported according to polystyrene (PS) calibration, universal calibration (UC) with individual polymer MH parameters from Table 3.1, UC with "universal" parameters for MCL PHA, and triple detector (TD) analysis. The average of three samples is reported.

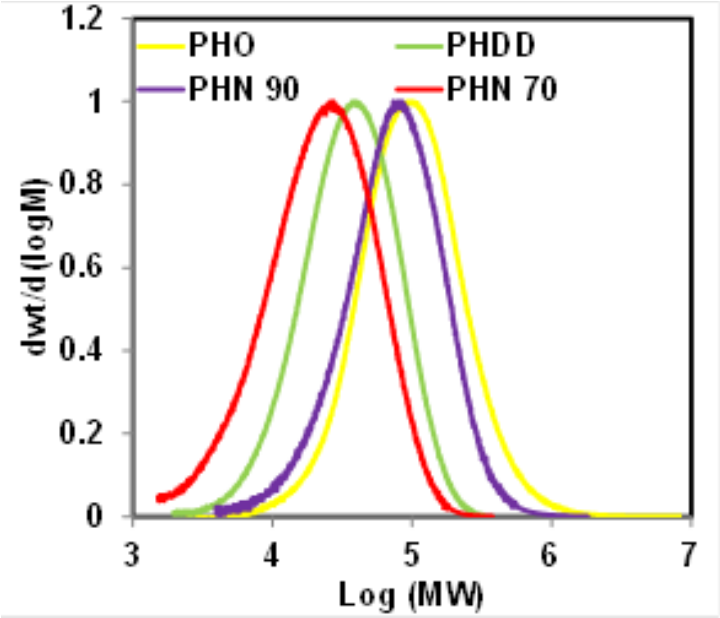

Figure 3.3 Molecular weight distributions of four MCL PHA polymers (Viscotek SEC, universal calibration).

reported in the literature for MCL PHAs [60,68].The difference in M_w values calculated using TD-SEC and DRI/UC methodologies is the largest for PHO, with the spread for the other three (lower M_w) samples less than 10%. This very good agreement (Table 3.1) validates the adoption of a "universal" set of MH parameters for MCL PHA samples analyzed in THF, and is independent of copolymer composition.

3.3.2 Thermal and rheological characterization

The thermal properties of MCl PHAs are summarized in Table 3.3. All the materials were highly amorphous, with PHO having the highest melting temperature and lowest crystallinity, whereas PHDD has highest crystallinity.

Table 3.3 Thermal properties of MCL PHAs

	T_M (°C)	T_g (°C)	Crystallinity (%)
PHO	63	-36	15
PHN 990	60	-46	17
PHN 970	50	-47	16
PHDD	61	-40	21

The bulk rheology of the four samples was also measured. All samples demonstrated Newtonian behavior. The zero shear viscosity scales with M_w with a slope of 1 at lower molecular weights, and has a slope of 3.8 which is higher than the slope of 3.4 anticipated for linear polymers at the higher molecular weights, as shown in Figure 3.4. This may be due to experimental error. The plot suggests an entanglement molecular weight around 8×10^4 Da (where the two fitted lines intersect), which is significantly higher than most conventional polymers, suggesting that these polymers may adopt folded helical conformations, similar to what has been proposed for PHB [76].

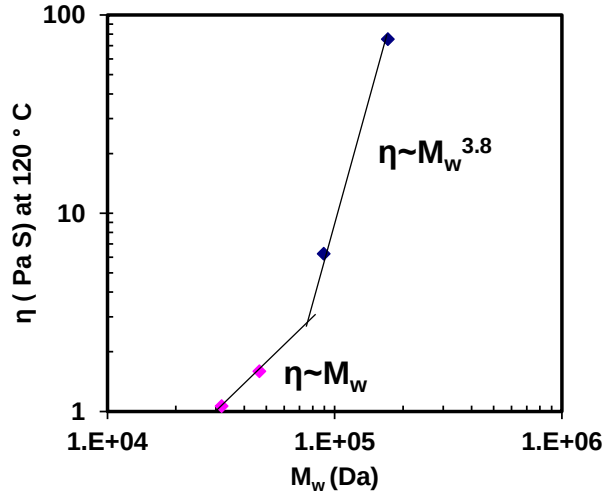

Figure 3.4 Viscosity as a function of molecular weight

3.4 Conclusion

This study provides the first determination of absolute MWDs and MW averages of MCL PHA copolymers. Fortuitously (and unlike PHB in chloroform), the relationship between polymer MW and intrinsic viscosity is very close to that determined through PS calibration. Thus, previously reported MW data [67,77] for MCL PHAs relative to polystyrene calibration can be considered, within experimental error, as absolute values. With these results, it will be possible to more closely examine the relationship between MCL PHA synthesis conditions and polymer MWs, and to better assess their processability using viscosity data. The latter will be of significant benefit in product development.

Chapter 4 Melt compounded blends of short and medium-chain-length poly-3-hydroxyalkanoates*

4.1 Introduction

Poly(3-hydroxyalkanoates) (PHAs) are microbially produced, biodegradable polymers derived from renewable resources [6]. Poly-3-hydroxybutyrate (PHB), the most studied short-chain-length (SCL) PHA, is a brittle polymer requiring modification to render it suitable for various engineering applications. Incorporation of 3-hydroxyvalerate (3HV) to form a copolymer of poly(3-hydroxybutyrate-*co*-3-hydroxyvalerate) (PHB-HV) results in improved ductility, impact properties, and lower tensile strength, moduli, melting temperatures and crystallinity [78].

Blends of PHB with other polymers have been studied extensively [79,80]. Parulekar et al. [19] achieved 440% improvement in the impact strength of PHB by adding a maleated polybutadiene to PHB/natural rubber blends. Substantial improvements in the impact resistance of PHB have been noted in immiscible blends of PHB with acrylonitrile-*g*-(ethylene-*co*-propylene-*co*-diene)-*g*-styrene, comprising of four phases: poly (ethylene-*co*-propylene-*co*-diene), poly (styrene-*co*-acrylonitrile), amorphous PHB and crystalline PHB [23]. Polycaprolactone (PCL)/PHB blends containing a PCL-PHB block copolymer as compatibilizer, exhibited dramatic increases in the elongation at break [21]. Blends of PHB containing a block copolymer of atactic poly((R, S)-3- hydroxybutyrate) and poly(ethylene glycol) resulted in increased elongation at break and lower modulus and tensile strength [22]. PHB/poly(methyleneoxide)(POM) blends exhibited modest improvements in mechanical

*A version of this chapter has been published. Nerkar, M., Ramsay, J.A., Ramsay, B.A., Kontopoulou, M., Journal of Polymers and the Environment, 2014 (22): 236-243

properties [20]. Blends of PHB with polymers derived from renewable sources, such as poly(lactic acid) (PLA), starch and chitosan have also been studied [80-82].

Medium-chain-length (MCL) PHAs, such as poly (3-hydroxyoctanoate) (PHO), have low crystallinity and exhibit elastomeric properties. PHO has been used to impact modify PLA via solution blending [9]. Epoxy functionalized MCL PHA resulted in further improvements in mechanical properties. These materials are therefore promising biopolymers as impact modifiers for PHB [60]. Dufresne et al. [83] noted a transition from elastomeric to brittle properties upon addition of PHB to PHO using a solvent mixing technique. Martelli et al. [84] noted 50% improvement in elongation at break of PHB-HV upon addition of MCL PHA using solution casting. However melt compounding, which is more industrially relevant, has not been investigated, in part due to the technical difficulties in producing sufficient quantities of MCL PHAs.

The objective of this chapter is to prepare and characterize melt compounded blends of MCL PHAs with PHB. In the previous chapter the properties of four different MCL PHAs with predominantly 3-hydroxyoctanoate (PHO), 3-hydroxynonanoate (PHN) or 3-hydroxydodecanoate (PHDD) content were reported. PHO had the highest melt viscosity and molecular weight. It also has low crystallinity and glass transition temperature (T_g). Based on these attributes PHO was chosen as the preferred candidate for impact modification in the present chapter. The morphology, mechanical, thermal and rheological properties of PHB/PHO blends are reported. Furthermore peroxide-initiated cross-linking of PHO is used to counteract the viscosity mismatch between the two components.

4.2 Experimental

4.2.1 Materials

An unmodified, additive free PHB (grade T19), with a weight-average molecular weight of 1,416,000 Da with a dispersity of 7, was supplied by BIOMER, Krailling, Germany in the form of powder. PHO, containing 98 mol % 3-hydroxyoctanoate and 2 mol % 3-hydroxyhexanoate, was produced and characterized as described previously in chapter 3 [85]. Its weight average molecular weight, determined by triple-detector size exclusion chromatography (SEC), was 172,000 Da with a dispersity of 1.75. Lauroyl peroxide (L-231) and ethyl ether anhydrous were obtained from Elf Atochem and Sigma Aldrich respectively and were used as received.

4.2.2 Compounding

PHB and PHO were dried in a vacuum oven at 100 °C and at room temperature respectively, to remove moisture. Blends containing 0-30 wt.% PHO were compounded in a DSM microcompounder at 190 °C for 3 min at a screw speed of 100 rpm. The compounder was operated under nitrogen blanket to limit polymer degradation. After compounding, the strands were quenched in cold water before chopping into pellets.

4.2.3 PHO cross-linking

Weighed amounts of lauroyl peroxide (0.06-0.5 wt.%) were dissolved in anhydrous ethyl ether and coated onto PHO pellets in a glass Petri dish. The coated pellets were placed in a vacuum oven overnight at room temperature to remove the solvent. Cross-linking was conducted in a Carver press at 155^{o}C for 10 min to ensure complete reaction (the half-life time of the lauroyl peroxide at 155^{o}C is 0.8 min). Cross-linked PHO was chopped into small pieces and dry mixed with PHB at appropriate ratios before feeding into compounder. For rheological

characterization, the cross-linked compression molded sheets were cut into 25 mm diameter disc and used for testing as described below.

The gel content of the peroxide-cross-linked MCL PHA was measured by dissolving the material in boiling tetrahydrofuran (THF) for 7 h. The polymer was sealed in stainless steel wire mesh (120 mesh) according to ASTM D 2765. The material was left for 1 h under the fumehood and subsequently dried overnight in a vacuum oven at room temperature. The % gel content was calculated using equation (4.1).

$$\text{Gel content} = \frac{\text{Final weight of sample}}{\text{Initial weight of sample}} \times 100 \qquad (4.1)$$

4.2.4 Blend Characterization

4.2.4.1 Differential scanning calorimetry (DSC)

DSC experiments were performed using a Q100 DSC from TA Instruments, under dry nitrogen. Since MCL PHAs crystallize slowly, the samples were preconditioned to eliminate their thermal history as follows: the polymer was heated at 100 °C for 10 min in a convection oven, and then kept at room temperature for two weeks before characterization. Samples weighing 10-12 mg were sealed in aluminum hermetic pans, equilibrated at -70 °C and kept isothermally for 5 min. Afterwards they were heated to 200 °C at a rate of 5 °C/min and held isothermally for 3 min before cooling to -70 °C at a rate of 5 °C/min. The samples were finally reheated to 200 °C at a rate of 5 °C/min. The % crystallinity of the polymers, X_c, was estimated using equation (4.2).

$$X_c = \frac{\Delta H_m}{\Delta H_{100}} \times 100 \qquad (4.2)$$

where ΔH_m is the enthalpy of fusion and ΔH_{100} is the theoretical fusion enthalpy of a 100% crystalline polymer, which is 146 J/g [74].

4.2.4.2 Thermogravimetric analysis (TGA)

TGA was conducted on a Q500 TGA from TA Instruments under nitrogen atmosphere, using 6-8 mg samples. The weight loss was evaluated by heating to 800 °C at a heating rate of 20 °C/min. Isothermal experiments were conducted at the compounding temperature of 190 °C for 20 min. The temperature at which 5 wt.% degradation occurred was reported as the degradation onset temperature.

4.2.4.3 Scanning electron microscopy

Blend morphologies were observed using a JEOL JSM-840 scanning electron microscope. Samples were first hot-pressed at 200^{o}C for 3 min, then immersed in liquid nitrogen for 3 min before brittle fracture. The MCL PHA phase was etched in acetone overnight at room temperature.

4.2.4.4 Rheology

Compression molded discs, 25 mm diameter and 2 mm thick, were prepared using a Carver press. The linear viscoelastic properties were measured in the oscillatory mode using a stress controlled rheometer, Visco Tech from Reologica, under nitrogen purge. Frequency sweeps were conducted at 190 °C using a cone and plate fixture having 25 mm diameter and 2° angle, at a frequency range between 1-100 rad/s. This range was chosen to limit the duration of the experiment to 100 s, given the sensitivity of PHB to degradation. Time sweeps were conducted at a frequency of 6.28 rad/s and temperatures ranging from 135 to 155 °C to obtain cure curves for the cross-linked PHO formulations.

4.2.4.5 Mechanical properties

The compounded materials were pre-dried in a vacuum oven at room temperature overnight. Specimens for mechanical property characterization were prepared by compression molding using a Carver press under 5000 N force, at 200 °C and a residence time of 3 min, then quenched in cold water. All specimens were conditioned at room temperature for 48 h after compression molding, prior to mechanical testing. Tensile tests were conducted in accordance with ASTM D638 using standard type V test specimens, with an Instron 3369 Universal tester, at a cross head speed (CHS) of 5 mm/min. The average of five measurements is reported. Un-notched Izod impact tests were conducted in accordance with ISO 180 using standard specimens on a SATEC Instron machine and the average of five specimens are also reported.

4.3 Results and discussion

4.3.1 Thermal and rheological properties

Thermal degradation is an important concern when processing PHB. The isothermal TGA curves (Figure 4.1) show that under nitrogen atmosphere PHB started to degrade at times longer than 10 min at the compounding temperature of 190 °C. Based on the TGA data, PHO had better thermal stability than PHB and its addition to PHB improved the thermal stability of the blend. The by-product of PHB degradation is mainly *trans*-2-butenoic acid [86], whereas the products of PHO degradation would be a mixture of *trans*-2-octenoic and *trans*-2-hexenoic acids. The presence of different decomposition products may affect the degradation kinetics of the mixture.

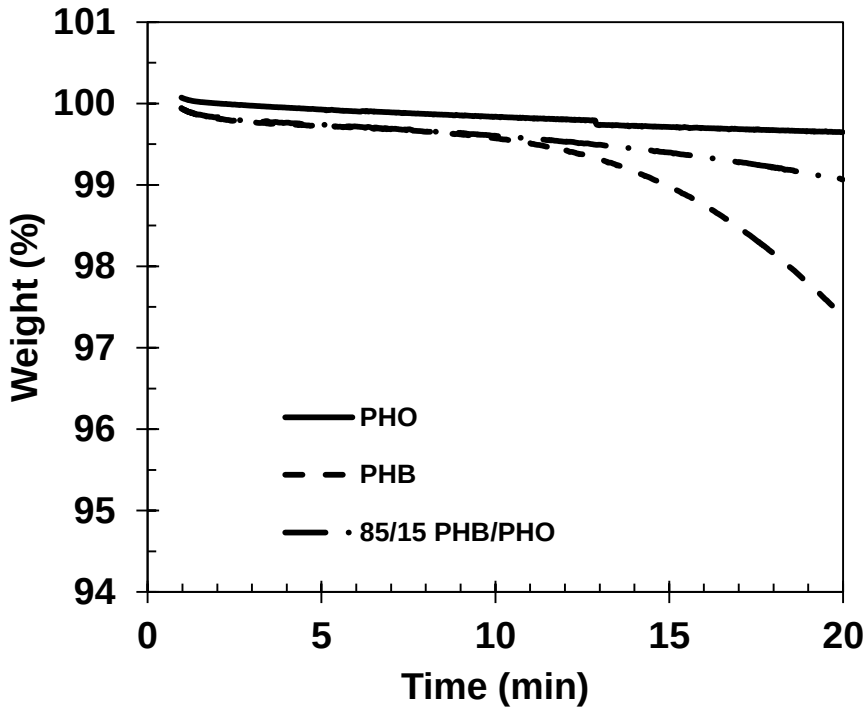

Figure 4.1 TGA curves for PHO, PHB and the 85/15 PHB/PHO blend at 190 °C

Table 4.1 summarizes the degradation onset temperatures of the blends in non-isothermal experiments. Addition of PHO gradually increased the degradation onset temperature of the blends. The shift in temperature was as high as 20 °C for the blends containing 30 wt.% PHO. Figure 4.2 shows the DSC thermograms of PHB and PHB/PHO blends. The first heating cycle of the PHB showed a single melting peak at 181 °C and a corresponding crystallinity of 66%. A double peak appeared during the second heating cycle (Figure 4.2a). The first melting peak at the lower temperature (171 °C) corresponds to crystals formed at the crystallization temperature and the second one at 177 °C is due to crystals that form during the heating cycle [83,87,88]. The upper peak is generally attributed to the presence of more stable crystals that

are favoured when unstable crystals melt and reorganize during the heating scan at slow cooling rates, such as the ones employed in DSC [88].

Table 4.1 Crystallization temperature (T_C), first and second melting peaks (T_{M1} and T_{M2} respectively), % crystallinity and degradation onset temperature for PHB and PHB/PHO blends.

PHB/PHO (wt.%/ wt.%)	T_C (°C)	T_{M1} (°C)	T_{M2} (°C)	Crystallinity (%)	Degradation onset temp (°C)
100/0	101	171	177	64	254
95/5	97	171	177	58	261
90/10	91	173	178	55	261
85/15	96	172	178	53	264
80/20	87	172	177	53	273
70/30	78	169	177	45	277

The relative magnitude and position of these peaks generally depends on the heating rate [89], and the blend composition [23]. In the present study, the high temperature endotherm became more prominent as the PHO content increased, suggesting that crystals that formed during the heating cycle were favored at higher PHO content. Moreover, as the amount of PHO was increased in the blend, the PHB crystallization peak shifted to lower temperatures (Figure 4.2b), suggesting that the PHB crystalline structure is affected in the presence of PHO.

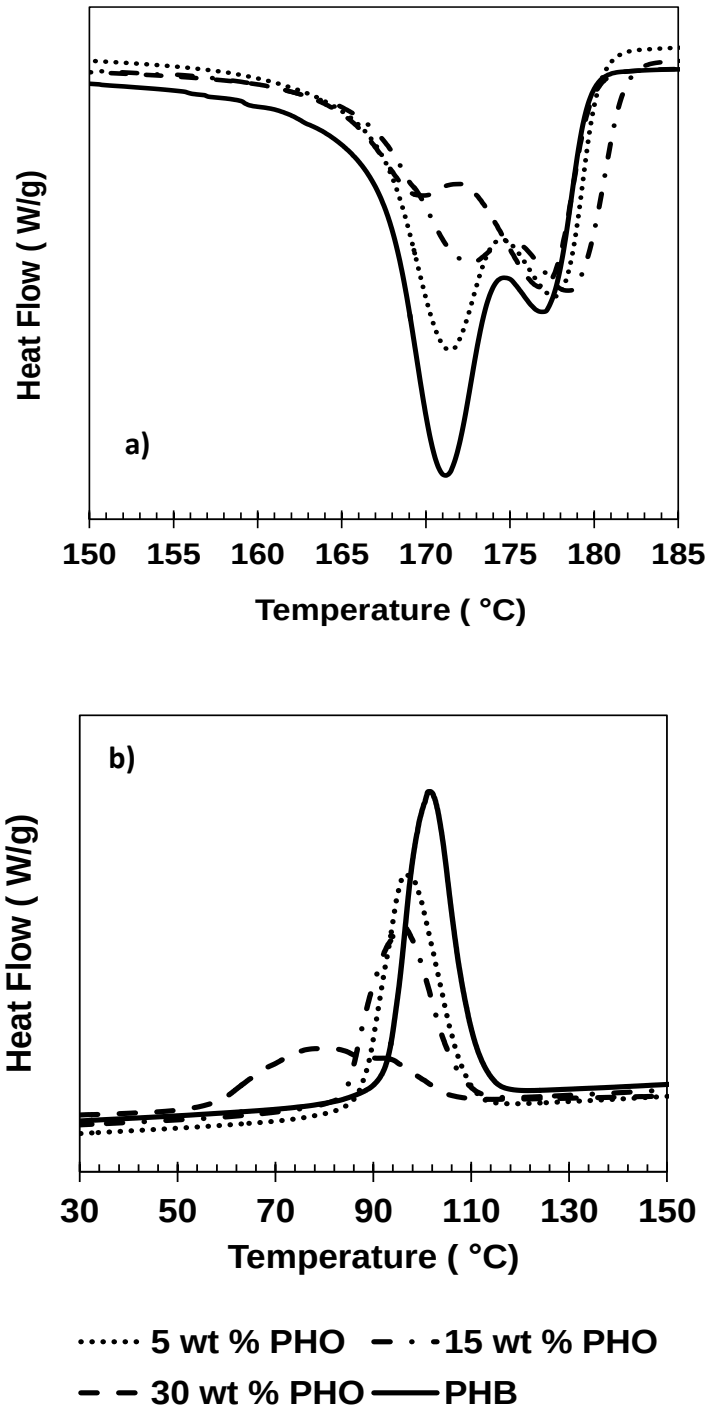

Figure 4.2 a) DSC endotherm (2nd heating cycle) and b) DSC exotherm of PHB and PHB/PHO blends

The PHO had very low crystallinity. A first heating cycle revealed a T_g of -36 °C, melting temperature of 63 °C and crystallinity of 15 %. Given its very low crystallization rates, PHO did not crystallize during the cooling cycle, therefore the second heating cycle was entirely featureless and is not shown in Figure 4.2. Addition of PHO to PHB resulted in a gradual decrease in the heat of fusion, resulting in decreased crystallinity, as shown in Table 4.1. This is a common phenomenon when an elastomeric material is added to a semi-crystalline one, and has also been noted when PHB was blended with amorphous polymers [81].

The linear viscoelastic properties of PHB and PHO are summarized in Figure 4.3. Both polymers exhibited Newtonian behavior, with no shear thinning over the frequency range investigated, as shown in Figure 4.3a. A large viscosity mismatch between the two polymers at the compounding temperature was noted, with PHB being significantly more viscous. This is obviously attributed to the differences in the molecular weight (172,000 Da and 1,416,000 Da for PHO and PHB respectively). The viscosity ratio, $\lambda = \eta_d/\eta_m$, (where η_d is the viscosity of the dispersed phase and η_m is the viscosity of the matrix) is very low, about 0.03 and affects negatively the dispersion of the dispersed phase within the matrix, as discussed in the following section.

4.3.2 Morphology

The PHB/PHO blends had droplet-matrix morphology, typical of immiscible polymer blends, as seen in the SEM images (Figure 4.4). The PHO domains were well dispersed within the PHB matrix at low PHO content, but as the level of PHO was increased, the domain sizes became larger and the morphology deteriorated. At 30 wt.% PHO, the coalescence of the dispersed

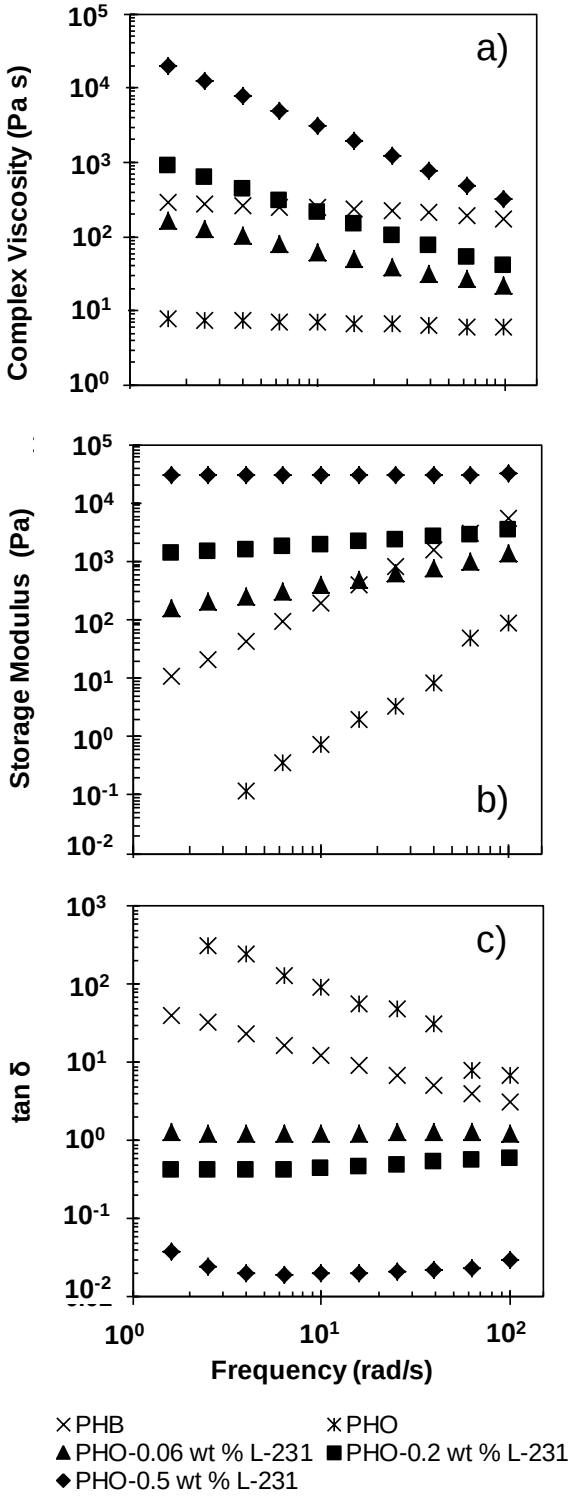

Figure 4.3 Rheological properties of PHB and PHO and effect of peroxide cross-linking on a) complex viscosity, b) storage modulus and c) loss tangent, tan δ, measured at 190 °C

phase resulted in a very coarse structure. As explained above, the tendency for coalescence may be attributed to the significant viscosity mismatch between the two blend components. Better morphology was reported in solution blending of PLA and PHO having similar viscosities [9]. However viscosity is not a factor during solution blending, therefore the results are not directly comparable.

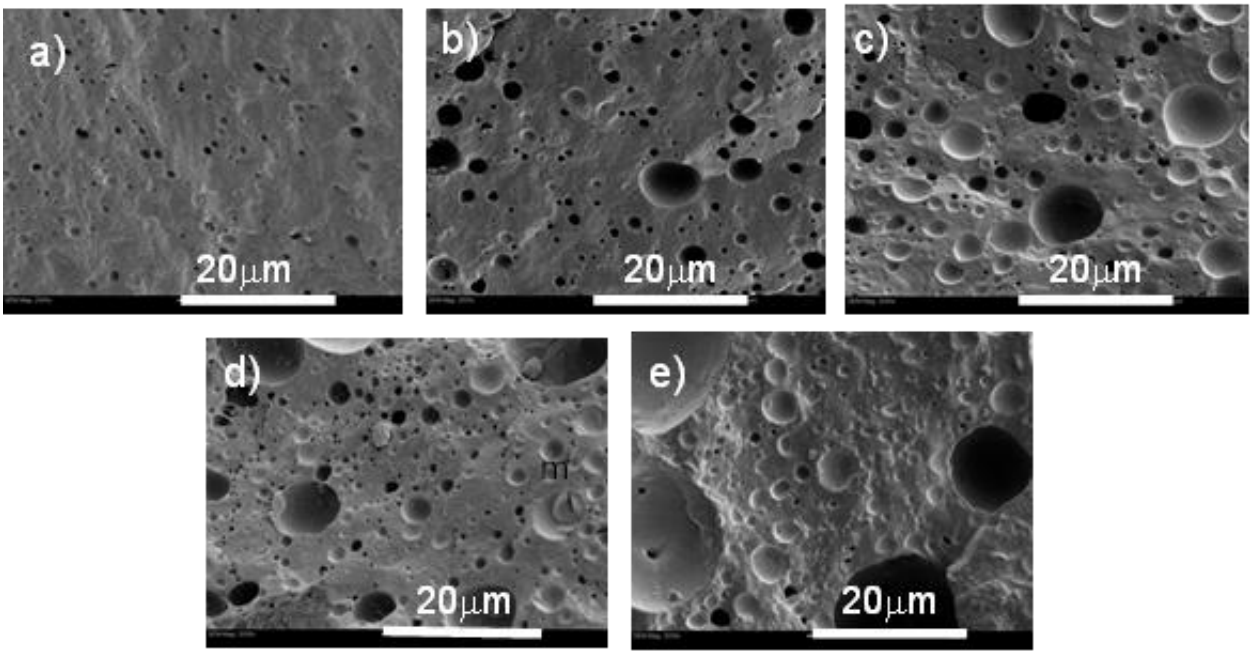

Figure 4.4 Scanning electron microscopy blends containing a) 5 wt.%, b) 10 wt.%, c) 15 wt.%, d) 20 wt.% and e) 30 wt.% of PHO at 2000x magnification

4.3.3 Mechanical properties

The tensile strain increased with the PHO content (Figure 4.5a). Considerable enhancement was observed above 15 wt.% PHO, indicating improved flexibility of the blends. At 30 wt.%, there was a decline in tensile strain. At this high PHO content, the PHO domains coalesced (Figure 4.4) and the deterioration in morphology caused the tensile strain to decrease. The un-notched impact strength of the blends improved by only 50% when 20 wt.% PHO was added, but

increased by 150% with 30 wt.% PHO compared to pristine PHB. On the other hand, the tensile stress and the Young's moduli decreased, as shown in Figure 4.5b. The decrease in tensile stress is typical of impact modification and can be justified by the decrease in crystallinity with the addition of PHO in the blend and the introduction of a softer component in the blend. Improvements in the strain at break, and a decrease in Young's modulus and tensile strength have been reported in PHB-HV/MCL PHA blends prepared by solution blending [84]. However in these blends MCL PHA contents above 5 wt.% led to phase separation and a decrease in strain at break. The results outlined above suggest that addition of PHO to PHB reduced the crystallinity of the blend, and moderately increased impact and elongation, which were counteracted by a decrease in the modulus. These are the expected results of impact modification. The extent of impact modification however remains limited, due to the coarse morphology, especially at high loadings which is attributed to the viscosity mismatch between the blend components, attributed to the very low viscosity of PHO.

4.3.4 Cross-linking of PHO

Chain extension of PHO through chemical cross-linking was employed, in an attempt to increase the viscosity of the dispersed phase to attain a more favourable viscosity ratio. Cross-linking of MCL PHAs can be achieved using peroxides, radiation, or sulfur cures. Gagnon et al. [90] cross-linked saturated and unsaturated MCL PHAs using four different types of peroxide with and without coagents. They found that cross-linking decreased the crystallinity of the polymer. Reduced tensile and tear strength was observed as a result of chain scission. Sulfur vulcanization was also used by Gagnon et al. [17], whereas Dufresne et al. [91] cross-linked MCL PHA by irradiation.

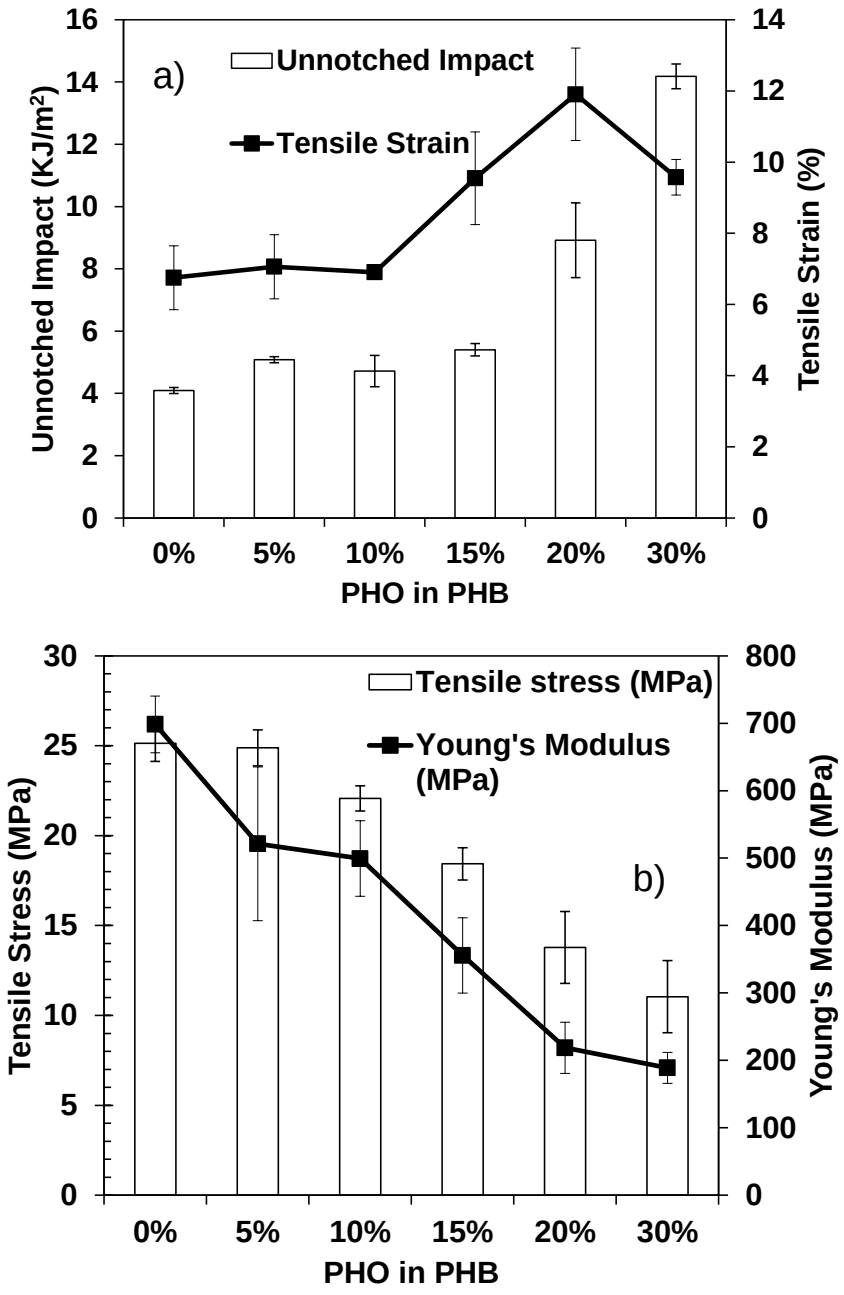

Figure 4.5 a) Un-notched impact strength and tensile strain b) tensile stress and Young's modulus of pristine PHB and its blends

In this work, given the sensitivity of the polymers to temperature, lauroyl peroxide was used, because it decomposes at relatively low temperatures. A series of time sweeps were conducted at various temperatures using the rheometer to generate a series of cure curves shown in Figure 4.6. Based on these data, 155 °C was chosen for the cross-linking reaction, aiming for the shortest possible reaction time.

Figures 4.3a-c show the effect of cross-linking on the linear viscoelastic properties of PHO. Addition of peroxide increased significantly the complex viscosity and storage modulus of PHO, whereas the loss tangent, tanδ, decreased below 1, revealing a transformation from viscoelastic liquid to a viscoelastic solid.

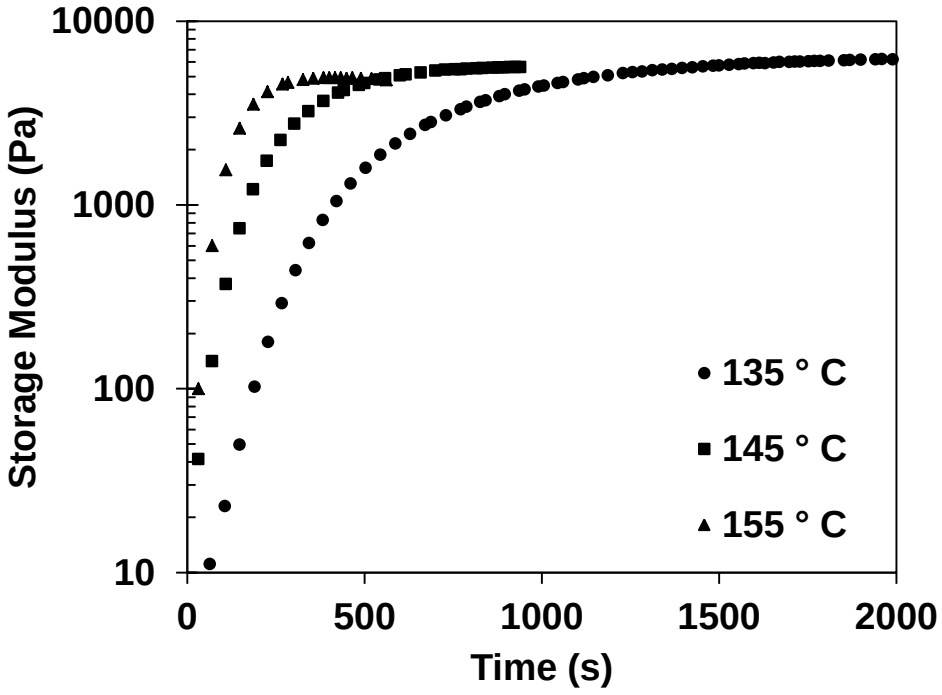

Figure 4.6 Cure curves of PHO with 0.1 wt.% lauroyl peroxide as a function of temperature at a frequency of 1 Hz.

A peroxide content of 0.06 wt.% was sufficient to achieve 67 wt.% gel content in the cross-linked PHO, resulting in a tanδ value of about 1. Further increases in peroxide to 0.2 and 0.5 wt.% resulted in almost fully gelled material with gel contents of 87 and 97% respectively.

It should be noted that cross-linking resulted in a significant drop in the crystallinity of PHO, as recorded from the 1st heating cycle, from 15 to 7% with 0.2 wt.% Lauroyl peroxide, whereas the fully cross-linked PHO was completely amorphous.

The increases in viscosity upon cross-linking were accompanied by a substantial increase in shear thinning behavior, and loss of the Newtonian plateau, as expected for cross-linked polymers having high cross-link densities. Given the change in the viscosity-shear rate dependence, cross-linked PHA can only match the viscosity of PHB in a very narrow frequency/shear rate range. Based on the data of Figure 4.3, in order to match the viscosity of PHO in the shear rate range of 10-100 s^{-1}, which is relevant to compounding, 0.2-0.5 wt.% of peroxide is needed.

The morphology of the blends containing 30 wt.% PHO cross-linked with different amounts of lauroyl peroxide is compared to that of the unreacted blends in Figure 4.7. The corresponding viscosity ratios, calculated at a representative shear rate of 50 s^{-1} from Figure 4.3a are shown in the caption of Figure 4.7. The dispersed PHO domain size became progressively smaller upon increasing the amount of cross-linking (Figure 4.7b and 4.7c). Significant improvement in morphology was seen upon addition of 0.2 wt.% Lauroyl peroxide. It was impossible to assess the domain size in the blends containing PHO cross-linked with 0.5 wt.% Lauroyl peroxide, because the high gel content did not allow for etching and thus sufficient contrast (Figure 4.7d).

The improvement in morphology correlates well with the decrease in the viscosity ratio achieved by using the cross-linked PHO dispersed phase.

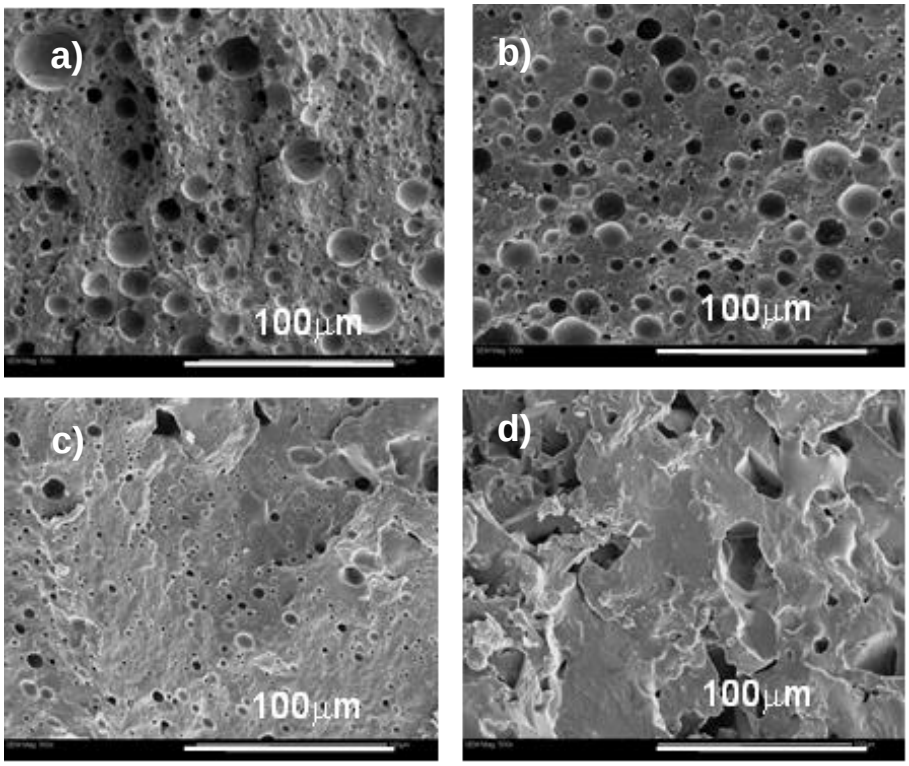

Figure 4.7 SEM of blends of PHB/cross-linked PHO 70/30 blends a) uncross-linked (viscosity ratio, λ=0.03) b) cross-linked with 0.06 wt.% of lauroyl peroxide (λ=0.15) c) cross-linked with 0.2 wt.% of lauroyl peroxide (λ=0.36) d) cross-linked with 0.5 wt.% of lauroyl peroxide (λ=3.73).

As shown in Table 4.2, there were significant improvements in the Young's modulus and strain at break of the blends containing cross-linked PHO, but the impact strength was unchanged. This may be due to the high cross-link densities and gel content of the cross-linked PHO, which alter its thermoplastic elastomer nature.

Table 4.2 Comparison of mechanical properties of PHB/PHO 70/30 blends containing uncross-linked and cross-linked PHO

PHB/PHO	Tensile stress (MPa)	Tensile strain at break (%)	Young's modulus (MPa)	Un-notched impact (KJ/m^2)
70/30	11.0 (±2.0)	9.6 (±0.5)	189 (±23)	14.2 (±0.4)
70/30 (0.2 wt.% lauroyl peroxide)	10 (±1.6)	14.4 (±0.3)	220 (±20)	13.3 (±1.4)
70/30 (0.5 wt.% lauroyl peroxide)	10.6 (±0.8)	14.5 (±0.4)	243 (±27)	14.2 (±0.5)

These results suggest that matching the viscosity of the blend components can result in finer morphology and improvements in the mechanical properties. However high cross-link densities and gel content of the cross-linked PHO, may present a limitation in terms of impact properties. Therefore tight control of the morphology, while avoiding the formation of excessive gels, is crucial to achieve desirable property improvements.

4.4 Conclusions

PHB/PHO blends had improved thermal stability, tensile strain at break and unnotched impact strength compared to the unmodified PHB. The ability of PHO to act as an impact modifier for PHB was limited by the viscosity mismatch between the two components, which resulted in a coarse blend morphology. Chain extension of PHO by peroxide cross-linking improved the

viscosity of PHO and led to better morphology and improved modulus and elongation at break of the blends.

Chapter 5 Dramatic improvements in strain hardening and crystallization kinetics of PLA by simple reactive modification in the melt state*

5.1 Introduction

Poly(lactic acid)(PLA) is a bioderived, biodegradable thermoplastic polyester [92], which can be processed using conventional thermoplastics processing equipment, including injection molding, blow molding, film casting and blowing [5]. However it has a very narrow processing window, because of the lack of melt strength and its slow crystallization rates. Additionally its poor engineering properties, including impact strength and heat resistance have mainly confined its applications to food packaging [38], as well as biomedical applications, such as drug delivery, where biocompatibility and biodegradability are desired [93]. The properties of PLA depend significantly upon its molecular weight and the stereochemical makeup of the backbone, which is controlled by polymerization with D-lactide, L-lactide, or D,L-lactide, to form random or block stereocopolymers [37]. Minimizing the amount of D-lactide is required to obtain PLA with higher crystallinity; however most commercial grades have low crystallinities and low crystallization rates, unless nucleating agents are used. The rheological properties of PLA depend on the molecular weight and molecular weight distributions, presence of branching, as well as its stereochemical makeup [94-98]. Strain hardening has been reported in melts containing a high molecular weight tail [94], and in amorphous PLA containing mixtures of the D and L isomers [96] at low temperatures, but otherwise it is generally accepted that commercially available linear PLA lacks the level of strain hardening, and therefore melt

*A version of this chapter is accepted. Nerkar, M., Ramsay, J.A., Ramsay, B.A., Kontopoulou, M. Macromolecular Materials and Engineering, accepted May2014.

strength, needed for normal processing operations. This restricts its processability in operations involving high stretch rates, such as film blowing, thermoforming, foaming etc. Given these shortcomings, approaches have been proposed to achieve chain extension and/or branching in PLA, with branching generally considered more beneficial [99]. Compared to the various synthetic routes that exist to synthesize branched PLA, methods that employ reactive modifications in the melt state are generally considered to be more convenient and industrially relevant. Various modification approaches to improve processability have been summarized by Pilla et al. [100] and Yu et al. [101]. These include chain extension in the presence of glycidol [46] and long chain branching via functional group reactions of pyromellitic dianhydride and triglycidyl isocyanurate [99]. Furthermore chain extenders, such as tris (nonylphenyl) phosphate, polycarbodiimide and multi-functional epoxy compounds have been used to counteract degradation in polyesters, such as PLA and to achieve chain extension [47,51,102,103].

Reactive extrusion of PLA using organic peroxides has been undertaken to increase the molecular weight, viscosity and melt strength with limited success, as the resulting branching is often counter-balanced by severe chain scission [52-54]. Radiation induced cross-linking in the presence of multi-functional coagents has been suggested as an alternative, but generally resulted in physical property reduction [104].

Peroxide-initiated reactive extrusion in the melt state, assisted by coagents is frequently employed as a means to introduce long-chain branching in linear polymers, such as polypropylene[105,106]. However there are only two reports, employing this approach in PLA. Yang et al. [107] used triallyl isocyanurate as a cross-linking agent together with dicumyl

peroxide (DCP), to obtain compounds with different levels of cross-linking. More recently, You et al. [108] reported that PLA prepared through reaction with DCP and pentaerythritol triacrylate (PETA) coagent had enhanced viscoelastic properties, which was attributed to branching. The resulting product had faster crystallization rates under isothermal conditions. However in these publications there was no mention about the properties of the resulting materials under uniaxial extension and the non-isothermal crystallization behavior of the polymers, which is relevant to processing, was not reported.

This chapter reports substantial improvements in the melt strength and non-isothermal crystallization kinetics, upon employing a simple chemical modification method in the melt state using solvent-free, peroxide-initiated grafting of a multi-functional coagent (triallyl trimesate, TAM). To the best of our knowledge this is the first time that simultaneous improvements in all these properties upon reactive modification are reported for PLA. These attributes are expected to enable use of these materials in operations such as foaming, injection moulding and film processing.

5.2 Experimental

PLA (grade 3251D, MFI 35 g/10 min at 190 °C/ 2.16 kg) was obtained from Natureworks®. TAM (98%, Monomer Polymer Inc.), dicumyl peroxide (DCP, 98%, Sigma-Aldrich), acetone (Sigma-Aldrich) and tetrahydrofuran (THF, Sigma-Aldrich) were used as received. Joncryl® ADR 4368 a multi-functional epoxide styrene-acrylic oligomeric chain extender, containing glycidyl methacrylate (GMA) functions was supplied by BASF. It has a functionality of 9 with epoxy equivalent weight 285 g/mol, and molecular weight 6,800 g/mol [51].

PLA was dried in a vacuum oven at 100 °C for 3 h to remove moisture. Peroxide-degraded PLA (PLA/DCP) was prepared by coating ground PLA powder (15 g) with an acetone solution containing DCP (0.045 g) and allowing the solvent to evaporate. The resulting mixture, containing 0.3 wt.% DCP, was charged to a DSM micro-compounder, equipped with twin-co-rotating screws, at 180 °C at 100 rpm for 6 min. Coagent-modified PLA was prepared as described for PLA/DCP from a mixture of PLA (14.8 g), DCP (0.045 g) and TAM (0.15 g), yielding PLA/TAM containing 0.3 wt.% DCP and 1 wt.% TAM. A compound containing 1.2 wt.% of GMA, which was the amount required to yield similar zero shear viscosity as the PLA/TAM was also prepared and used for comparison. Neat PLA was processed under the same conditions outlined above, to provide a suitable basis for comparison. After compounding, the strands were quenched in cold water before chopping into pellets for further characterization.

Samples were prepared for size exclusion chromatography (SEC) analysis by dissolving 10 mg of polymer in 1 mL of distilled THF overnight to ensure complete dissolution, and filtered through a 0.2 µm nylon filter. Polymer molecular weight distributions (MWD) were determined with respect to polystyrene standards using a Viscotek 270max separation module with triple detection by differential refractive index (DRI), viscosity (IV) and light scattering (low angle LALS and right angle RALS), which was maintained at 40 °C and contained two porous PolyAnalytik columns in series. Distilled THF was used as the eluent at a flow rate of 1 mL/min.

The linear viscoelastic properties were measured in the oscillatory mode using a stress controlled rheometer (Visco Tech by Reologica). Frequency sweeps were conducted at 180 °C using 20 mm parallel plates, under nitrogen purge. Samples were further characterized in uniaxial extension using an SER-2 universal testing platform from Xpansion Instruments hosted

on an MCR-301 Anton Paar rheometer. Measurements were conducted at 180 °C at Hencky strain rates ranging from 0.10 to 10 s^{-1}. The linear viscoelastic (LVE) oscillatory measurements obtained at 180 °C were used to calculate the LVE stress growth curve, η^+, and to check the consistency of the extensional measurements. The curve corresponding to $3\eta^+$ represents the LVE envelope in uniaxial extension, according to Trouton's law.

Differential scanning calorimetry (DSC) was conducted using a DSC Q 100 by TA Instruments. Samples were scanned between 0 and 200 °C at a heating rate of 5 °C/min. After the first heating, each sample was held isothermally at 200 °C for 3 min before cooling at rates between 2.5 and 20 °C/min, to determine the crystallization onset and peak temperatures according to ASTM D3418. The % crystallinity of PLA, was estimated using Equation (5.1)

$$X_c = \frac{\Delta H_m - \Delta H_{cc}}{\Delta H_{100}} \times 100 \qquad (5.1)$$

where ΔH_m is the apparent fusion enthalpy, ΔH_{cc} is the exothermic enthalpy that is absorbed by crystals formed during the heating scan and ΔH_{100} is the theoretical fusion enthalpy of a 100% crystalline polymer, which is 93.6 J/g for PLA [109].

Isothermal studies involved heating the sample to 200 °C and holding it for 3 min, followed by cooling at 50 °C/min to temperatures ranging from 135-155 °C, where they were held isothermally until completion of crystallization. The analysis included evaluations of the relative crystallinity as a function of time and standard Avrami kinetics [110].

5.3 Results and Discussion

5.3.1 Rheological characterization

The linear viscoelastic properties of neat PLA, PLA reacted with 0.3 wt.% DCP (PLA/DCP) and with 0.3 wt.% DCP/ 1 wt.% TAM (PLA/TAM) are summarized in Figure 5.1. PLA/DCP had essentially unaltered flow characteristics compared to the unmodified PLA (Figure 5.1a) and linear architecture, as revealed by the Van Gurp-Palmen plots of Figure 5.1b, tend to the limit of 90°. This suggests that peroxide-induced degradation was compensated by chain extension, without branching. This is corroborated by the minimal differences in the molar mass distributions between these two compounds (Table 5.1).

On the contrary, PLA/TAM demonstrated a substantial increase in molar mass (Table 5. 1) and melt viscosity (Figure 5.1a). It is well-known that solvent-free processing with multi-functional coagents involves simultaneous chain scission and cross-linking, the balance of which controls the molecular weight and branching distributions of the final product. In general, reaction with coagents bearing multiple acrylate, allylic or styrenic groups results in bimodal molecular weight and branched distribution, comprised of a linear chain population of relatively low molecular weight, and a high molecular weight hyper-branched chain population, which can progress above the gel point [56,111]. Furthermore it has been reported that systems containing polypropylene reacted with coagent and peroxide can undergo a precipitation polymerization, which results in the formation of a separate phase of highly cross-linked, coagent-rich sub-micron sized particles [56,112]. The resulting products possess a creamy appearance in the melt state, owing to the presence of these cross-linked nano-particles [56].

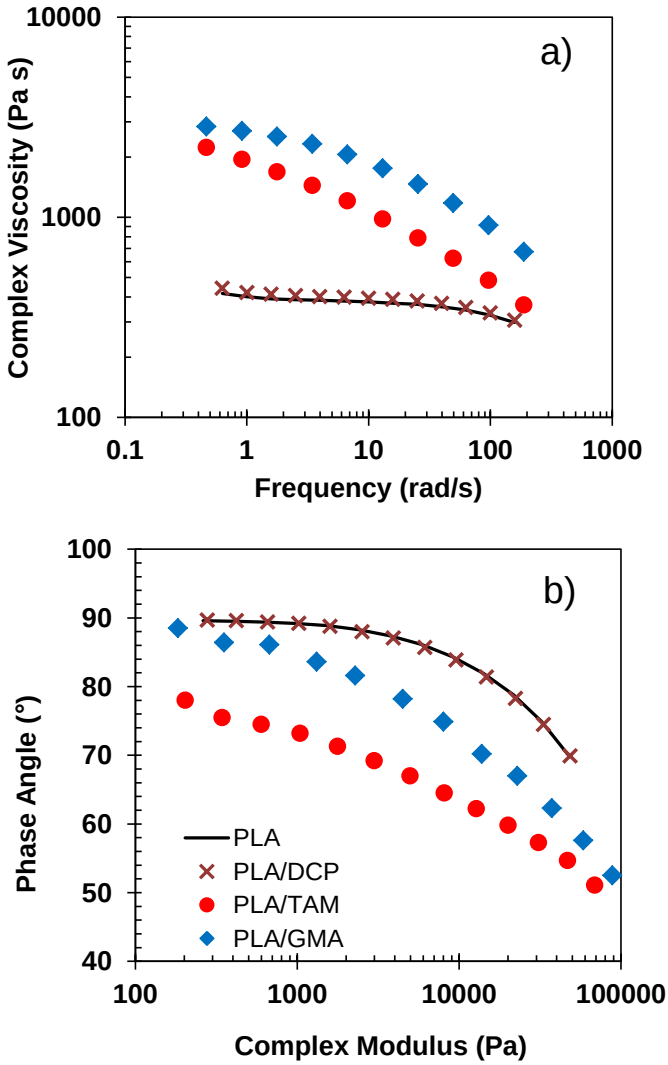

Figure 5.1 a) Complex viscosity as a function of frequency and b) phase degree as a function of complex modulus at 180 °C.

In the present case, treatment with 0.3 wt.% DCP and 0.1 wt.% TAM produced a creamy (as opposed to the transparent PLA and PLA/DCP), gel-free product with increased melt elasticity, and shear thinning, as observed in Figure 5.1, consistent with the presence of branching [57]. We compared the properties of PLA/TAM to those of PLA chain extended using a multi-

functional epoxide styrene-acrylic oligomeric chain extender, containing GMA functions (trade name Joncryl® from BASF).

Table 5.1 Material characterization

Material	**Mw**[a)]	**PDI**[b)]	T_M	T_C	$T_{C,onset}$	T_{CC}	**Crystallinity**
	[g/mol]		**[°C]**	**[°C]**	**[°C]**	**[°C]**	[%]
PLA	98,140	1.7	173	N/A	N/A	109	24
PLA/DCP	90,600	1.8	170	N/A	N/A	94	35
PLA/TAM	143,020	2.0	169	133	149[c)], 142[d)]	N/A	52
PLA/GMA	115,000	1.7	168	105	124[c)], 123[d)]	95	34

[a)]Mw: Weight average molar mass; [b)]PDI: polydispersity index; [c)]at cooling rate of 2.5 °C, [d)]at cooling rate of 5 °C.

The chain extended (PLA/GMA) was prepared by reacting PLA with 1.2 wt.% Joncryl®, which was the amount needed to match the zero shear viscosity of PLA/TAM. The epoxy functions contained within multi-functional epoxies can react with the –OH and –COOH end groups of PLA, resulting in random branching and/or cross-linking [51]. The low levels of Joncryl® used herein, produced a gel-free product with higher molar mass than the parent PLA (Table 5.1) increased viscosity and deviations from the terminal flow behavior (Figure 5.1).

The different shear thinning characteristics and shapes of the Van Gurp-Palmen plots of PLA/GMA compared to PLA/TAM point to different branching levels and chain topologies. PLA/TAM presumably contained small amounts of a hyper-branched population, which are characteristic of this coagent modification, whereas reaction with multi-functional epoxies

produces random branching. In spite of the different mechanisms of chain extension/branching, the ultimate strain hardening characteristics of PLA/TAM and PLA/GMA were very similar, as shown in Figure 5.2. Pronounced strain hardening was present in both materials, providing evidence of long chain branching. Note that the viscosities of the parent PLA and PLA/DCP were below the threshold needed to support extensional viscosity experiments.

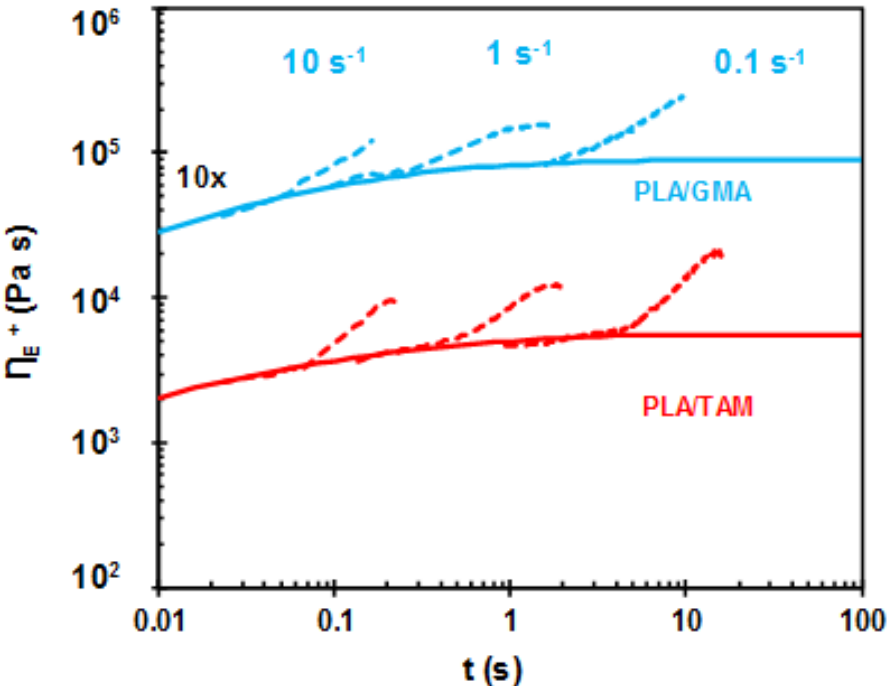

Figure 5.2 Tensile stress growth coefficient (η_E^+) of TAM and GMA modified PLA as a function of strain rate and time at Hencky strain rates of 0.1, 1 and 10 s^{-1} at 180 °C. Curves are shifted by an arbitrary factor for the sake of clarity. Solid lines represent the LVE envelop ($3\eta_E^+$) for each sample.

5.3.2 Thermal properties

Detailed DSC data are presented in Table 5.1 and Figure 5.3. The glass transition temperature (T_g) of PLA was 62 °C and remained unchanged in all modified materials. PLA had a cold crystallization peak, T_{cc}, at 109 °C, a melting peak, T_M, at 173 °C (Table 5.1 and Figure 5.3a). PLA/DCP had reduced cold crystallization temperature and increased crystallinity. These findings are commonly associated to PLA degradation [51,108]. Neither of these two materials crystallized during the cooling cycle.

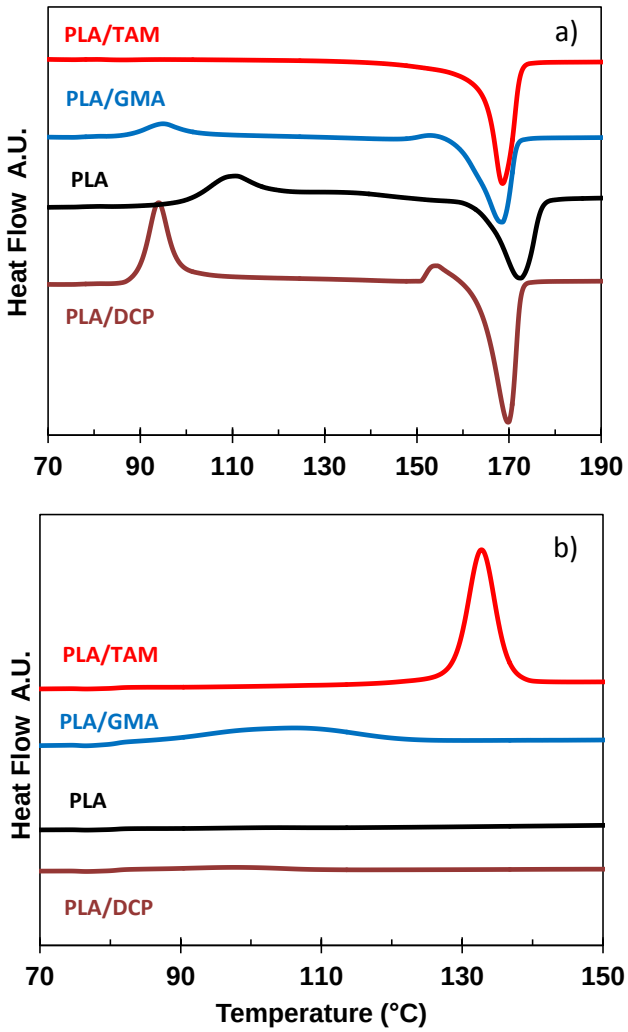

Figure 5.3 DSC a) 2nd heating scan at rate of 5 °C/min b) cooling scan at the rate of 5 °C/min

On the contrary, the branched PLAs showed exothermal crystallization peaks. PLA/GMA had a weak crystallization peak, T_C, around 105 °C, suggesting a moderate effect of this modification on the ability of the chains to crystallize. On the other hand, coagent modified PLA had a clear and sharp crystallization peak at 133 °C (Figure 5.3b). This was accompanied by the disappearance of the cold crystallization peak, and a significant increase in crystallinity by 117 % with respect to neat PLA and 50 % with respect to PLA/DCP. Even though changes in the cold crystallization of PLA upon modification with a PETA coagent have been mentioned previously [108] this is the first time that the presence of an exothermic crystallization peak arising during the cooling cycle, which is indicative of the capability of the material to crystallize upon cooling during normal polymer processing operations, is reported.

The ability of our modified materials to crystallize was evident not only by the appearance of an exothermic crystallization peak, but also by their isothermal and non-isothermal crystallization kinetics (Figure 5.4). The PLA and PLA/DCP formulations did not crystallize and therefore are not included in this comparison. Plots of the evolution of relative crystallinity as a function of time revealed a crystallization half-time ($t_{1/2}$) of 9.3 min at 135 °C for PLA/GMA, whereas the half-time of PLA/TAM at this temperature was only 0.6 min. The results of the Avrami analysis for temperatures ranging from 135-155 °C are presented in Table 5.2. The Avrami exponents suggest similar crystal growth habit in all cases. Introduction of branching in polymers such as polypropylene has been associated previously to changes in the crystallization kinetics [113]. The relative crystallinity as a function of time, recorded during non-isothermal crystallization experiments is shown in Figure 5.4b. While cooling from the melt state, PLA/TAM started to

crystallize significantly earlier, with $t_{1/2}$ of 2.6 and 1.8 min at cooling rates of 2.5 and 5°C/min respectively, as compared to 8.4 and 3.9 min for PLA/GMA.

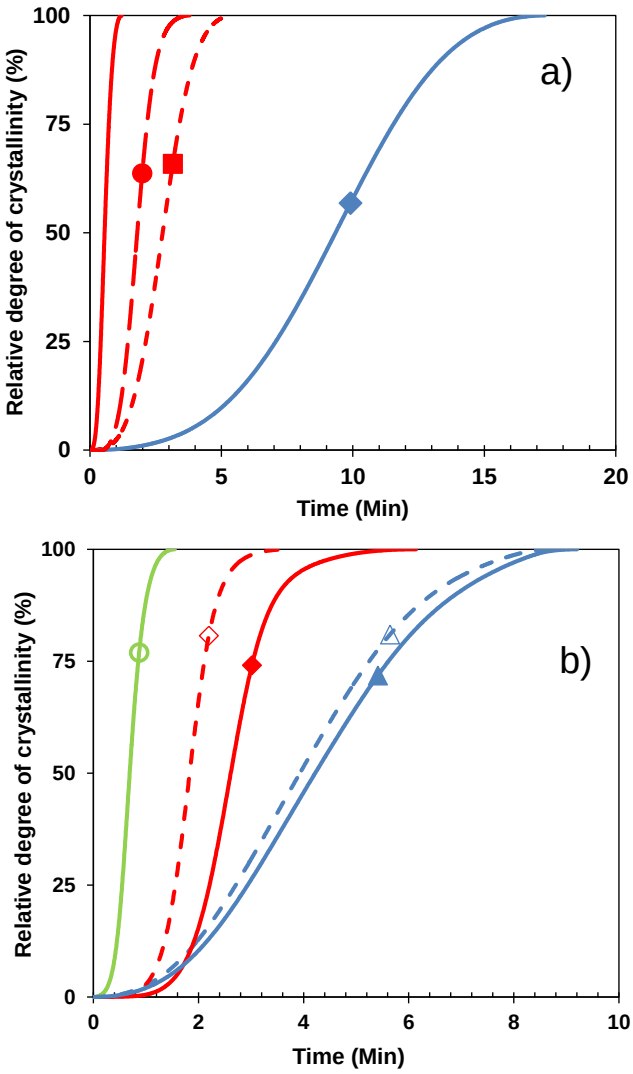

Figure 5.4 Relative degree of crystallinity as a function of time a) isothermal crystallization experiments; (-) PLA/TAM at 135 °C, (●)PLA/TAM at 140 °C, (■)PLA/TAM at 150 °C, (◆) PLA/GMA at 135 °C and (b) non-isothermal crystallization experiments; (◇)PLA/TAM at 2.5 °C/min, (◆)PLA/TAM at 5 °C/min, (o)PLA/TAM at 20 °C/min, (△)PLA/GMA at 2.5 °C/min, (▲)PLA/GMA at 5 °C/min

Furthermore PLA/TAM had $t_{1/2}$ of 0.96, 0.73 and 0.66 min at cooling rates of 10, 15 and 20 °C respectively, whereas PLA/GMA did not crystallize at these conditions.

Table 5.2 Isothermal Avrami constants and crystallization half time for PLA/GMA and PLA/TAM at various temperatures

	Temperature [°C]	**n**	**K [min^{-1}]**	**$t_{1/2}$ [min]**
PLA/GMA	135	2.9	0.0001	9.3
PLA/TAM	135	3.0	4.27	0.6
PLA/TAM	145	3.4	0.14	1.6
PLA/TAM	150	3.3	0.02	2.8
PLA/TAM	155	2.6	0.01	6.1

The findings reported above point to a nucleating effect, which occurred in spite of the absence of a nucleating agent. As explained earlier, a nucleating effect attributed to the formation of a separate phase of coagent-rich particles that forms upon reactive modification as a result of TAM oligomerization [55], was reported recently in coagent modified polypropylene. We suggest that a similar nucleation effect is responsible for the enhancements in crystallinity and crystallization rates in the reactively modified PLA/TAM product.

5.4 Conclusions

PLA with long chain branching was produced by a simple radical mediated peroxide-initiated grafting of TAM coagent in the melt state. The resulting product demonstrated strain hardening,

consistent with its long chain branched characteristics, and significantly enhanced crystallinity and crystallization rates, suggesting that this is a promising approach to enhance the processing characteristics and properties of PLA.

Chapter 6 Improvements in the extensional rheology, thermal properties and morphology of poly(lactic acid)/ poly-3-hydroxyoctanoate blends through reactive modification

6.1 Introduction

Among the key challenges associated with more wide-spread acceptance of biopolyesters, such as poly(lactic acid) (PLA) and polyhydroxyalkanoates (PHA) in engineering applications are their high production costs, brittle nature, slow crystallization rates and low melt strength, which restrict their processability under common polymer processing operations, as well as their hygroscopic nature, and susceptibility to degradation.

The advantages and drawbacks of PLA and PHAs as well as the current state-of-the-art of the various modification methods that have been employed to overcome their limitations have been reviewed recently [24,36,38,79,104,114]. Blending with ductile polymers and addition of plasticizers are commonly used to improve the properties and processability of PLA [36,114], and poly-3-hydroxybutyrate (PHB) [79,115]. Furthermore, to achieve fully bio-based formulations, blends of biopolymers have been studied extensively [79,80,116].

PHAs and their copolymers have been used to enhance the toughness of PLA through solution blending [117] or melt blending [117-119]. As already shown in Chapter 4, medium-chain-length (MCL) PHAs can serve as impact modifiers for PHB, due to their low crystallinity and elastomeric character [84,100,101].

To address the problem of lack of melt strength and suitable rheological properties of biopolyesters, reactive modifications in the melt state have been employed to achieve chain extension. Various modification approaches of PLA have been summarized by Pilla et al. [100],

and Yu et al. [101]. These include chain extension of PLA in the presence of glycidol [46] and introduction of long chain branching via functional group reactions of pyromellitic dianhydride and triglycidyl isocyanurate [99]. Furthermore chain extenders, such as tris (nonylphenyl) phosphite, polycarbodiimide and epoxy-functionalized oligomeric acrylic copolymer (trade name Joncryl® from BASF) have been considered to counteract degradation in PLA and introduce chain extension [47,102,103]. In-situ cross-linked hyperbranched polymers have been used to improve the toughness of PLA [120,121]. Reactive extrusion of PLA using organic peroxides and coagents has also been undertaken [52-54,104,107,108]. On the other hand, as discussed in Chapter 4, cross-linking of MCL PHAs can be achieved using peroxides, radiation, or sulfur cures [17,90,91].

Reactive blending of biopolyesters, such as PHB and polyhydroxybutyrate-co-valerate (PHBV) with polybutylene succinate (PBS) [31], and PLA with polycaprolactone (PCL) [122], PLA with PBS [123], PLA with Poly(butylene adipate-co-terephthalate) (PBAT) [124] and PHB [125] using peroxides has been employed to produce in-situ compatibilized blends having improved properties. Another proposed chemical modification involved blending of PLA with MCL-PHAs using diisocyanate chain extenders, which are highly toxic compounds [4]. Epoxy functionalities have been introduced in MCL PHA to react with the hydroxyl groups of PLA, thus increasing the interfacial interaction and improving the blend morphology and compatibility [117]. This approach was also tested in the present thesis (Appendix A) with limited success.

In chapter 5, we presented a simple reactive modification approach, utilizing solvent-free, peroxide-initiated grafting of a multi-functional coagent, to introduce branching and achieve substantial improvements in the strain hardening characteristics of PLA. This approach resulted

in faster crystallization kinetics, both under isothermal and under non-isothermal conditions. The present chapter investigates chain extension of PHO and PLA/PHO blends using the same approach. The properties of the reactively modified blends are compared to those of unmodified blends.

6.2 Experimental

6.2.1 Materials

Polyhydroxyoctanoate (PHO) containing ~98 mol% of 3-hydroxyoctanoate and ~2 mol% of 3-hydroxyhexanoate was produced from glucose and octanoic acid, using bacterial fermentation, as described by Xuan et al. [70,72]. The weight average molecular weight of the PHO, determined by triple-detector size exclusion chromatography (SEC), was 172,000 Da with a dispersity of 1.75 [126]. PLA (grade 3251D, MFI 35 g/10 min at 190 °C/ 2.16 kg) was obtained from Natureworks®. Triallyl trimesate (TAM, 98%, Monomer Polymer Inc.), dicumyl peroxide (DCP, 98%, Sigma-Aldrich), acetone (Sigma-Aldrich), and tetrahydrofuran (THF, Sigma-Aldrich) were used as received.

6.2.2 Compounding

PLA and PHO were dried in a vacuum oven at 100 °C and at room temperature respectively, to remove moisture. PLA/PHO blends containing 0-20 wt.% PHO were compounded in a DSM microcompounder at 180 °C for 3 min at a screw speed of 100 rpm. The compounder was operated under nitrogen blanket to limit polymer degradation. After compounding, the strands were quenched in cold water before chopping into pellets. The neat materials were compounded under the same conditions for comparison.

Peroxide-degraded PHO and PLA/PHO blends were prepared by coating ground PHO and PLA powders with an acetone solution containing DCP and allowing the solvent to evaporate. The resulting mixtures of PHO were charged to a DSM micro-compounder, equipped with twin-co-rotating screws, at 180 °C at 100 rpm for 6 min. Coagent-modified PHO and PLA reacted with DCP and TAM were prepared as described above from PHO or PLA, yielding various compositions containing 0.2-0.5 wt.% DCP and amounts of TAM ranging from 0.5-2 wt.%. Similarly coagent-modified PLA/PHO blends containing DCP and TAM were prepared. The various compounds are designated using the name of the polymer, followed by the amounts of DCP and TAM (i.e. PHO/0.3/1 denotes PHO reacted with 0.3 wt.% DCP and 1 wt.% TAM).

The gel content of coagent modified PHO and PLA/PHO blend was measured by dissolving the material in chloroform for 7 h. The polymer was sealed in stainless steel wire (120 mesh) according to ASTM D 2765. The material was left to stand for 1 h and subsequently dried overnight in a vacuum oven at room temperature. The % gel content was calculated using equation (6.1).

$$\text{Gel content} = \frac{\text{Final weight of sample}}{\text{Initial weight of sample}} \times 100 \qquad (6.1)$$

6.2.3 Characterization

6.2.3.1 Rheology

Compression molded discs, 25 mm diameter and 2 mm thick, were prepared using a Carver press. The linear viscoelastic properties were measured in the oscillatory mode using a stress controlled rheometer (Visco Tech from Reologica). Frequency sweeps were conducted at 180 °C using 20 mm parallel plates.

Reactively modified PLA/PHO blends were further characterized in simple uniaxial extension using an SER-2 universal testing platform from Xpansion Instruments hosted on the MCR-301 Anton Paar rheometer. Measurements were conducted at 180 °C at Hencky strain rates ranging between 0.10 and 10 s^{-1}. Specimens were prepared by compression molding the polymer samples between polyester films to a gauge of about 0.75 mm, using a hydraulic press. Individual polymer specimens were then cut to a width of 10 mm. Linear viscoelastic (LVE) oscillatory measurements obtained at 180 °C were used to calculate the LVE stress growth curve and check the consistency of the extensional measurements.

6.2.3.2 Differential scanning calorimetry (DSC)

DSC experiments were performed using a Q100 DSC from TA Instruments, under dry nitrogen. Since MCL PHAs crystallize slowly, the samples were preconditioned to eliminate their thermal history as follows: the polymer was heated at 100 °C for 10 min in a convection oven, and then kept at room temperature for two weeks before characterization. Samples weighing 10-12 mg were sealed in aluminum hermetic pans, equilibrated at -70 °C and kept isothermally for 5 min. Afterwards they were heated to 200 °C at a rate of 5 °C/min and held isothermally for 3 min before cooling to -70 °C at a rate of 5 °C/min. The samples were finally reheated to 200 °C at a rate of 5 °C/min. The % crystallinity of the polymers, X_c, was estimated using equation (6.2).

$$X_c = \frac{\Delta H_m - \Delta H_{cc}}{\Delta H_{100}} \times 100 \qquad (6.2)$$

where, ΔH_m is the enthalpy of fusion, ΔH_{cc} is the exothermic enthalpy (cold crystallization) recorded during DSC heating cycle and ΔH_{100} is the theoretical fusion enthalpy of a 100% crystalline polymer. The heat of fusion for 100% crystalline PLA is 93.6 J/g [109].

6.2.3.3 Heat deflection temperature (HDT)

Specimens (127 mm X 13 mm X 3 mm) were prepared by compression molding using a Carver press under 5000 N force, at 200 °C with a residence time of 3 min, then quenched in cold water. Specimens were lowered in a silicon oil bath and the temperature was raised from 23 ^{o}C at a heating rate of 120 ^{o}C/h. until 0.25 mm deflection occurred under a load of 1.82 MPa, in accordance with ASTM D 648. At least three specimens were tested and the average value was reported.

6.2.3.4 Mechanical properties

Specimens for mechanical property characterization were prepared by compression molding using a Carver press under 5000 N force, at 200 °C and a residence time of 3 min, then quenched in cold water. All specimens were conditioned at room temperature for 48 h after compression molding, prior to mechanical testing. Tensile tests were conducted in accordance with ASTM D638 using standard type V test specimens, with an Instron 3369 Universal tester, at a cross head speed (CHS) of 5 mm/min. The average of five measurements is reported. Un-notched Izod impact tests were conducted in accordance with ISO 180 using standard specimens on a SATEC Instron machine and the average of five specimens are reported.

6.2.3.5 Scanning electron microscopy

Blend morphologies were observed using a JEOL JSM-840 scanning electron microscope. Samples were first hot-pressed at 200 ^{o}C for 3 min, then immersed in liquid nitrogen for 3 min before brittle fracture. The MCL PHA phase was etched in acetone overnight at room temperature. The coagent modified blend samples were examined without etching as MCL PHA was partially cross-linked and could not be dissolved.

6.2.3.6 Hot stage microscopy

Isothermal crystallization experiments were performed using a Linkam CSS 450 hot stage mounted on an Olympus BX51 optical microscope. The sample was first heated to 200 °C at a rate of 30 °C /min and held for 10 min to eliminate the heat history. The melt was then cooled to 135 °C at 30 °C/min. The crystallization process was recorded isothermally at 135 °C using a Sony ExwaveHAD 3 CCD digital recorder.

6.3 Results and Discussion

6.3.1 Blends of PLA with PHO

PLA and PHO form an immiscible blend system, having droplet-matrix morphology at compositions up to 30 wt.% PHO, as shown in Figure 6.1. These blends have very coarse morphology, with the average dispersed domain size changing from 1.5 ($\pm$0.2) µm for 95/05 PLA/PHO blend to 5 ($\pm$0.6), 7 ($\pm$2) and 7.6 ($\pm$2) µm for 90/10, 85/15 and 80/20 blend respectively. This is consistent with the findings reported in Chapter 4 on PHB/PHO blends, and is attributed to the significant viscosity mismatch between the blend components. PLA and PHO had an almost Newtonian behavior, with viscosities of 660 Pa.s and 13 Pa.s for PLA and PHO respectively, at the compounding temperature of 180 °C, resulting in a viscosity ratio (defined as the ratio of the viscosity of the dispersed phase over the viscosity of the matrix) of 0.02. Generally viscosity ratios as close as possible to 1 are required to achieve optimum blend morphology, whereas viscosity ratios much higher or lower than 1 result in coarse morphologies and tendency toward coalescence during melt compounding.

Table 6.1 summarizes the mechanical properties of the blends. Significant improvement was observed in the elongation and impact properties, accompanied by a decrease in Young's modulus and tensile strength. The decline in these properties was associated with the decrease in crystallinity of the blend, which is expected because of the addition of an amorphous minor phase.

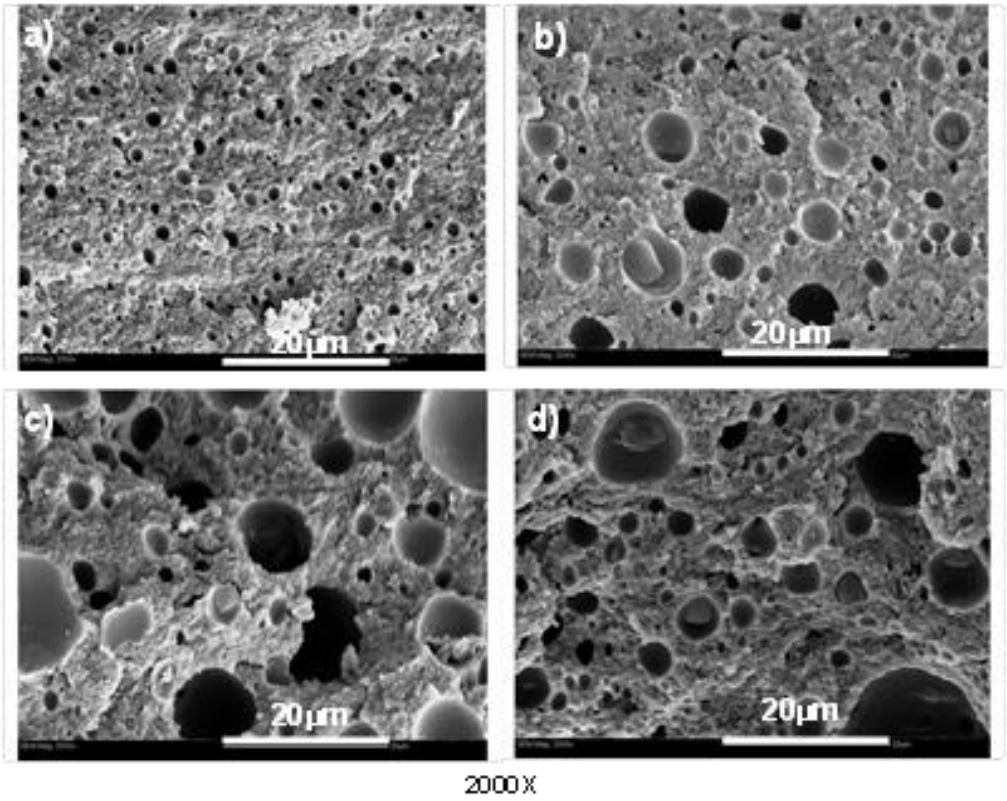

Figure 6.1 Scanning electron microscope images of PLA blend containing a) 5 wt.%, b) 10 wt.%, c) 15 wt.% and d) 20 wt.% of PHO.

From Table 6.1 it is obvious that the optimum levels of impact strength were obtained at compositions between 10 and 15 wt.% PHO, whereas the values decreased when higher

amounts were added. This is attributed to the morphology of the blend, which became much coarser at compositions above 10 wt.% PHO, as shown in Figure 6.1.

Table 6.1 Mechanical properties of PLA and PLA/PHO blends

PHO (wt.%)	Tensile stress (MPa)	Young's Modulus (MPa)	Elongation at break (%)	Unnotched Impact (KJ/m^2)	Crystallinity (%)
0	74 (±3)	670 (±74)	14 (±1)	32 (±5)	24
5	56 (±4)	582 (±68)	24 (±10)	63 (±6)	17
10	50 (±4)	696 (±29)	35 (±15)	65 (±5)	16
15	45 (±3)	571 (±22)	47 (±10)	53 (±9)	16
20	34 (±3)	442 (±34)	24 (±3)	40 (±5)	16

As mentioned in the previous chapters, low melt viscosities, viscosity mismatch and absence of melt strength are factors that make processing of biopolyesters and their blends difficult, resulting in a need for chain extension. In Chapter 4, we proposed peroxide-mediated cross-linking of the PHO dispersed phase to achieve higher viscosity, and therefore to improve the morphology of the blend. However, this approach produced high gel contents and limited property improvements in blends with PHB. A similar attempt at blending peroxide cross-linked PHO with PLA, shown in Appendix A, also resulted in limited success.

In the present chapter, a reactive modification procedure was implemented using peroxide and coagent, similar to the approach described in Chapter 5, to achieve branching and therefore

chain extension, while avoiding excessively high gel contents. The following sections describe the effects of coagent modification on PHO, PLA and PLA/PHO blends.

6.3.2 Reactive modification of PHO

PHO was reacted with various amounts of TAM and DCP, aiming in general at choosing formulations that would use the least amounts of reagents possible, while still achieving acceptable improvements in viscosity and elasticity, without excessive gel contents.

As shown in Figure 6.2, the flow characteristics of PHO remained unaltered when reacted with 0.3 wt.% DCP (PHO/0.3). The absence of changes in the presence of DCP is opposite to what was observed in Chapter 4, when lauroyl peroxide was used. This suggests that in the presence of DCP chain extension/cross-linking in the presence of peroxide is counteracted by significant chain scission, possibly because of the higher compounding temperatures needed for DCP compared to lauroyl peroxide.

When the multifunctional coagent, TAM, was added to the formulation, significant changes were noted in the rheological properties of PHO. Two distinct groupings are noted in Figure 6.2a. When TAM amounts up to 0.75 wt.% were added (sample PHO/0.3/0.75), the increase in complex viscosity was relatively small. On the contrary, addition of 1 wt.% TAM resulted in a pronounced increase in viscosity, shear thinning behavior, and elasticity. Above this level of TAM, the properties showed a tendency to plateau.

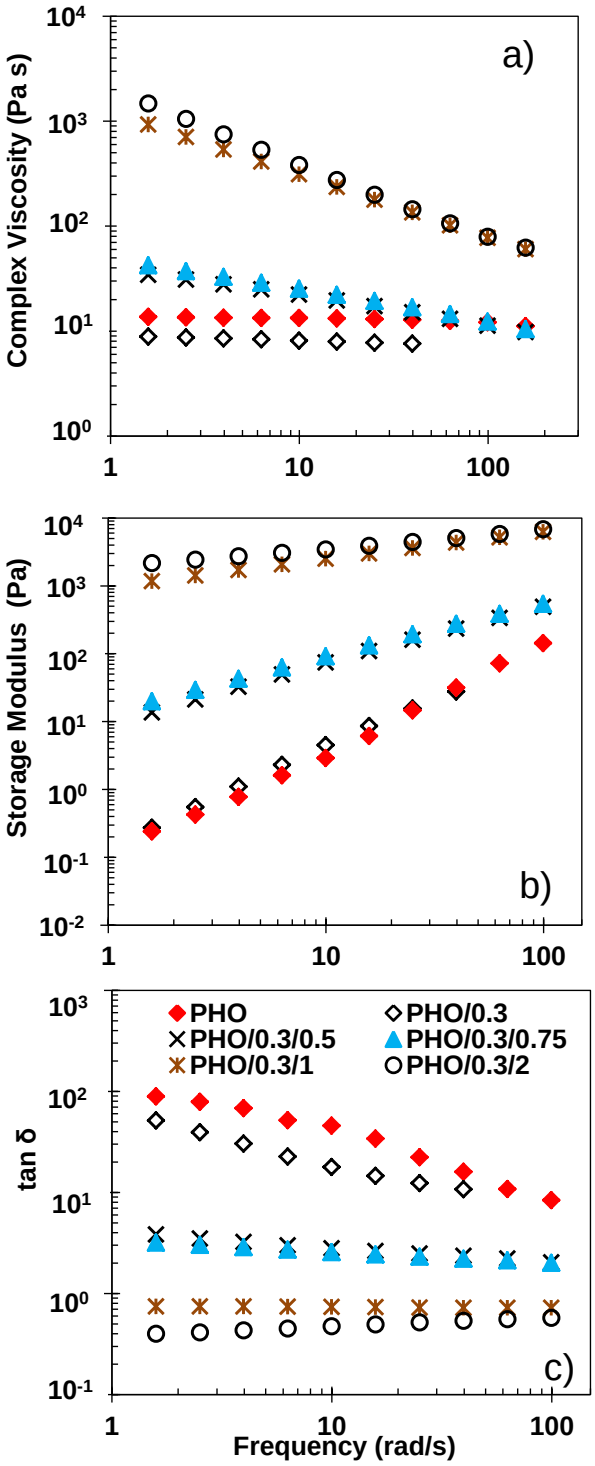

Figure 6.2 Effect of TAM content on the rheological properties of PHO with DCP content remaining constant a) complex viscosity b) storage modulus and c) tan δ

Reactive modification was accompanied by changes in the appearance of the extrudate. The PHO formulations containing low amounts of TAM were sticky and did not form strands when extruded. On the contrary, addition of 1 wt.% TAM resulted in the formation of strands that were not sticky and were easy to handle for further processing and characterization as shown in Figure 6.3.

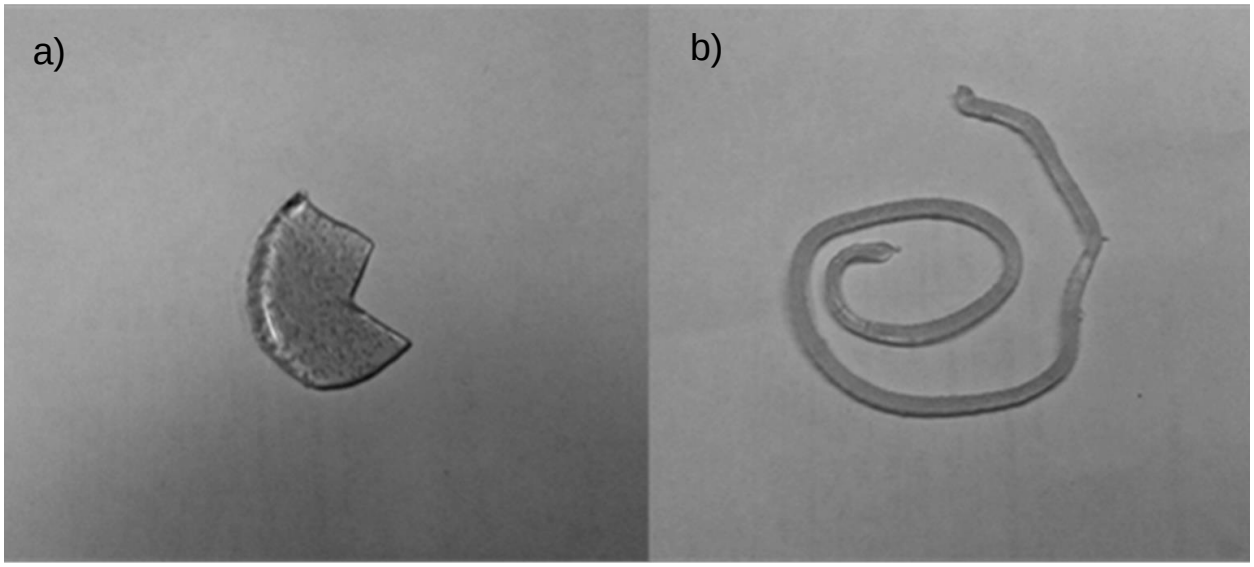

Figure 6.3 a) unmodified PHO after extrusion b) PHO/0.3/1 after extrusion

In an effort to achieve an optimum formulation, the amount of DCP was varied, while keeping the amount of TAM constant at 1 wt.% (Figure 6.4). From this figure, it is obvious that amounts of DCP above 0.3 wt.% were necessary to obtain significant improvements in complex viscosity and elasticity. However the material reacted with 0.5 wt.% DCP was highly cross-linked, with a gel content of 42 %. Based on the above results, the formulation containing 0.3 wt.% of DCP with 1 wt.% of TAM showed the best improvement in viscosity, while maintaining a moderate gel content of 23%.

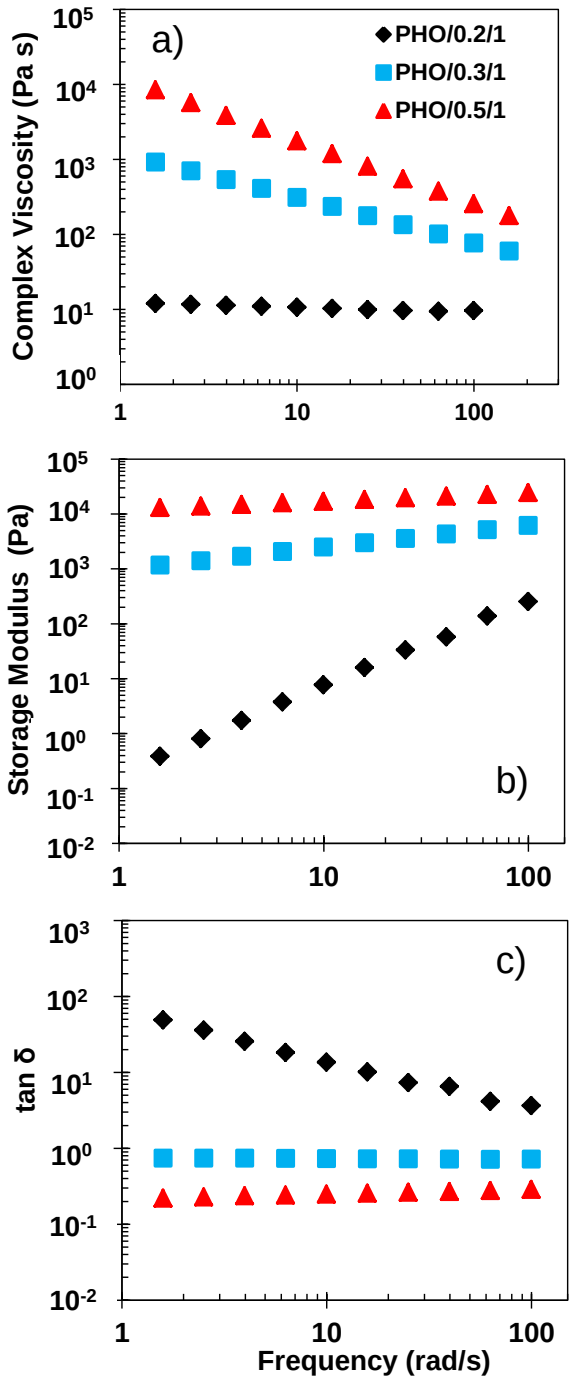

Figure 6.4 Effect of DCP amount on a) complex viscosity b) storage modulus and c) tan δ of coagent modified PHO (PHO 0.3/1 and PHO 0.5/1 yielded 23 and 42 % gel respectively)

In spite of the dramatic changes in the rheological properties, the thermal properties of the reactively modified PHO, including the glass transition temperature ($T_{g)}$ remained unaltered, whereas the material remained highly amorphous, with no obvious melting transition.

6.3.3 Reactive modification of PLA

The reactive modification of the PLA matrix to provide branched PLA has been described in detail in Chapter 5. Figure 6.5 shows the rheological properties of PLA reacted with two different amounts of coagent and comparison with PHO/0.3/1. The formulation reacted with 2 wt.% TAM had very high viscosity, and appeared fully crosslinked and hard to process. On the contrary, PLA/0.3/1 had negligible gel content, therefore this composition was deemed suitable for the blend compositions described in Section 6.3.3. below.

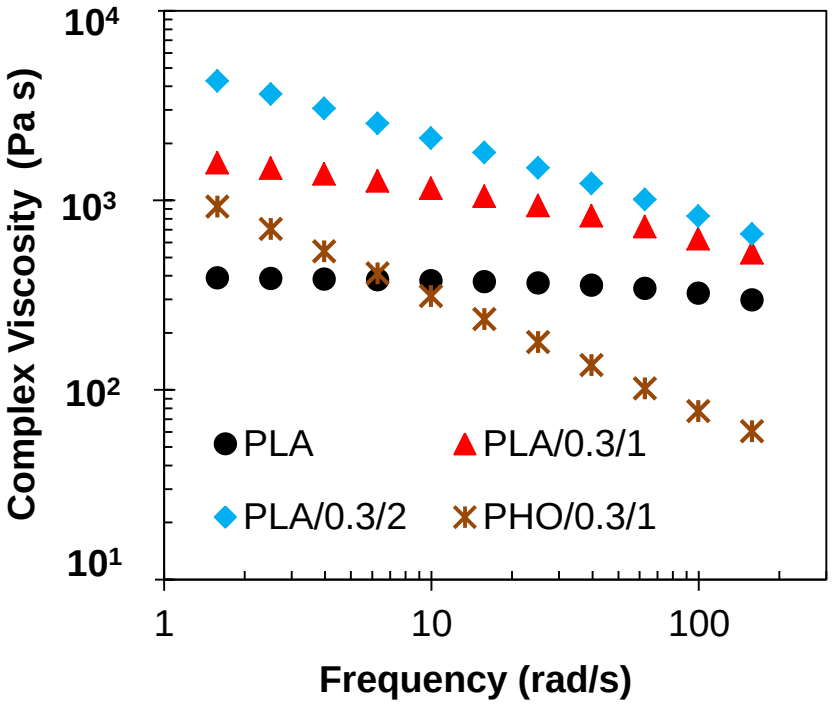

Figure 6.5 Effect of coagent modification on the complex viscosity of PLA and PHO

The extensional properties of the PLA/0.3/1 are summarized in Figure 6.6. As explained in Chapter 5, reactive modification resulted in substantial strain hardening, which provides solid evidence of a branched structure.

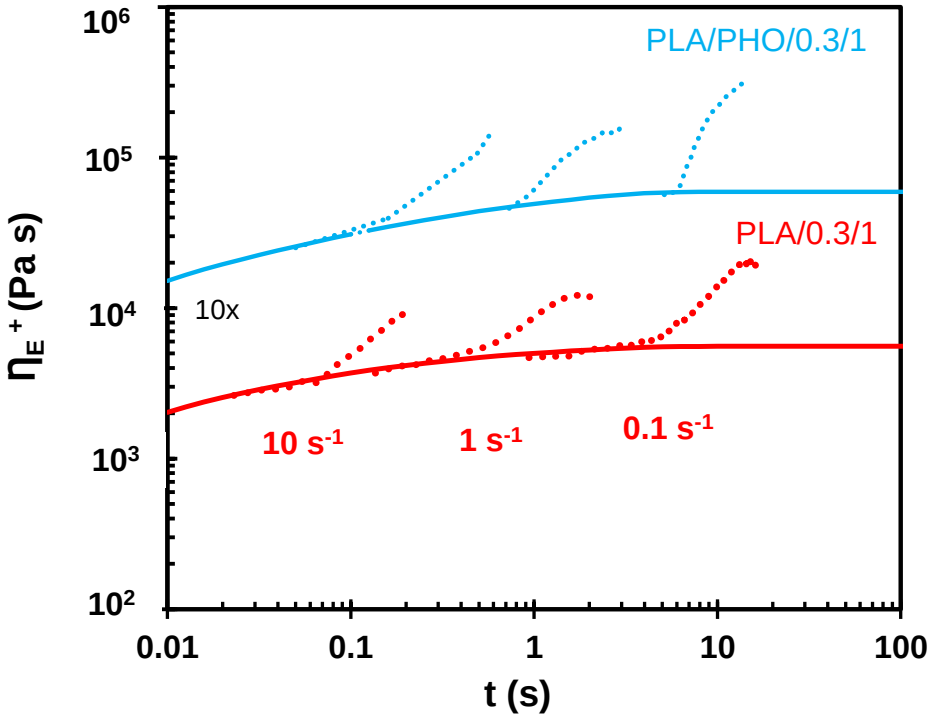

Figure 6.6 Tensile stress growth coefficient (η_E^+) of PLA/0.3/1 and (PLA/PHO)/0.3/1 as a function of strain rate and time at Hencky strain rates of 0.1, 1 and 10 s^{-1} at 180 °C. Curves are shifted by an arbitrary factor for the sake of clarity. Dotted lines represent the LVE envelop for each sample.

In addition to the enhancements in viscosity and strain hardening, the coagent modified PLA had substantially different thermal properties compared to the neat PLA, as shown in Table 6.2, including the appearance of a sharp crystallization peak in the DSC exotherm (Figure 6.7), disappearance of the cold crystallization peak and increase in crystallinity.

Table 6.2 Thermal properties of neat, DCP and coagent modified PHO, PLA and PHO/PLA blend

	T_M (°C)	T_C (°C)	T_{CC} (°C)	Crystallinity (%)
PLA	173	NA	109	24
PLA/0.3	170	NA	94	35
PLA/0.3/1	169	133	NA	52
PLA/PHO	170	NA	105	16
(PLA/PHO) /0.3	170	NA	104	17
(PLA/PHO) /0.3/1	169	138	NA	56

As reported in Chapter 5, the crystallization kinetics of PLA appeared significantly enhanced, both in isothermal, and non-isothermal experiments. This finding was attributed to the formation of a separate phase of coagent-rich particles that forms upon reactive modification, which results in a nucleating effect [55].

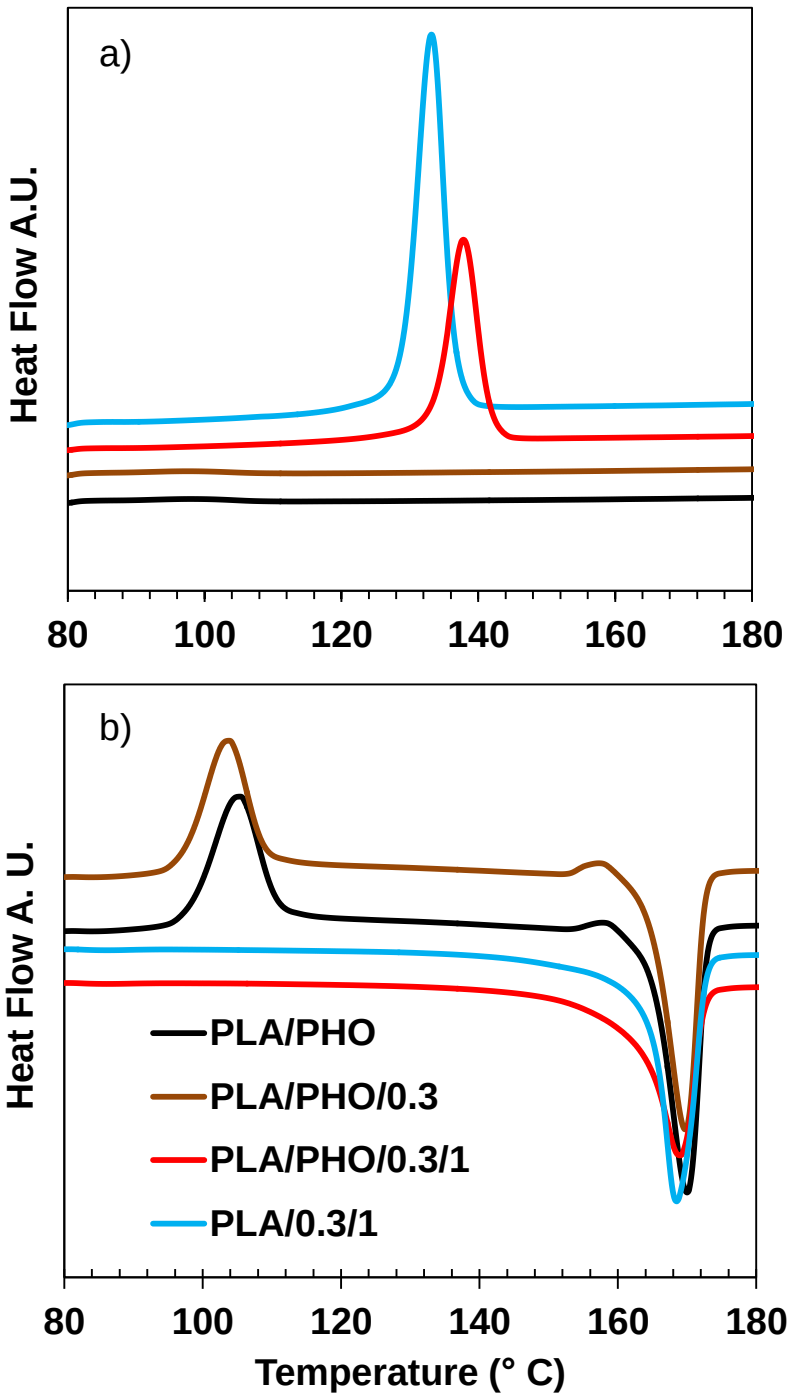

Figure 6.7 DSC (a) cooling exotherm (b) heating endotherm of coagent-modified PLA and PLA/PHO blends

Further evidence of the altered crystalline structure of these materials upon coagent modification is provided by the optical microscope images in Figure 6.8, which depict PLA and PLA/0.3/1 samples crystallized under isothermal conditions at 135 °C. The unmodified PLA did not show evidence of crystal structure formation when cooled for 5 min, whereas the coagent-modified sample is characterized by the formation of a dense spherulitic structure.

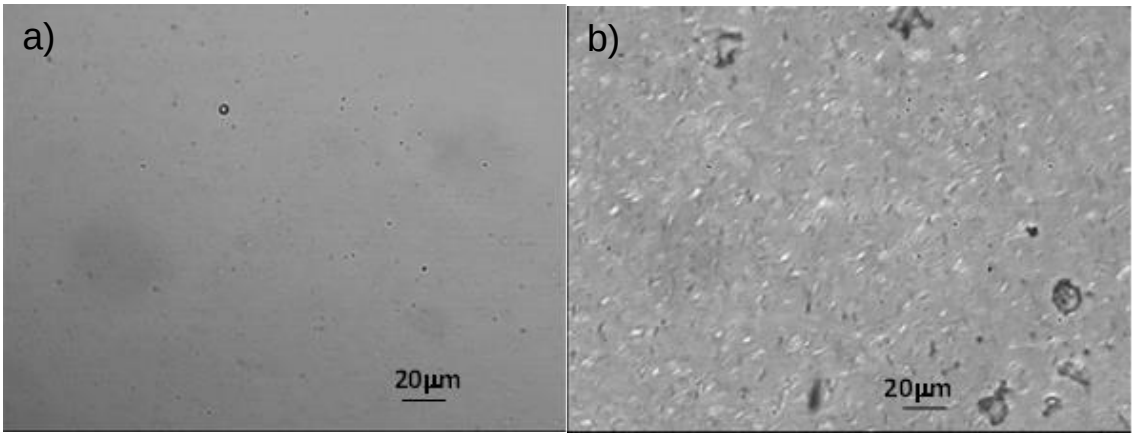

Figure 6.8 Hot stage microscopy of a) PLA, b) PLA/0.3/1 at 135 °C

The profound changes in the thermal and rheological properties of PLA are expected to have a major impact on the properties of reactively compounded blends of PLA with PHO, when PLA is the matrix phase. These blends are presented in section 6.3.4 – 6.3.7 below.

6.3.4 Reactive compounding of PLA with PHO

Based on the analysis presented in section 6.3.1, blends of PLA/PHO containing 10 wt.% PHO, were used as this was identified as the optimum composition in terms of mechanical properties. An additional reason for keeping the PHO content as low as possible is its high cost. For simplicity these blends will be noted below as PLA/PHO.

6.3.5 Thermal and rheological properties

Reaction of PLA/PHO blends with various amounts of peroxide and coagent resulted in similar trends as noted in the sections above, i.e. increase in the complex viscosity, loss of Newtonian plateau, increased shear thinning and elasticity of the blends. The values of all viscoelastic properties were in-line with those seen for the PLA matrix at equivalent contents (Figures 6.5 and 6.9), with what appears to be limited influence of the minor PHO dispersed phase. Similarly, the extensional stress growth data showed strain hardening behavior, following the same trends as those seen for the branched PLA matrix (Figure 6.6).

In agreement with the findings reported for the reactively modified PLA, the modified PLA/PHO showed a clear and sharp crystallization peak at 138 °C (Figure 6.7a). This was accompanied by the disappearance of the cold crystallization peak, and significantly higher crystallinities compared to the unreacted materials (Figure 6.7b). The thermal properties of all the reactively modified compounds and their unreacted counterparts are summarized in Table 6.2.

6.3.6 Blend morphology

Compounding of PLA and PHO in the presence of DCP alone, resulted in a significant reduction in the PHO domain size, as seen in Figure 6.10. The size of the PHO dispersed domains decreased from 5 ($\pm$0.6) µm to 1 ($\pm$0.2) and 1.2 ($\pm$0.2) µm when 0.5 and 1 wt. % of DCP was added. Since, based on the rheological evaluations presented above, DCP alone did not influence the rheological properties of the constituents of the blend, the most likely explanation for this observation is a compatibilizing effect in the presence of DCP. This could be attributed to the formation of small amounts of copolymer, by cross-termination of free radical chains of PLA and PHO during the compounding procedure. In-situ compatibilization by reactive

blending of biopolyesters through reaction with peroxides to produce blends with finer morphologies has been reported previously [17,123-125].

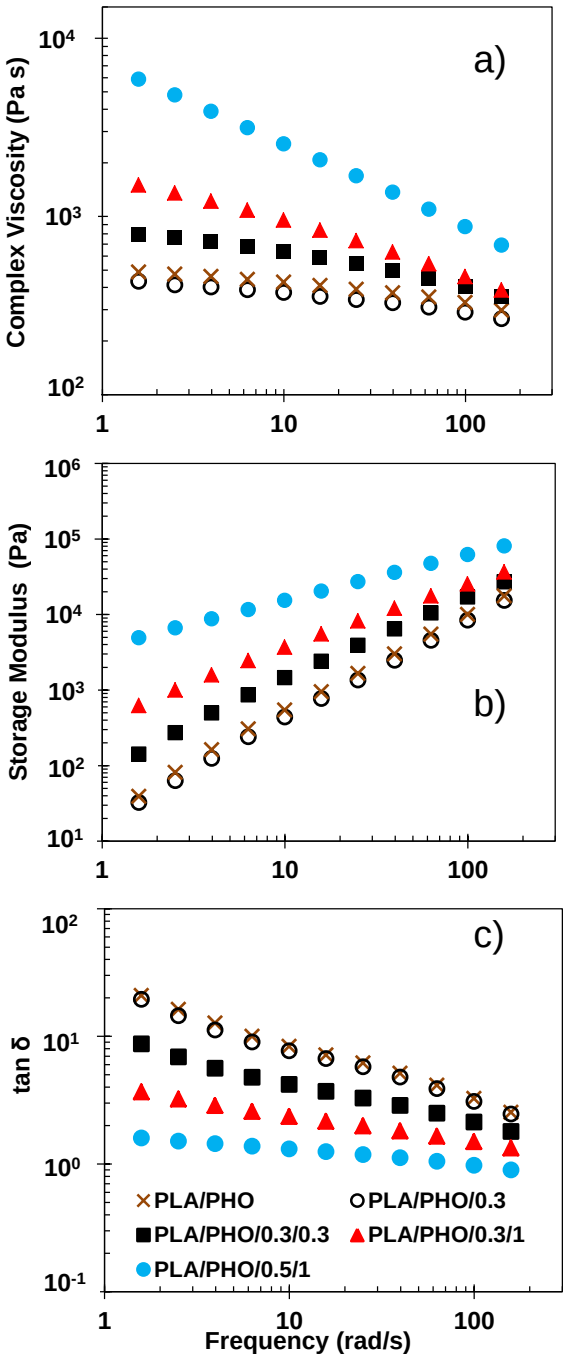

Figure 6.9 Effect of DCP and TAM on a) complex viscosity b) storage modulus and c) tan δ of PLA/PHO blends

Ma et al. [124,127] and Dong et al. [125] attributed the compatibilization effect to the combination of macroradicals that form in the presence of DCP via hydrogen abstraction. The macroradicals may further recombine to form complex products, including copolymer at the interface, resulting in a compatibilization effect.

Addition of TAM to the formulation resulted in further refinement in the morphology, which is may be attributed to the improved viscosity of the PHO. The PHO domain size reduced from 1.5 ($\pm$0.2) to 0.55 ($\pm$0.08) μm and from 5 ($\pm$0.6) to 1 ($\pm$0.16) μm for 95/5 and 90/10 PLA/PHO blends respectively. In case of 80/20 the blend morphology changed from droplet-matrix to co-continuous. Figure 6.11 shows the altered morphologies obtained in the presence of TAM, in blends containing various amounts of PHO. In addition to the finer morphology noted previously, these blends exhibited a different, co-continuous morphology at a PHO content of 20 wt.%. Such changes in morphology are common in thermoplastic vulcanizates, consisting of PP and EPDM [128] but have never been noted for these biopolyester blends.

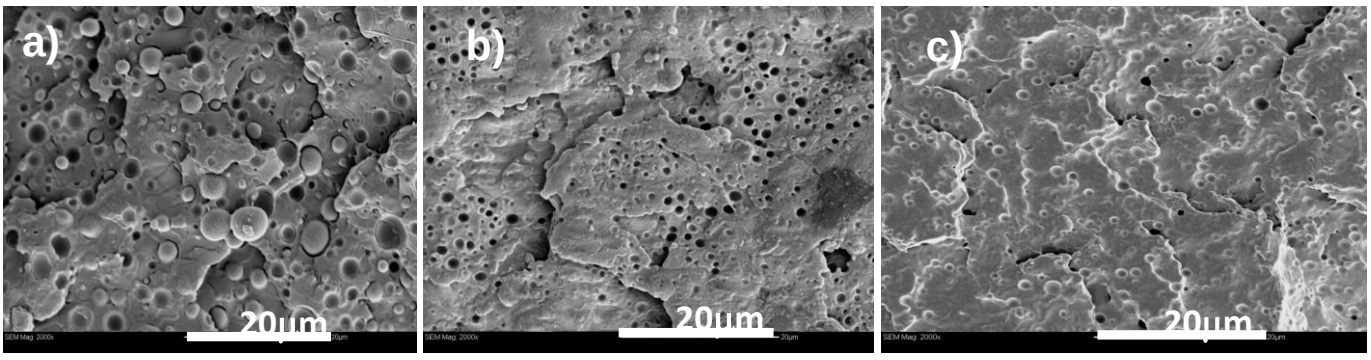

Figure 6.10 Scanning electron microscopy of PLA/PHO (90/10) blend a) unmodified b) (PLA/PHO)/0.5 c) (PLA/PHO)/1

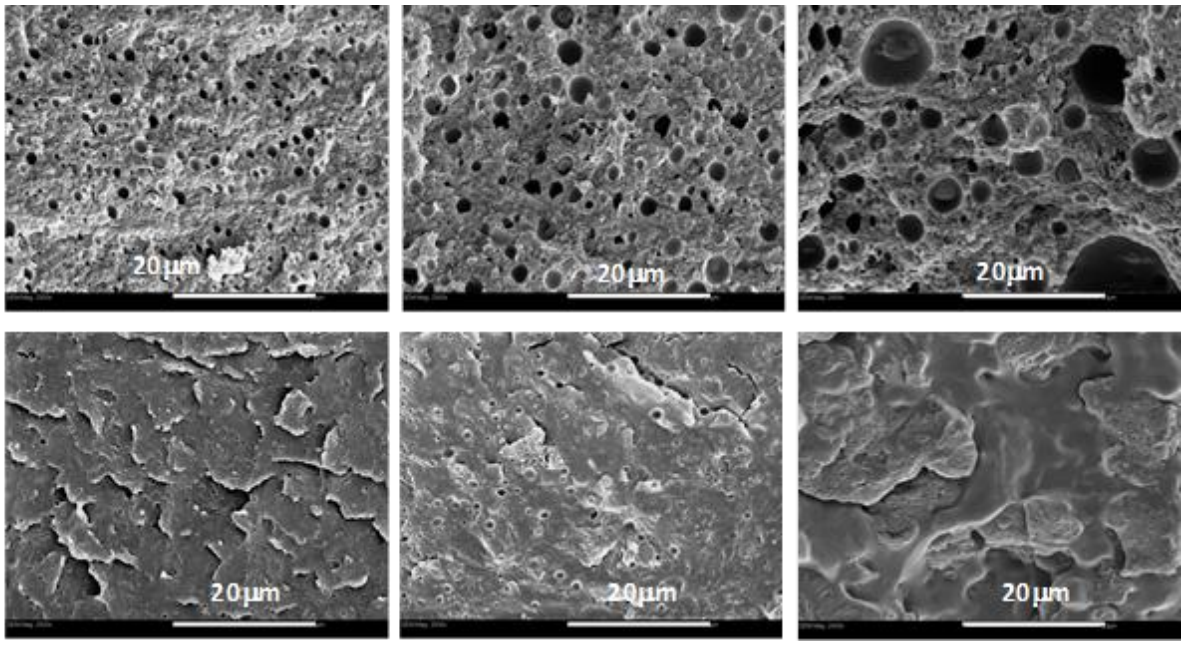

Figure 6.11 Effect of coagent modification on morphology of PLA/PHO blends a) 95/05 b) 90/10 c) 80/20 (wt./wt.%) (samples reacted with coagent were not etched); Top row without coagent; bottom row with coagent

6.3.7 Mechanical properties

The reactively modified PLA/PHO blend had better tensile strain and unnotched impact strength compared to pristine PLA, however, its properties were not as good as the unmodified blend, in spite of the improved morphology (Table 6.3). The gel content of coagent modified PLA/PHO blend was 20 %, revealing the presence of cross-linked chains in the modified blend. These gels might have compromised the ductility of the blend, thus explaining the drop in ductility and impact strength compared to the unmodified blend. Addition of PHO to PLA, as well as reactive modification, did not affect its heat deflection temperature (HDT) (Table 6.3).

Table 6.3 Mechanical properties and heat deflection temperature of neat and coagent modified PLA, and PLA/PHO blends

	Tensile stress (MPa)	Tensile strain (%)	Unnotched Impact (KJ/m^2)	Young's Modulus (MPa)	HDT (°C)
PLA	74 (±3)	14 (±1)	32 (±5)	670 (±74)	55
PLA/0.3/1	77 (±1)	13 (±2)	35 (±2)	837 (±74)	56
PLA/PHO	50 (±1)	35 (±15)	65 (±5)	696 (±7)	55
(PLA/PHO)/0.3/1	49 (±3)	24 (±4)	55 (±3)	677 (±34)	54

These findings suggest that avoiding gels is crucial for the optimization of the properties of these materials. Cross-linking/gelation is also expected to affect negatively the biodegradability of these materials. Therefore optimization of the compositions to avoid the formation of gels should be a high priority.

These results have shown that coagent modification improves significantly the processability of the materials, by improving the melt strength and crystallization rates, while the mechanical properties remain relatively unaffected when the specimens are prepared under the same conditions. The differences noted in thermal properties and morphology however suggests that processing conditions during the solidification stage may be tuned to further impart change in the mechanical properties. This should be a topic of further investigation.

6.4 Conclusions

Addition of PHO to PLA increased the impact strength and elongation at break of PLA, at the expense of the Young's modulus, while the HDT remained unaffected. The droplet-matrix morphology of the blends was coarse, because of the very low viscosity of PHO, resulting in a viscosity mismatch between the blend components.

The viscosity of PHO was successfully increased through partial cross-linking, using solvent-free chemical modification using DCP and TAM coagent. In addition to the substantial increase in viscosity and melt elasticity, the resulting product exhibited improved extrudate appearance.

Reactively modified PLA/PHO in the presence of DCP and TAM displayed the enhancements in strain hardening and crystallization rates, previously observed for the matrix modified PLA. Furthermore these blends had finer morphology, which was attributed to a compatibilizing effect possibly arising from copolymer formation at the interface. Coagent modification further resulted in changes in the morphology, and possible phase inversion in blends containing higher PHO contents.

Chapter 7 Thesis overview

7.1 Thesis overview

Ongoing need for alternate options to conventional petroleum based polymers has resulted in significant attention to various biopolyesters, including poly(lactic acid) (PLA) and poly-(3-hydroxyalkanoates) (PHAs), which are bioderived and biodegradable. However, most of these materials typically suffer from high production costs, brittleness, slow crystallization rates and low melt strength, which restrict their processability under common polymer processing operations. This thesis focused on the improvement of properties and processability of biopolyesters through blending and reactive compounding. Specifically the potential of elastomeric medium-chain-length (MCL) PHAs, as potential impact modifiers for PLA and brittle poly-3-hydroxybutyrate (PHB) was assessed, using conventional melt compounding.

In spite of the relatively high molar masses (ranging from 18,200 to 172,000 g/mole), MCL PHAs melts have low viscosity, presumably due to their helical conformation. Melt blending of these materials with PLA and PHB resulted in coarse blend morphologies due to the large viscosity mismatch, however, remarkable improvement was observed in ductility and impact strength of PHB and PLA. As expected these improvements were accompanied by a decline in tensile stress and Young's modulus. Free-radical mediated cross-linking of polyhydroxyoctanoate (PHO) using a peroxide resulted in improved blend morphology, because of the increased viscosity of PHO; however the impact properties did not show further improvements, presumably because of the high gel content. Furthermore chain extension using epoxidized PHO (ePHO) were explored. This approach lowered the interfacial tension between PLA and PHO, because of the

interactions between the epoxy groups of ePHO with the carboxylic acid end group of PLA, thus resulting in improved compatibility. However the morphology remained coarse, because of the extremely low viscosity of ePHO.

The inability of the previously suggested approaches to produce substantial improvements in the processability and properties of these polyesters led to the development of a simple reactive compounding approach, involving reaction with a peroxide and coagent. This method resulted in substantially improved crystallization rates, viscosity, elasticity and melt strength of PLA and its blends with PHO, as well as improved the compatibility between the blend components, resulting in a very fine morphology. This approach has resulted in blends having simultaneously improved toughness, increased viscosity, strain hardening and crystallinity and represents a significant technological advance in these materials.

These results suggest that simple free-radical mediated reactive compounding of biopolyesters in the melt state can produce the rheological enhancements needed in processes such as film blowing and casting, blow molding, thermoforming and foaming, as well as the enhanced crystallization rates needed in injection molding, thus significantly broadening the applicability of these polymers in conventional polymer processing operations. This should enable the introduction of these compounds to new products/markets and may lead to the possible identification of new applications for these biopolymers.

7.2 Conclusions

Absolute molecular weight (MW) distributions were determined for different MCL PHAs with predominantly 3-hydroxyoctanoate (PHO), 3-hydroxynonanoate (PHN) or 3-hydroxydodecanoate (PHDD) content via triple-detector size exclusion chromatography (SEC),

combined with analyses using various detectors, using tetrahydrofuran (THF) as the carrier solvent. Unlike with the short-chain-length (SCL) PHB, the uncorrected polystyrene calibration in THF provided a good estimate (within 10 %) of absolute MW values for the tested MCL PHAs, irrespective of side chain length. Weight-average MW values ranged from 172,000 Da for PHO to 18,200 for PHN with 30 mol% 3-hydroxyheptanoate, and dispersities of all samples were close to two. Melt viscosity data suggested an entanglement molecular weight around 8 X 10^4 Da, significantly higher than most thermoplastics.

Blends of PHO with PHB, were prepared by melt compounding. Coarsening of the droplet-matrix morphology of the blends was noted as the PHO content increased beyond 5 wt.%; this was attributed to the significant viscosity mismatch between the components. Addition of PHO improved the thermal stability of the blends, reduced their crystallinity and resulted in shifts in their melting and crystallization temperatures. The blends had improved tensile strain at break. The unnotched impact strength showed a threefold increase at 30 wt.% PHO content. Cross-linking of PHO using a peroxide initiator increased its viscosity, thus improving the morphology and mechanical properties of the blends.

Blends of PLA with PHO were also investigated. In spite of the viscosity mismatch between the blend components, addition of PHO resulted in increased elongation at break and impact strength of PLA accompanying decrease in tensile strength and modulus. These improvements can be explained by a reduction in the crystallinity of the PLA, whereas the melting point and glass transition temperature (T_g) remained unaffected. Further increase of the PHO content resulted in a drop in properties, and attributed to the coarse morphology. The heat deflection temperature (HDT) of PLA did not change upon addition of 10 wt.% PHO. Peroxide cross-linking

of PHO to increase its melt viscosity, and introduction of epoxy groups led to only moderate improvements in blend properties.

In order to improve melt and crystallization properties, PLA was chemically modified by radical mediated solvent-free, peroxide-initiated grafting of triallyl trimesate (TAM) coagent in the melt state. When compared with the parent material and with PLA samples treated with peroxide alone, coagent-modified materials demonstrated higher molar mass and improved melt rheological properties, including substantial improvements in melt elasticity and strain hardening under uniaxial extension. The properties of coagent modified PLA were compared to those PLA modified by a multi-functional epoxide oligomeric chain extender (Joncryl®). Although the rheological properties were comparable, the coagent-modified material demonstrated significantly enhanced crystallinity and crystallization rates. The appearance of a distinct crystallization exothermic peak and the disappearance of the cold crystallization temperature point to a nucleation effect in the coagent modified PLA, which together with the rheological enhancements can promote the processability of this material in conventional thermoplastics operations.

Reactive compounding in the presence of the dicumyl peroxide (DCP) and TAM was also evaluated in PHO and its blends with PLA. The viscosity and elasticity of PHO increased substantially following reactive compounding indicative of partial cross-linking, while it retained its amorphous nature. In addition to the substantial increase in viscosity and melt elasticity, the resulting product exhibited improved extrudate appearance. Reactively modified PLA/PHO blends in the presence of DCP and TAM displayed enhancement in strain hardening and crystallization rates, previously observed for the matrix, modified PLA. Furthermore these

blends had finer morphology, which was attributed to a compatibilizing effect possibly arising from copolymer formation at the interface. Coagent modification further resulted in changes in the morphology, and possible phase inversion in blends containing higher PHO content, while the mechanical properties and HDT remained relatively unaffected by this coagent modification.

7.3 Significant contributions

This thesis has completed a very thorough and complete characterization of various MCL PHAs, which are possible candidates to replace conventional elastomeric polymers. For the very first time, the true molecular weight of MCL PHAs was determined. Based on the findings, molar mass determinations based on polystyrene standards can be used as the molecular weight of these materials.

MCL PHAs have very low viscosities and crystallize very slowly, requiring 8-12 h to solidify after processing. This makes their handling and post-processing very difficult. The work in this thesis developed a method to improve processing and handling of MCL PHA, through a simple reactive modification using a peroxide and coagent.

It was shown that PHO, a bioderived and biodegradable polymer, can be used to impact modify brittle biopolymers to offer a complete biosystem. Addition of PHO improved elongation and impact properties of brittle PLA and PHB.

The most important contribution of this thesis is that it provided a solution to improve the melt strength of PLA and its blends with PHO. This should extend its use in applications such as blow molding, thermoforming, blown film and foaming that involve stretching. The improvements in the total crystallinity and crystallization rates of PLA and its blends with PHO without the need

to add nucleating agents, are another significant finding of this thesis, which will likely have broad implications in their potential to extend to new applications.

7.4 Recommendation for future work

i) Optimization of coagent content is needed to reduce gel content so that the elastomeric properties of MCL PHA can be retained and its ability to impact modify brittle polymers can fully be utilized.

ii) Most of the MCL PHAs, with the exception of poly(3-hydroxydodecanoate) (PHDD) were highly amorphous. It may be worthwhile to pursue coagent modification of PHDD, to investigate the potential to impart some improved crystallinity to this material.

iii) The solid-state properties of coagent modified MCL PHAs should be investigated, as these materials could be used as replacements for conventional thermoplastic elastomers.

iv) The effect of coagent modification on pristine PHB and its blends with MCL PHA can be investigated in detail to see whether the properties of these blends can be enhanced.

v) Further detailed investigations of the improvements in crystallization in the presence of coagent should be carried out, including detailed optical microscopy, X-ray diffraction (XRD) analysis, as well as investigation of coagent-rich particle formation in these compounds. The improvements in the morphology of PLA/MCL PHA blends in the presence of peroxide and coagent should also be studied.

vi) The mechanical properties of coagent modified materials should be influenced by the differences in their crystallinity. Detailed investigation of this, including different cooling rates during sample preparation, as well as different molding procedures, (injection and compression molding) should be carried out to exploit this effect.

References

1. Azapagic A, Emsley A, Hamerton I. Polymer – The environment and sustainable development. Hamerton I, Wiley, 2003.

2. Gerald S. Degradable polymers: principles and applications. Netherlands: Kluwer academic publishers, 2002.

3. Opportunities in chemistry by National research council. Washington DC: National academy press, 1985.

4. Lee J, McCarthy S. Biodegradable poly(lactic acid) blends with chemically modified polyhydroxyoctanoate through chain extension. J Polym Environ 2009;17(4):240-247.

5. Lim L, Auras R, Rubino M. Processing technologies for poly(lactic acid). Progress in Polymer Science 2008;33(8):820-852.

6. Hanggi U. Requirements on bacterial polyesters as future substitute for conventional plastics for consumer goods. FEMS Microbiol Rev 1995;16(2-3):213-220.

7. Lemoigne M. Ann.Inst.Pasteur,Paris. 1925,(39):144.

8. Steinbuchel A, Valentin H. Diversity of bacterial polyhydroxyalkanoic acids. FEMS Microbiol Lett 1995;128(3):219-228.

9. Takagi Y, Yasuda R, Yamaoka M, Yamane T. Morphologies and mechanical properties of polylactide blends with medium chain length poly(3-hydroxyalkanoate) and chemically modified poly(3-hydroxyalkanoate). J Appl Polym Sci 2004;93(5):2363-2369.

10. Gassner F, Owen A. Physical properties of poly(beta-hydroxybutyrate) poly(epsilon-caprolactone) blends. Polymer 1994;35(10):2233-2236.

11. Grassie N, Murray EJ, Holmes PA. The thermal degradation of poly(-(d)-β-hydroxybutyric acid): Part 1—Identification and quantitative analysis of products. Polym Degrad Stab 1984;6(1):47-61.

12. Hong S, Gau T, Huang S. Enhancement of the crystallization and thermal stability of polyhydroxybutyrate by polymeric additives. J Therm Anal Calorim 2011;103(3):967-975.

13. Huisman G, Deleeuw O, Eggink G, Witholt B. Synthesis of poly-3-hydroxyalkanoates is a common feature of fluorescent *pseudomonads*. Appl Environ Microbiol 1989;55(8):1949-1954.

14. Jiang X. Process development for the production and separation of medium-chain-length poly (3-hydroxyalkanoates) by *Pseudomonas putida KT2440*. Ph.D. Thesis, 2010.

15. Diard S, Carlier J, Ageron E, Grimont P, Langlois V, Guerin P, Bouvet O. Accumulation of poly(3-hydroxybutyrate) from octanoate, in different *Pseudomonas* belonging to the rRNA homology group I. Syst Appl Microbiol 2002;25(2):183-188.

16. Sun Z, Ramsay JA, Guay M, Ramsay BA. Fermentation process development for the production of medium-chain-length poly-3-hyroxyalkanoates. Appl Microbiol Biotechnol 2007;75(3):475-485.

17. Gagnon K, Lenz R, Farris R, Fuller R. Crystallization behavior and its Influence on the mechanical properties of a thermoplastic elastomer produced by *Pseudomonasoleovorans*. Macromolecules 1992;25(14):3723-3728.

18. Utracki LA. Polymer blends handbook. Kluwer academic publishers, 2002.

19. Parulekar Y, Mohanty A. Biodegradable toughened polymers from renewable resources: blends of polyhydroxybutyrate with epoxidized natural rubber and maleated polybutadiene. Green Chem 2006;8(2):206-213.

20. Avella M, Martuscelli E. Poly-d-(-)(3-hydroxybutyrate) poly(ethylene oxide) blends - phase-diagram, thermal and crystallization behavior. Polymer 1988;29(10):1731-1737.

21. Hori Y, Takahashi Y, Hongo H, Yamaguchi A, Hagiwara T. Takasago Int. 1996(EP 723 983).

22. Kumagai Y, Doi Y. Journal of Environmental Polymer Degradation 1993;1(2):81.

23. de Carvalho FP, Quental AC, Felisberti MI. Polyhydroxybutyrate/acrylonitrile-g-(ethylene-co-propylene-co-diene)-g-s tyrene blends: Their morphology and thermal and mechanical behavior. J Appl Polym Sci 2008;110(2):880-889.

24. Asrar J, Hill J. Biosynthetic processes for linear polymers. J Appl Polym Sci 2002;83(3):457-483.

25. Ceccorulli G, Pizzoli M, Scandola M. Plasticization of bacterial poly(3-hydroxybutyrate). Macromolecules 1992;25(12):3304-3306.

26. Riande E, Markovitz H, Plazek D, Raghupathi N. Viscoelastic behavior of polystyrene - tricresyl phosphate solutions. Journal of Polymer Science Part C-Polymer Symposium 1975(50):405-430.

27. Ishikawa K, Kawaguchi Y, Doi Y. Plasticization of bacterial polyester by the addition of acylglycerols and its enzymatic degradability. Kobunshi Ronbunshu 1991;48(4):221-226.

28. Withey R, Hay J. The effect of seeding on the crystallisation of poly(hydroxybutyrate), and co-poly(hydroxybutyrate-co-valerate). Polymer 1999;40(18):5147-5152.

29. Alata H, Hexig B, Inoue Y. Effect of poly(vinyl alcohol) fine particles as a novel biodegradable nucleating agent on the crystallization of poly(3-hydroxybutyrate). J Polym Sci Pt B-Polym Phys 2006;44(13):1813-1820.

30. Maiti P, Batt CA, Giannelis EP. New biodegradable polyhydroxybutyrate/layered silicate nanocomposites. Biomacromolecules 2007;8(11):3393-3400.

31. Kosan B, Michels C, Meister F. Dissolution and forming of cellulose with ionic liquids. Cellulose 2008;15(1):59-66.

32. Ljungberg N, Cavaille JY, Heux L. Nanocomposites of isotactic polypropylene reinforced with rod-like cellulose whiskers. Polymer 2006;47(18):6285-6292.

33. Danyadi L, Janecska T, Szabo Z, Nagy G, Moczo J, Pukanszky B. Wood flour filled PP composites: Compatibilization and adhesion. Composites Sci Technol 2007;67(13):2838-2846.

34. Nanocrystalline cellulose as strong as Kevlar and extracted from plants is heading to commercialization in Canada. http://nextbigfuture.com 2011.

35. Lucia LA. The nanoscience and technology of renewable biomaterials. John Wiley and Sons, 2009.

36. Rasal RM, Janorkar AV, Hirt DE. Poly(lactic acid) modifications. Prog Polym Sci 2010;35(3):338-356.

37. Saeidlou S, Huneault MA, Li H, Park CB. Poly(lactic acid) crystallization. Prog Polym Sci 2012;37(12):1657-1677.

38. Nampoothiri KM, Nair NR, John RP. An overview of the recent developments in polylactide (PLA) research. Bioresour Technol 2010;101(22):8493-8501.

39. Zaman HU, Song JC, Park L, Kang I, Park S, Kwak G, Park B, Yoon K. Poly(lactic acid) blends with desired end-use properties by addition of thermoplastic polyester elastomer and MDI. Polym Bull 2011;67(1):187-198.

40. Gui Z, Xu Y, Gao Y, Lu C, Cheng S. Novel polyethylene glycol-based polyester-toughened polylactide. Mater Lett 2012;71:63-65.

41. Murariu M, Ferreira ADS, Pluta M, Bonnaud L, Alexandre M, Dubois P. Polylactide (PLA)-CaSO4 composites toughened with low molecular weight and polymeric ester-like plasticizers and related performances. Eur Polym J 2008;44(11):3842-3852.

42. Li H, Huneault MA. Effect of nucleation and plasticization on the crystallization of poly(lactic acid). Polymer 2007;48(23):6855-6866.

43. Battegazzore D, Bocchini S, Frache A. Crystallization kinetics of poly(lactic acid)-talc composites. Express Polym Lett 2011;5(10):849-858.

44. Yang G, Su J, Su R, Zhang Q, Fu Q, Na B. Toughening of poly(l-lactic acid) by annealing: The effect of crystal morphologies and modifications. J Macromol Sci Part B-Phys 2012;51(1-3):184-196.

45. Corre Y, Duchet J, Reignier J, Maazouz A. Melt strengthening of poly (lactic acid) through reactive extrusion with epoxy-functionalized chains. Rheol Acta 2011;50(7-8):613-629.

46. Deenadayalan E, Lele AK, Balasubramanian M. Reactive extrusion of poly(l-lactic acid) with glycidol. J Appl Polym Sci 2009;112(3):1391-1398.

47. Najafi N, Heuzey MC, Carreau PJ, Wood-Adams PM. Control of thermal degradation of polylactide (PLA)-clay nanocomposites using chain extenders. Polym Degrad Stab 2012;97(4):554-565.

48. Villalobos M, Awojulu A, Greeley T, Deeter G. Oligomeric chain extenders for economic reprocessing and recycling of condensation plastics, 2004.

49. Bikiaris DN, Karayannidis GP. Chain extension of polyesters PET and PBT with two new diimidodiepoxides .2. Journal of Polymer Science Part A-Polymer Chemistry 1996;34(7):1337-1342.

50. Villalobos M, Awojulu A, Greeley T, Turco G, Deeter G. Oligomeric chain extenders for economic reprocessing and recycling of condensation plastics. Energy 2006;31(15):3227-3234.

51. Al-Itry R, Lamnawar K, Maazouz A. Improvement of thermal stability, rheological and mechanical properties of PLA, PBAT and their blends by reactive extrusion with functionalized epoxy. Polym Degrad Stab 2012;97(10):1898-1914.

52. Dean KM, Petinakis E, Meure S, Yu L, Chryss A. Melt strength and rheological properties of biodegradable poly(lactic acid) modified via alkyl radical based reactive extrusion processes. J Polym Environ 2012;20(3):741-747.

53. Rytlewski P, Zenkiewicz M, Malinowski R. Influence of dicumyl peroxide content on thermal and mechanical properties of polylactide. International Polymer Processing 2011;26(5):580-586.

54. Carlson D, Dubois P, Nie L, Narayan R. Free radical branching of polylactide by reactive extrusion. Polym Eng Sci 1998;38(2):311-321.

55. Zhang Y, Tiwary P, Parent JS, Kontopoulou M, Park CB. Crystallization and foaming of coagent-modified polypropylene: Nucleation effects of cross-linked nanoparticles. Polymer 2013;54(18):4814-4819.

56. Parent JS, Sengupta SS, Kaufman M, Chaudhary BI. Coagent-induced transformations of polypropylene microstructure: Evolution of bimodal architectures and cross-linked nano-particles. Polymer 2008;49(18):3884-3891.

57. Parent JS, Bodsworth A, Sengupta SS, Kontopoulou M, Chaudhary BI, Poche D, Cousteaux S. Structure-rheology relationships of long-chain branched polypropylene: Comparative analysis of acrylic and allylic coagent chemistry. Polymer 2009;50(1):85-94.

58. Vaidya A, Pandey R, Mudliar S, Kumar M, Chakrabarti T, Devotta S. Production and recovery of lactic acid for polylactide - an overview. Crit Rev Environ Sci Technol 2005;35(5):429-467.

59. Global biopolymers market analysis and forecasts to 2015. 2009;GMDCH0018MR.

60. Rai R, Yunos DM, Boccaccini AR, Knowles JC, Barker IA, Howdle SM, Tredwell GD, Keshavarz T, Roy I. Poly-3-hydroxyoctanoate P(3HO), a medium chain length polyhydroxyalkanoate homopolymer from *Pseudomonas mendocina*. Biomacromolecules 2011;12(6):2126-2136.

61. Nerkar M, Ramsay J, Ramsay B, Kontopoulou M. Morphology and mechanical properties of blends of short-chain-length and medium-chain-length poly-3-hydroxyalkanoates. Polymer Processing Society, 2012;358-359.

62. Akita S, Einaga Y, Miyaki Y, Fuita H. Solution Properties of poly(d-beta-hydroxybutyrate) .1. biosynthesis and characterization. Macromolecules 1976;9(5):774-780.

63. Marchessault R, Okamura K, SU C. Physical properties of poly(beta-hydroxy butyrate) .2. conformational aspects in solution. Macromolecules 1970;3(6):735-&.

64. Miyaki Y, Einaga Y, Hirosy T, Fujita H. Solution properties of poly(d-beta-hydroxybutyrate) .2. light-scattering and viscosity in trifluoroethanol and behavior of highly expanded polymer coils. Macromolecules 1977;10(6):1356-1364.

65. Cornibert J, Marchessault RH, Benoit H, Weill G. Physical properties of poly(beta-hydroxy butyrate) .3. folding of helical segments in 2,2,2-trifluoroethanol. Macromolecules 1970;3(6):741.

66. Berger E, Ramsay BA, Ramsay JA, Chavarie C, Braunegg G. PHB Recovery by hypochlorite digestion of non-PHB biomass. Biotechnol Tech 1989;3(4):227-232.

67. Ramsay J, Berger E, Voyer R, Chavarie C, Ramsay B. Extraction of poly-3-hydroxybutyrate using chlorinated solvents. Biotechnol Tech 1994;8(8):589-594.

68. Shozui F, Matsumoto K, Sasaki T, Taguchi S. Engineering of polyhydroxyalkanoate synthase by Ser477X/Gln481X saturation mutagenesis for efficient production of 3-hydroxybutyrate-based copolyesters. Appl Microbiol Biotechnol 2009;84(6):1117-1124.

69. Daly P, Bruce D, Melik D, Harrison G. Thermal degradation kinetics of poly(3-hydroxybutyrate-co-3-hydroxyhexanoate). J Appl Polym Sci 2005;98(1):66-74.

70. Jiang X, Sun Z, Marchessault R, Ramsay J, Ramsay B. Biosynthesis and properties of medium-chain-length polyhydroxyalkanoate with enriched content of the dominant monomer. Biomacromolecules 2012;13(9):2926-2932

71. Sun Z, Ramsay J, Guay M, Ramsay B. Enhanced yield of medium-chain-length polyhydroxyalkanoates from nonanoic acid by co-feeding glucose in carbon-limited, fed-batch culture. J Biotechnol 2009;143(4):262-267.

72. Jiang X, Ramsay JA, Ramsay BA. Acetone extraction of mcl-PHA from *Pseudomonas* putida KT2440. J Microbiol Methods 2006;67(2):212-219.

73. Dupont A, Harrison G. Conformation and dn/dc determination of cellulose in N,N-dimethylacetamide containing lithium chloride. Carbohydr Polym 2004;58(3):233-243.

74. Barham P, Keller A, Otun E, Holmes P. Crystallization and morphology of a bacterial thermoplastic - poly-3-hydroxybutyrate. J Mater Sci 1984;19(9):2781-2794.

75. Beuermann S, Buback M, Davis T, Gilbert R, Hutchinson R, Kajiwara A, Klumperman B, Russell G. Critically evaluated rate coefficients for free-radical polymerization, 3 - Propagation rate coefficients for alkyl methacrylates. Macromol Chem Phys 2000;201(12):1355-1364.

76. Marchessault R, Monasterios C, Morin F, Sundararajan P. Chiral poly(beta-hydroxyalkanoates) - an adaptable helix influenced by the alkane side-chain. Int J Biol Macromol 1990;12(2):158-165.

77. Kim DY, Kim HW, Chung MG, Rhee YH. Biosynthesis, modification, and biodegradation of bacterial medium-chain-length polyhydroxyalkanoates. J Microbiol 2007;45(2):87-97.

78. Ma P, Hristova-Bogaerds DG, Lemstra PJ, Zhang Y, Wang S. Toughening of PHBV/PBS and PHB/PBS blends via in situ compatibilization using dicumyl peroxide as a free-radical grafting initiator. Macromol Mater Eng 2012;297(5):402-410.

79. Ha CS, Cho WJ. Miscibility, properties, and biodegradability of microbial polyester containing blends. Prog Polym Sci 2002;27(4):759-809.

80. Yu L, Dean K, Li L. Polymer blends and composites from renewable resources. Prog Polym Sci 2006;31(6):576-602.

81. Zhang M, Thomas NL. Preparation and properties of polyhydroxybutyrate blended with different types of starch. J Appl Polym Sci 2010;116(2):688-694.

82. Zhang M, Thomas NL. Blending polylactic acid with polyhydroxybutyrate: The effect on thermal, mechanical, and biodegradation properties. Adv Polym Technol 2011;30(2):67-79.

83. Dufresne A, Vincendon M. Poly(3-hydroxybutyrate) and poly(3-hydroxyoctanoate) blends: Morphology and mechanical behavior. Macromolecules 2000;33(8):2998-3008.

84. Martelli SM, Sabirova J, Fakhoury FM, Dyzma A, de Meyer B, Soetaert W. Obtention and characterization of poly(3-hydroxybutyricacid-co-hydroxyvaleric acid)/mcl-PHA based blends. Fod Sci Technol-Leb 2012;47(2):386-392.

85. Nerkar M, Ramsay J, Ramsay B, Kontopoulou M, Hutchinson R. Determination of Mark-Houwink Parameters and absolute molecular weight of medium-chain-length poly(3-hydroxyalkanoates). J Polym Environ 2013;21(1):24-29.

86. Sin MC, Gan SN, Annuar MSM, Tan IKP. Thermodegradation of medium-chain-length poly(3-hydroxyalkanoates) produced by *Pseudomonas* putida from oleic acid. Polym Degrad Stab 2010;95(12):2334-2342.

87. Pearce R, Marchessault R. Melting and crystallization in bacterial poly(beta-hydroxyvalerate), PHV, and Blends with Poly(beta-hydroxybutyrate-co-hydroxyvalerate). Macromolecules 1994;27(14):3869-3874.

88. Owen A, Heinzel J, Skrbic Z, Divjakovic V. Crystallization and melting behavior of PHB and PHB/HV copolymer. Polymer 1992;33(7):1563-1567.

89. Organ S, Barham P. On the equilibrium melting temperature of Polyhydroxybutyrate. Polymer 1993;34(10):2169-2174.

90. Gagnon K, Lenz R, Farris R, Fuller R. Chemical modification of bacterial elastomers .1. peroxide cross-linking. Polymer 1994;35(20):4358-4367.

91. Dufresne A, Reche L, Marchessault R, Lacroix M. Gamma-ray crosslinking of poly (3-hydroxyoctanoate-co-undecenoate). Int J Biol Macromol 2001;29(2):73-82.

92. Park SJ, Kim TW, Kim MK, Lee SY, Lim S. Advanced bacterial polyhydroxyalkanoates: Towards a versatile and sustainable platform for unnatural tailor-made polyesters. Biotechnol Adv 2012;30(6):1196-1206.

93. Platel RH, Hodgson LM, Williams CK. Biocompatible initiators for lactide polymerization. Polym Rev 2008;48(1):11-63.

94. Palade L, Lehermeier H, Dorgan J. Melt rheology of high L-content poly(lactic acid). Macromolecules 2001;34(5):1384-1390.

95. Dorgan J, Williams J, Lewis D. Melt rheology of poly(lactic acid): entanglement and chain architecture effects. J Rheol 1999;43(5):1141-1155.

96. Othman N, Acosta-Ramirez A, Mehrkhodavandi P, Dorgan JR, Hatzikiriakos SG. Solution and melt viscoelastic properties of controlled microstructure poly(lactide). J Rheol 2011;55(5):987-1005.

97. Othman N, Xu C, Mehrkhodavandi P, Hatzikiriakos SG. Thermorheological and mechanical behavior of polylactide and its enantiomeric diblock copolymers and blends. Polymer 2012;53(12):2443-2452.

98. Othman N, Jazrawi B, Mehrkhodavandi P, Hatzikiriakos SG. Wall slip and melt fracture of poly(lactides). Rheol Acta 2012;51(4):357-369.

99. Liu J, Lou L, Yu W, Liao R, Li R, Zhou C. Long chain branching polylactide: structures and properties. Polymer 2010;51(22):5186-5197.

100. Pilla S, Kim SG, Auer GK, Gong S, Park CB. Microcellular extrusion-foaming of polylactide with chain extender. Polym Eng Sci 2009;49(8):1653-1660.

101. Yu L, Toikka G, Dean K, Bateman S, Yuan Q, Filippou C, Tri Nguyen. Foaming behaviour and cell structure of poly(lactic acid) after various modifications. Polym Int 2013;62(5):759-765.

102. Meng Q, Heuzey M, Carreau PJ. Effects of a multifunctional polymeric chain extender on the properties of polylactide and polylactide/clay nanocomposites. Int Polym Proc 2012;27(5):505-516.

103. Najafi N, Heuzey MC, Carreau PJ. Crystallization behavior and morphology of polylactide and PLA/clay nanocomposites in the presence of chain extenders. Polym Eng Sci 2013;53(5):1053-1064.

104. Maharana T, Mohanty B, Negi YS. Melt-solid polycondensation of lactic acid and its biodegradability. Prog Polym Sci 2009;34(1):99-124.

105. Graebling D. Synthesis of branched polypropylene by a reactive extrusion process. Macromolecules 2002;35(12):4602-4610.

106. Passaglia E, Coiai S, Augier S. Control of macromolecular architecture during the reactive functionalization in the melt of olefin polymers. Prog Polym Sci 2009;34(9):911-947.

107. Yang S, Wu Z, Yang W, Yang M. Thermal and mechanical properties of chemical crosslinked polylactide (PLA). Polym Test 2008;27(8):957-963.

108. You J, Lou L, Yu W, Zhou C. The preparation and crystallization of long chain branching polylactide made by melt radicals reaction. J Appl Polym Sci 2013;129(4):1959-1970.

109. Fukada E. Poiseuille Medal Award Lecture: Piezoelectricity of biopolymers. Biorheology 1995;32(6):593-609.

110. Long Y, Shanks R, Stachurski Z. Kinetics of polymer crystallization. Prog Polym Sci 1995;20(4):651-701.

111. El Mabrouk K, Parent JS, Chaudhary BI, Cong R. Chemical modification of PP architecture: strategies for introducing long-chain branching. Polymer 2009;50(23):5390-5397.

112. Wu W, Parent JS, Sengupta SS, Chaudhary BI. Preparation of crosslinked microspheres and porous solids from hydrocarbon solutions: a new variation of precipitation polymerization chemistry. J Polym Sci Pol Chem 2009;47(23):6561-6570.

113. Tian J, Yu W, Zhou C. Crystallization kinetics of linear and long-chain branched polypropylene. J Macromol Sci Phys 2006;45(5):969-985.

114. Anderson KS, Schreck KM, Hillmyer MA. Toughening polylactide. Polym Rev 2008;48(1):85-108.

115. Verhoogt H, Ramsay BA, Favis BD. Polymer blends containing poly(3-hydroxyalkanoate)s. Polymer 1994;35(24):5155-5169.

116. Imre B, Pukanszky B. Compatibilization in bio-based and biodegradable polymer blends. Eur Polym J 2013;49(6):1215-1233.

117. Schreck KM, Hillmyer MA. Block copolymers and melt blends of polylactide with Nodax (TM) microbial polyesters: Preparation and mechanical properties. J Biotechnol 2007;132(3):287-295.

118. Noda I, Satkowski M, Dowrey A, Marcott C. Polymer alloys of Nodax copolymers and poly(lactic acid). Macromol Biosci 2004;4(3):269-275.

119. Ma P, Spoelstra AB, Schmit P, Lemstra PJ. Toughening of poly (lactic acid) by poly (beta-hydroxybutyrate-co-beta-hydroxyvalerate) with high beta-hydroxyvalerate content. Eur Polym J 2013;49(6):1523-1531.

120. Bhardwaj R, Mohanty AK. Modification of brittle polylactide by novel hyperbranched polymer-based nanostructures. Biomacromolecules 2007;8(8):2476-2484.

121. Nyambo C, Misra M, Mohanty AK. Toughening of brittle poly(lactide) with hyperbranched poly(ester-amide) and isocyanate-terminated prepolymer of polybutadiene. J Mater Sci 2012;47(13):5158-5168.

122. Semba T, Kitagawa K, Ishiaku U, Hamada H. The effect of crosslinking on the mechanical properties of polylactic acid/polycaprolactone blends. J Appl Polym Sci 2006;101(3):1816-1825.

123. Wang R, Wang S, Zhang Y, Wan C, Ma P. Toughening modification of PLLA/PBS blends via in-situ compatibilization. Polym Eng Sci 2009;49(1):26-33.

124. Ma P, Cai X, Zhang Y, Wang S, Dong W, Chen M, Lemstra PJ. In-situ compatibilization of poly(lactic acid) and poly(butylene adipate-co-terephthalate) blends by using dicumyl peroxide as a free-radical initiator. Polym Degrad Stab 2014;102:145-151.

125. Dong W, Ma P, Wang S, Chen M, Cai X, Zhang Y. Effect of partial crosslinking on morphology and properties of the poly(beta-hydroxybutyrate)/poly(D,L-lactic acid) blends. Polym Degrad Stab 2013;98(9):1549-1555.

126. Nerkar M, Ramsay JA, Ramsay BA, Kontopoulou M, Hutchinson RA. Determination of Mark-Houwink Parameters and Absolute Molecular Weight of Medium-Chain-Length Poly(3-Hydroxyalkanoates). J Polym Environ 2013;21(1):24-29.

127. Ma J, La LTB, Zaman I, Meng Q, Luong L, Ogilvie D, Kuan H. Fabrication, structure and properties of epoxy/metal nanocomposites. Macromol Mater Eng 2011;296(5):465-474.

128. Abdousabets S, Patel R. Morphology of elastomeric alloys. Rubber Chem Technol 1991;64(5):769-779.

129. Palierne J. Linear Rheology of viscoelastic emulsions with Interfacial tension. Rheologica Acta 1990;29(3):204-214.

130. Wu S. Formation of dispersed phase in incompatible polymer blends - interfacial and rheological effects. Polym Eng Sci 1987;27(5):335-343.

Appendix A - Improved viscosity ratio and compatibility of poly (lactic acid) and polyhydroxyoctanoate blends

Introduction

In Chapter 6 it was reported that the reason for the very coarse morphology of poly (lactic acid) **(**PLA)/polyhydroxyoctanoate (PHO) blend is the significant viscosity mismatch between the blend components. This is evident from Figure A.1, which summarizes the complex viscosities of the materials under consideration. Both polymers had Newtonian behavior, with viscosities of 661 Pa.s and 13 Pa.s for PLA and PHO respectively, at 180°C, resulting in a viscosity ratio (defined as the ratio of the viscosity of the dispersed phase over the viscosity of the matrix) of 0.02.

The shortcoming of viscosity mismatch between PHO and poly-3-hydroxybutyrate (PHB) was addressed in chapter 4 by free radical mediated cross-linking using peroxide. In this appendix, the same approach is followed to increase the viscosity of PHO and reduce the viscosity mismatch with PLA. Additionally epoxidation of PHO was explored to improve its compatibility with PLA by reaction of epoxy groups with hydroxyl and carboxyl groups of PLA. Furthermore it was anticipated that the epoxy groups would act as a chain extender to improve the viscosity of PHO [1].

Experimental

Cross-linking of PHO

PHO was crosslinked as described in Chapter 4 (Section 4.2.3) and dry mixed with PLA before feeding in the DSM micro compounder. The gel content of the peroxide cross-linked MCL PHA was measured as described in chapter 4.

Epoxidation of PHO

10-epoxyundecanoic acid was prepared as described below and was used to prepare epoxidized PHO (ePHO). 50 g of 10-undecenoic acid were dissolved in 25 ml of anhydrous dichloromethane and the solution was placed in an ice bath (0 ^{o}C). m-Chloroperbenzoic acid (mCPBA) was purified by washing with a phosphate buffer solution of pH 7.5 and dried under reduced pressure at room temperature. 65 g of purified mCPBA dissolved in 450 ml of anhydrous dichloromethane were added to the 10-undecenoic solution drop wise, under continuous stirring with a magnetic stirrer in an ice bath. The solution was then stirred for 24h until a white precipitate formed. After filtration to eliminate the m-chlorobenzoic acid the filtrate was washed with a 0.80 M solution of sodium sulphite until peroxide was no longer detectable with peroxide test paper. The organic layer was finally washed with distilled water until pH test paper indicated that the washings were neutral. The solution was then dried under reduced pressure to yield a dry white powder.

Nuclear magnetic resonance characterization

Proton (^{1}H) and carbon (^{13}C) NMR spectra were recorded on a Bruker DPX300 NMR spectrometer at 300 MHz in deuterated chloroform ($CDCl_3$) as solvent. The chemical shifts (ppm) for ^{1}H and ^{13}C NMR were referenced relative to tetramethylsilane (TMS, 0.00 ppm) as the

internal reference. The solution concentration was 0.5 w/v% (20 mg of sample in the NMR tube) and the solution was filtered prior to placing it in the NMR tube.

Yield = 99%; mp = 39 ^{o}C. ^{1}H-NMR (300 MHz, $CDCl_3$, δ ppm); 1.9-1.3 (m, 12H, $(CH_2)_6$; 2.3 (t, 2H, CH_2-CO_2H); 2.5 (dd, 1H, CH epoxy); 2.8 (t, 1H, H_a of CH_2 epoxy); 2.9 (d, 1H, H_b of CH_2 epoxy).

Results and Discussion

Cross-linked PHO (xPHO)

Complex viscosities of the xPHO, are summarized in Figure A.1. Cross-linking led to significant increase in shear thinning behavior and loss of the Newtonian plateau as expected for cross-linked polymer with high cross-linked densities.

Given the change in the viscosity-shear rate dependence, xPHO can only match the viscosity of PLA in a very narrow frequency/shear rate range. As shown in Figure A.1, lower peroxide loading (0.06 wt.%) matched the viscosity of PLA at lower frequency region. At higher peroxide level, 0.2 wt.%, the viscosity of PHO was equivalent to PLA viscosity in the mid frequency region. In order to match the viscosity of PHO at high shear rates of about 100 s^{-1} (equivalent to shear rate in processing), 0.5 wt.% of peroxide was needed, hence PHO was cross-linked using 0.5 wt.% peroxide and blended with PLA for further evaluations.

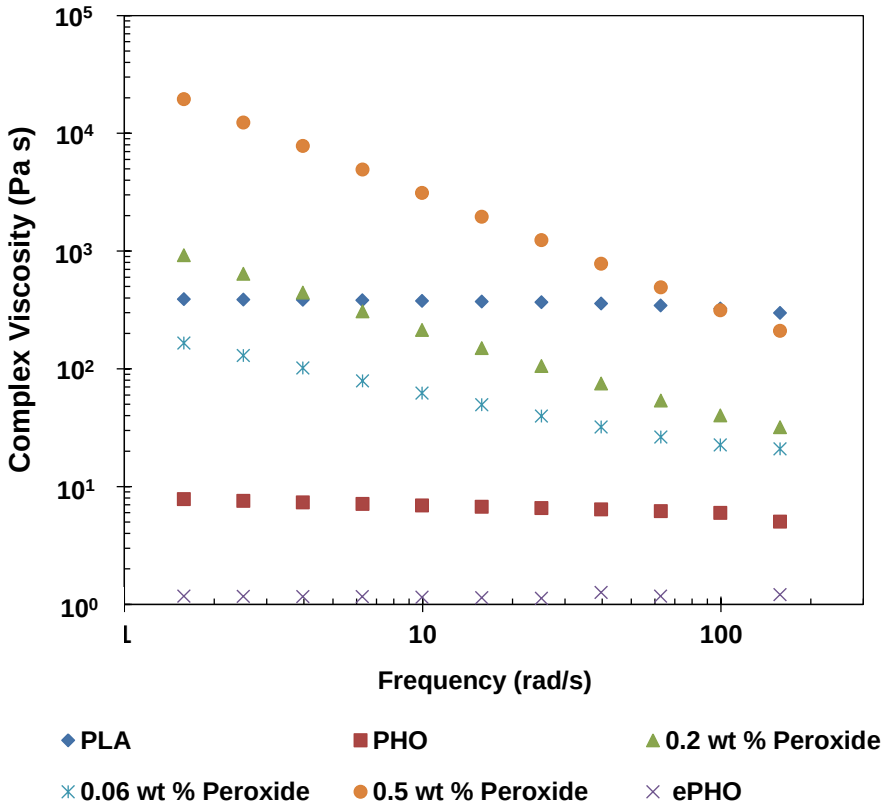

Figure A.1 Complex viscosity of PLA, PHO, xPHO and ePHO at 180°C

The mechanical properties of PLA blends containing xPHO and ePHO are summarized in Table A.1. xPHO matched the viscosity of PLA in the high frequency region and had pronounced shear thinning characteristics, however, it did not show any improvement in mechanical properties as the elastic nature of PHO was altered due to the high gel content (97%) of xPHO.

Table A.1 Mechanical properties of PLA and blends containing PHO, ePHO and xPHO

	Tensile stress (MPa)	Tensile Strain (%)	Unnotched Impact (KJ/m^2)	Young's Modulus (MPa)
PLA	74 (±3)	14 (±1)	32 (±5)	670 (±74)
10 % PHO	50 (±4)	35 (±15)	65 (±5)	696 (±29)
10 % xPHO	40 (±2)	11 (±1)	23 (±1)	567 (±29)
10 % ePHO	47 (±4)	32 (±8)	57 (±11)	551 (±36)

Epoxidized PHO

The compositions of the prepared 10-epoxyundecanoic acid and the ePHO were determined by ^{1}H NMR spectroscopy. The spectra were consistent with the expected structures. The epoxidation reaction of 10-undecanoic acid was followed by ^{1}H-NMR. During the epoxidation the characteristic signals corresponding to the unsaturated side group (2.0 ppm –CH_2-, 4.9 ppm =CH_2, 5.8 ppm –CH=) disappear and are replaced by peaks associated with the oxirane group at 2.5 ppm (c, 0-CH-, multiplet) and 2.75-2.9 ppm (a and b, -O-CH_2, triplet and multiplet, respectively), while the –CH_2- group is now found at 1.3 ppm (e). The ^{1}H NMR spectrum of ePHA, together with the corresponding chemical shift assignments, is presented in Figure A.2. The percentage of epoxy groups in the prepared ePHA was calculated by comparing the oxirane signals (i and j in particular, due to the fact the h is overlapped by the CH_2 side chain groups) with the -CH_3 signal of the unmodified side chain (f). The content of epoxy modified monomer in the resulting ePHO was 12 mole %, as determined by the ^{1}H NMR.

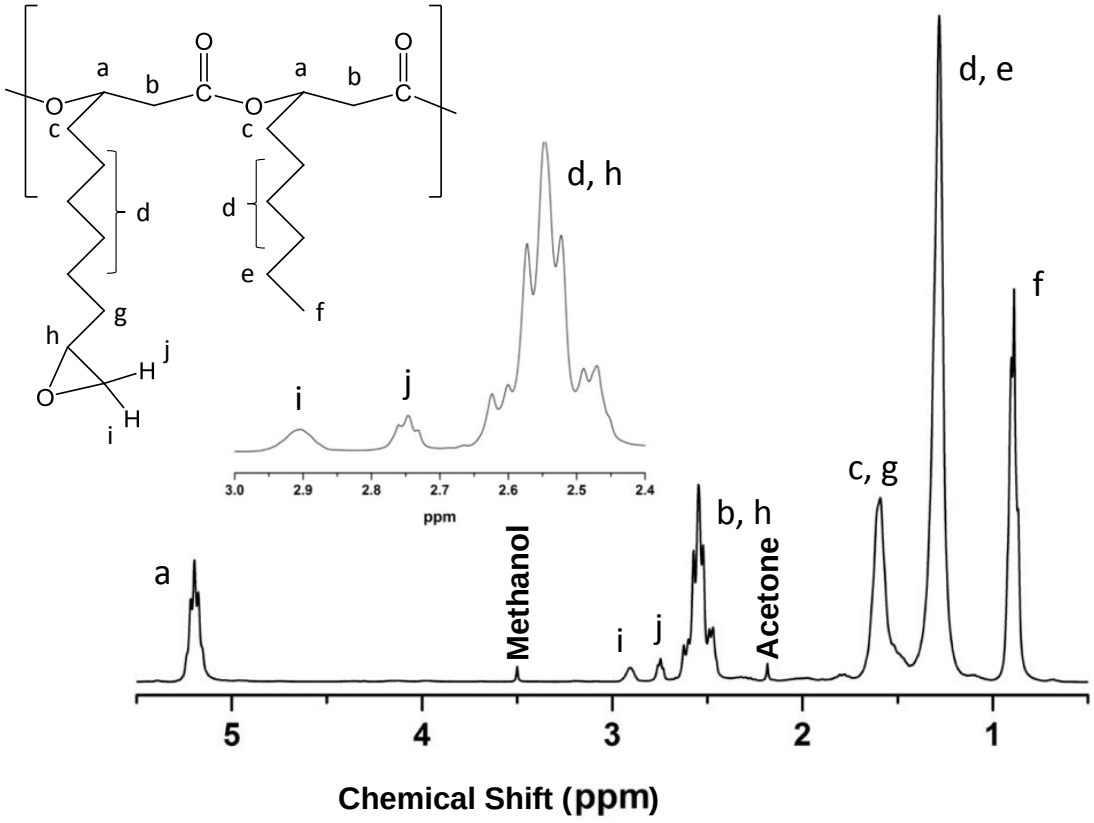

Figure A.2. NMR spectra of ePHA (12% mol/mol 10-epoxyundecanoic acid/unmodified monomer)

Epoxidation of PHO did not show any increase in viscosity of PHO rather it was diminished (Figure A.1).

Blends of PLA with ePHO

The compatibility of the blend components in immiscible blends is associated with their interfacial tension. The Palierne model [2] was used to obtain an estimate of the interfacial tension between PLA and PHO by fitting the complex modulus of the blend as a function of frequency (A.3).

The Palierne model relates viscoelasticity of emulsion with the viscoelasticity of matrix and dispersed phase, droplet size and droplet size distribution of dispersed phase and the interphase surface tension of the blend components. It can be expressed as

$$G^*(\omega) = G^*m(\omega)\left(\frac{1+3\phi H(\omega)}{1-2\phi H(\omega)}\right) \qquad \text{(A.1)}$$

$$H(\omega) = \frac{4\left(\frac{\alpha}{R}\right)[2G_m^*+5G_d^*]+[G_d^*-G_m^*][16G_m^*+19G_d^*]}{40\left(\frac{\alpha}{R}\right)[G_m^*+G_d^*]+[2G_d^*+3G_m^*][\,16G_m^*+\,19G_d^*]}$$

G_d^* and G_m^* are complex moduli of the dispersed phase and matrix respectively, α, the interfacial tension, ϕ, the volume fraction of disperse phase, ω is the studied frequency and R is the particle radius.

Immiscible blends of PLA and PHO formed droplet-matrix morphology with PLA as matrix phase and PHO forming spherical dispersed phase. Scanning electron microscopy (SEM) with details mentioned in chapter 4 was used to characterize blend morphology. Volume average diameter of PHO domain determined using image analysis software SigmaScan Pro was 1.73 μm. Interfacial tension was calculated by substituting volume average diameter and volume fraction of PHO in equation A.1. The estimated interfacial tensions were 2.1 and 0.6 N/mm for PLA-PHO and PLA-ePHO respectively. The epoxy groups of ePHO plausibly reacted with carboxylic acid end group of PLA improving their compatibility and hence reducing interfacial tension.

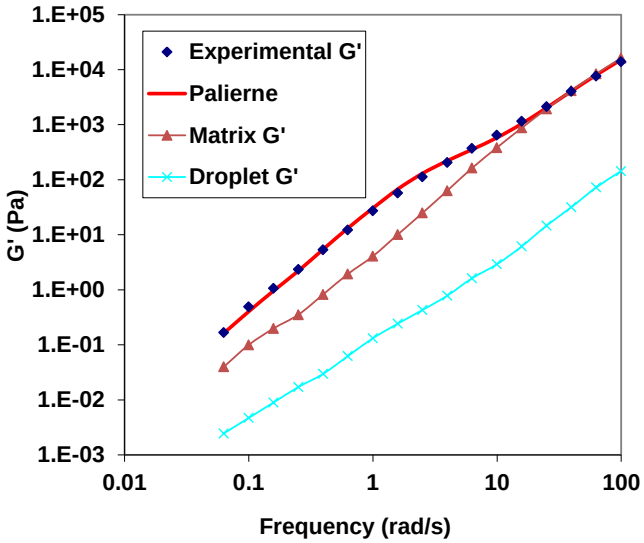

Figure A.3 Elastic modulus, G', of the PLA (matrix), PHO (droplet) and the 95/5 PLA/PHO blend as a function of frequency at 180°C, and fit of the data using the Palierne model.

The mechanical properties of PLA/ePHO blend are depicted in Table A.1. Irrespective of improved compatibility as a result of epoxidation, enhancement in properties was not equivalent to that of neat PHO. ePHO that had viscosity lower than neat PHO, yielded a higher viscosity mismatch and a coarser blend morphology (Figure A.4).

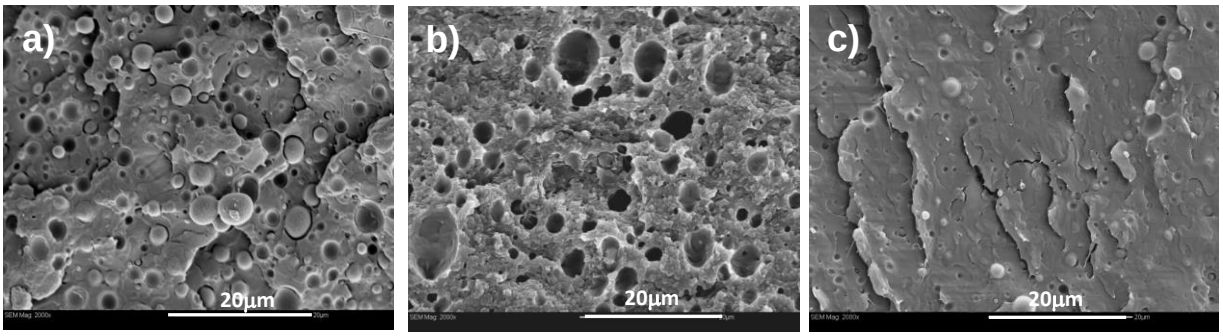

Figure A.4 Scanning electron microscopy of PLA blends containing 10 % of a) PHO, b) ePHO and c) xPHO (0.5 wt.% of peroxide)

To further identify the mechanism for the morphology development the droplet size of PHO and ePHO in PLA matrix was predicted using Wu model [3] for viscoelastic liquids as shown in equation A.2 and further it was compared with particle size obtained from SEM images.

The model correlates viscosity of blend components, interfacial tension, droplet size and shear rate according to

$$\frac{\dot{\gamma}\eta_m D}{\sigma} = 4\left(\frac{\eta_m}{\eta_d}\right)^{\pm 0.84} \quad \text{(A.2)}$$

where, $\dot{\gamma}$ – shear rate, η_m- viscosity of matrix, η_d- viscosity of dispersed, σ- surface tension, D- diameter of particle (+ve sign for λ>1, -ve for λ<1)

The predicted particle size at a shear rate of 100 S^{-1} was 4μm which is fairly close to the particle size obtained from SEM images. The particle size of ePHO was higher at 8μm

In spite of the lower interfacial tension in ePHO/PLA, blend morphology was coarser, indicating that effect of viscosity mismatch was more prominent than the interfacial tension reduction. This explains the lack of improvements in morphology and hence mechanical properties.

Conclusion

Epoxidation of PHO improved its compatibility with PLA, however did not show any improvement in elongation and impact properties due to increased viscosity mismatch with PLA. Cross-linking of PHO improved its viscosity substantially. Irrespective of lowering viscosity mismatch, xPHO/PLA blend did not enhance ductility, mainly due to high gel content altering its elastic nature.

References

1. Al-Itry R, Lamnawar K, Maazouz A. Improvement of thermal stability, rheological and mechanical properties of PLA, PBAT and their blends by reactive extrusion with functionalized epoxy. Polym Degrad Stab 2012;97(10):1898-1914.

2. Palierne J. Linear rheology of viscoelastic emulsions with interfacial tension. Rheologica Acta 1990;29(3):204-214.

3. Wu S. Formation of dispersed phase in incompatible polymer blends - interfacial and rheological effects. Polym Eng Sci 1987;27(5):335-343